

SMALL VOLUME CELL CULTURE TECHNOLOGY
FOR THE ANALYSIS OF CLONAL HETEROGENEITY
IN MAMMALIAN CELL POPULATIONS

by

Darek Sikorski

B.Sc. (Honours), University of Western Ontario, 2007

A THESIS SUBMITTED IN PARTIAL FULFILLMENT
OF THE REQUIREMENTS FOR THE DEGREE OF

DOCTOR OF PHILOSOPHY

in

The Faculty of Graduate and Postdoctoral Studies

(Biomedical Engineering)

THE UNIVERSITY OF BRITISH COLUMBIA
(Vancouver)

April 2017

© Darek Sikorski, 2017

Abstract

The ability to culture individual cells provides a unique method to assess the heterogeneity of mammalian cell populations. However, there are many challenges when scaling down culture systems due to the complexity of re-creating a stimulating environment at the clonal level. Small volume culture systems such as integrated microfluidic platforms offer the potential to radically alter the throughput of clonal screening through the use of time-lapse imaging, dynamic stimulus control and economy of scale. In particular, the use of automated fluidic control allows for the characterization of single cells in a dynamic microenvironment similar to large-scale culture. This thesis describes how small volume cell culture practices such as the use of conditioned medium and microfluidic technology can be implemented to isolate large numbers of cells in small volumes and evaluate clonal populations under precise medium conditions. For a Chinese Hamster Ovary (CHO) cell system normal growth kinetics and specific productivity were sustained in small volumes. When exposed to conditioned medium from a parental CHO line, clones cultured at sub-mL scales matched the performance of large-scale cultures. A microfluidic bead assay was developed to detect Immunoglobulin G titers secreted from clones in nL volumes. The combination of microfluidic conditioned medium perfusion with the magnetic bead assay allowed for clonal productivity to be evaluated under simulated fed-batch conditions. Lastly, microfluidic cell culture was demonstrated on a human embryonic stem cell (hESC) system through the robust generation of colonies derived from single cells. hESCs propagated in the microfluidic system were observed to match the growth kinetics, marker expression and colony morphologies of larger cultures, while resolving response heterogeneity during

differentiation induction. This thesis demonstrates how high-throughput, small volume culture systems can be used to screen clonal populations for therapeutic applications under complex culture conditions.

Preface

The research presented in this thesis is part of a larger collaboration to design and implement microfluidic technology for the clonal analysis of mammalian cell populations.

Chapter 2 is a version of a manuscript to be submitted for publication. I designed the experiments with input from the following undergraduates as well as from my supervisors Drs. James Piret and Carl Hansen. June Wong wrote the Hamilton Methods, performed the automated re-suspension experiments and cultured the cells. Angela McLaughlin performed the preliminary manual experiments, tested the feeds and cultured the cells. Amir Reza Meysami Fard performed the enzyme-linked immunosorbent assays. A fellow graduate student Navid Ghaffari designed the preliminary Hamilton Methods and tested the automated cell re-suspension. I performed all microfluidic experiments. June Wong, Angela McLaughlin and I performed the data analysis, statistical tests and generated all the figures. I primarily wrote the manuscript with input from June Wong, Angela McLaughlin as well as Drs. James Piret and Carl Hansen.

Chapter 3 is also a version of a manuscript that will be submitted for publication. I designed all experiments with input from Drs. James Piret, Carl Hansen and Charles Haynes. June Wong cultured the cells and supplied the CHO samples for microfluidic culture. Amir Reza Meysami Fard performed the large-scale enzyme-linked immunosorbent assays. I designed the microfluidic assay with input from Veronique Lecault and Anupam Singhal. I fabricated the devices and did all of the microfluidic experiments. I wrote the Matlab algorithms to automatically segment the beads and

measure intensities while performing all manual bead intensity and intracellular fluorescence analysis. I generated all the figures and primarily wrote the manuscript with input from Drs. James Piret, Carl Hansen and Charles Haynes.

A version of Chapter 4 was published in the *Biotechnology Journal*:

- Sikorski, D. J., Caron, N. J., VanInsberghe, M., Zahn, H., Eaves, C. J., Piret, J. M. & Hansen, C. L. Clonal analysis of individual human embryonic stem cell differentiation patterns in microfluidic cultures. *Biotechnology Journal*, 10, 1546-1554 (2015)

This work was part of a collaborative project between 3 research groups: Dr. Carl Hansen (Centre for High-Throughput Biology, University of British Columbia, Vancouver, BC, Canada), Dr. James Piret (Michael Smith Laboratories, University of British Columbia, Vancouver, BC, Canada), and Dr. Connie Eaves (Terry Fox Laboratory, BC Cancer Agency, Vancouver, BC, Canada). Dr. Nicolas Caron and I designed the experiments with input from Drs. Connie Eaves, James Piret and Carl Hansen. Dr. Nicolas Caron performed the preliminary scale up experiments and cultured the cells. Michael Vaninsberghe and I wrote the custom Labview software. Hans Zahn designed and built the custom microscope enclosure and helped set up the custom incubator system. I performed all microfluidic experiments. I performed the data analysis, statistical tests and generated all the figures. I primarily wrote the manuscript with input from Drs. Nicolas Caron, Connie Eaves, James Piret and Carl Hansen.

Table of Contents

ABSTRACT	ii
PREFACE	iv
TABLE OF CONTENTS	vi
LIST OF FIGURES	viii
LIST OF ABBREVIATIONS	ix
ACKNOWLEDGEMENTS	xi
CHAPTER 1 INTRODUCTION	1
1.1 THESIS OUTLINE	1
1.2 RECOMBINANT PROTEIN PRODUCTION IN MAMMALIAN CELLS	3
1.2.1 <i>Chinese hamster ovary cells</i>	4
1.2.2 <i>Selection of high-producing cell lines</i>	5
1.2.3 <i>Fed-batch culture and small volume evaluation</i>	7
1.2.4 <i>Heterogeneity in CHO cell lines</i>	8
1.2.5 <i>Single CHO cell measurements and limitations</i>	9
1.3 HUMAN EMBRYONIC STEM CELLS.....	11
1.3.1 <i>Stem cell potential and pluripotency</i>	11
1.3.2 <i>Heterogeneity in ESC populations</i>	12
1.3.3 <i>Clonal analysis of hESCs</i>	14
1.4 MICROFLUIDICS	15
1.4.1 <i>Microfluidic large scale integration</i>	15
1.4.2 <i>Single cells and microfluidic chips</i>	17
1.4.3 <i>Challenges of microfluidic mammalian cell culture</i>	18
1.5 THESIS OBJECTIVES	20
CHAPTER 2 SIMULATING FED-BATCH CHO CELL CULTURES USING CONDITIONED MEDIUM FOR CLONAL ANALYSIS	23
2.1 INTRODUCTION	23
2.2 MATERIALS AND METHODS	26
2.2.1 <i>Cell lines and cell culture</i>	26
2.2.2 <i>Fed-batch culture</i>	28
2.2.2 <i>Conditioned medium harvesting and re-suspension</i>	29
2.2.3 <i>Cell culture and assay automation</i>	31
2.2.4 <i>ELISA</i>	31
2.2.5 <i>Microfluidic cell culture</i>	32
2.2.6 <i>Statistical analysis</i>	33
2.3 RESULTS	34
2.3.1 <i>Feed screening and pH control</i>	34
2.3.2 <i>Automating conditioned medium re-suspension</i>	35
2.3.3 <i>Effect of cell concentration on conditioned medium re-suspension</i>	36
2.3.4 <i>Conditioned medium re-suspension applied to other clones and cell lines</i>	37
2.3.5 <i>Microfluidic conditioned medium perfusion</i>	39
2.4 DISCUSSION	40
CHAPTER 3 A DYNAMIC MICROFLUIDIC BEAD ASSAY TO DETECT IGG IN NL VOLUMES	49
3.1 INTRODUCTION	49
3.2 MATERIALS AND METHODS	52
3.2.1 <i>Dynamic microfluidic bead assay protocol</i>	52

3.2.2 <i>Image acquisition and assay automation</i>	53
3.2.3 <i>Bead segmentation</i>	54
3.2.4 <i>Cell culture</i>	54
3.2.5 <i>Parental cell line fed-batch culture</i>	56
3.2.5 <i>Conditioned medium harvesting</i>	56
3.2.6 <i>ELISA</i>	57
3.2.7 <i>Flow cytometry</i>	58
3.2.8 <i>Microfluidic cell culture</i>	58
3.3 RESULTS.....	60
3.3.1 <i>Microfluidic secretion assay development</i>	60
3.3.2 <i>Automated bead segmentation</i>	63
3.3.3 <i>Dynamic precise measurements of IgG in nL chambers</i>	64
3.3.4 <i>Evaporation considerations and cell culture optimization</i>	66
3.3.5 <i>Microfluidic productivity assessment of CHO-S D2 clones</i>	67
3.4 DISCUSSION.....	70
CHAPTER 4 MICROFLUIDIC CELL CULTURE FOR THE CLONAL ANALYSIS OF HESC POPULATIONS	80
4.1 INTRODUCTION.....	80
4.2 MATERIALS AND METHODS.....	82
4.2.1 <i>Microfluidic device design and operation</i>	82
4.2.2 <i>Cell culture</i>	83
4.2.3 <i>Microfluidic hESC culture</i>	84
4.2.4 <i>Colony recovery and RT-qPCR</i>	85
4.2.5 <i>Immunostaining</i>	87
4.2.6 <i>Flow cytometry</i>	88
4.2.7 <i>Statistical analysis</i>	88
4.3 RESULTS.....	89
4.3.1 <i>Design features and clonal culture performance</i>	89
4.3.2 <i>Quantification of cell proliferation and colony morphology</i>	90
4.3.3 <i>Transcript analysis of recovered samples</i>	91
4.4 DISCUSSION.....	94
CHAPTER 5 CONCLUSIONS & FUTURE DIRECTIONS	107
5.1 SIGNIFICANCE OF WORK.....	107
5.2 FUTURE RECOMMENDATIONS.....	108
5.2.1 <i>Conditioned medium perfusion and re-suspension</i>	108
5.2.2 <i>Microfluidic clone selection</i>	111
5.2.3 <i>Microfluidic human embryonic stem cell culture</i>	114
5.3 FINAL THOUGHTS.....	116
BIBLIOGRAPHY	117
APPENDICES	139
APPENDIX A: HAMILTON METHODS.....	139
APPENDIX B: MICROFLUIDIC FABRICATION PROTOCOLS.....	176
APPENDIX C: BEAD SEGMENTATION ALGORITHM.....	182

List of Figures

Figure 1.1	Schematic of typical cell line selection	22
Figure 2.1	CHO-S D2 performance comparison for different feed strategies.....	42
Figure 2.2	3 mL deep well plate and 25 mL shake flask CHO-S D2 performance comparison.....	43
Figure 2.3	Schematic for automated conditioned medium perfusion/re-suspension.....	44
Figure 2.4	Concentration matching for conditioned medium re-suspension method....	45
Figure 2.5	Conditioned medium re-suspension performance for multiple clones.....	46
Figure 2.6	Conditioned medium re-suspension reproducibility for CHO-S D2 and applicability to CHOm56 cell line.....	47
Figure 2.7	Conditioned medium perfusion in microfluidic CHO-S cultures.....	48
Figure 3.1	Bead assay development.....	72
Figure 3.2	Schematic for dynamic microfluidic bead assay	74
Figure 3.3	Automated bead segmentation	75
Figure 3.4	Magnetic bead assay validation on fixed IgG concentrations	76
Figure 3.5	Microfluidic productivity assessments during clonal CHO culture	77
Figure 3.6	Microfluidic clone ranking in fed-batch conditioned medium.....	78
Figure 4.1	Design of the microfluidic culture device.....	96
Figure 4.2	Validation of RT-qPCR analysis of clonal CA1S populations.....	98
Figure 4.3	Validation of on-chip undifferentiated CA1S cell growth and immunohistochemical features.....	100
Figure 4.4	Effect of differentiation induction on CA1S colony formation.....	101
Figure 4.5	Effect of differentiation induction on colony morphology.....	102
Figure 4.6	Growth rate heterogeneity of individual CA1S colonies.....	103
Figure 4.7	Flow cytometric analysis of CA1S cells before and after induction of their differentiation.....	104
Figure 4.8	Heterogeneity in OCT4 transcript levels and relation to different culture conditions.....	106

List of Abbreviations

CAD	Computer assisted design
cDNA	Complementary deoxyribonucleic acid
CHO	Chinese hamster ovary
CM	Conditioned medium
CI	Confidence interval
CRISPR	Clustered regularly interspaced short palindromic repeats
CT	Cycle threshold
DAPI	4',6-diamidino-2-phenylindole
DHFR	Dihydrofolate reductase
DIC	Differential interference contrast
DMEM/F12	Dubelcco's modified Eagle medium nutrient mixture F12
DNA	Deoxyribonucleic acid
dO ₂	Dissolved oxygen
DWP	Deep well microtiter plate
EB	Embryoid body
ELISA	Enzyme-linked immunosorbent assay
ELISPOT	Enzyme-linked immunosorbent spot
EGFP	Enhanced green fluorescent protein
ESC	Embryonic stem cell
FACS	Fluorescence-activated cell sorting
FBS	Fetal bovine serum
FITC	Fluorescein isothiocyanate

GAPDH	Glyceraldehyde 3-phosphate dehydrogenase
GFP	Green fluorescent protein
GS	Glutamine synthase
hESC	Human embryonic stem cell
IgG	Immunoglobulin G
mAb	Monoclonal antibody
MSL	Multilayer soft-lithography
MSX	Methionine sulfoximine
MTX	Methotrexate
NTC	No template control
OCT	Octamer binding protein
PBS	Phosphate buffered saline
PCR	Polymerase chain reaction
PDMS	Polydimethylsiloxane
PTFE	Polytetrafluoroethylene
RNA	Ribonucleic acid
ROCK	Rho-associated kinase
RT-qPCR	Reverse transcription quantitative polymerase chain reaction
SSEA	Stage specific embryonic antigen
q_p	Specific productivity
tPA	Tissue plasminogen activator
TRA	Teratocarcinoma related antigen
VCD	Viable cell density

Acknowledgements

Many people have helped make this work possible all of whom I cannot thank enough. First and foremost I would like to thank my supervisors, Dr. James Piret and Dr. Carl Hansen, who have been outstanding throughout the course of my degree. Jamie, thank you for your unwavering mentorship and support, your constant encouragement and optimism have allowed me to accomplish far more than I could have ever imagined. I will always be grateful for the opportunities you have given me and the countless doors you have opened for me. Carl, thank you for your constant ambition, drive and holding everything to a higher standard. Working in your lab was an honor and a privilege, which I shall always cherish.

I would also like to thank my committee members, Dr. Charles Haynes and Dr. Bhushan Gopaluni for their support, encouragement and advice throughout my PhD. Chip, thank you for your continuing mentorship and critical eye, your involvement has enabled my research to reach a level far beyond what I ever thought possible. Bhushan, your enthusiasm, guidance and praise have kept me going throughout this long journey.

I wish to thank my countless colleagues from the Piret and Hansen labs. Thank you Pascal, Corinne, Mario, Marta, Roger, Bronwyn and all my coworkers in the Piret lab. Your scientific opinions have been invaluable to me and it has been a pleasure to work alongside you. Thank you Nick for introducing me to the lab, human embryonic stem cells and your wonderful cell line. A special thanks to Chris for keeping the Piret lab running and for many longwinded and rewarding conversations over the years. From the Hansen lab I would like to thank Kaston, Jens, Kevin, Bertin, Tim, Keith, Georgia,

Mark, Carolina, Oleh, Marketa, Marijn, among many others who have made my time there go smoothly and have provided limitless help. In particular Mike, Hans and Dan, your friendship and assistance have made this work possible. All of our adventures outside the lab have helped me to unwind when needed. I sincerely thank you Anupam for your mentorship, advice and support in setting up the CHO project; I will always remember our discussions of science, philosophy and life fondly. I would also like to thank Carmen for her constant advice and wisdom about graduate school while keeping the Hansen lab running in tip-top shape. Paul, Donna, Sean, Amir, Sarah and the numerous students who have worked with me deserve special mention as they have all contributed substantially to this project. Sincere thanks to June and Angela in particular for helping develop the conditioned medium re-suspension, it would not have been possible without you. Lastly and most importantly, I have to deeply thank Adam and Navid. You have been true friends for life on top of colleagues whose support, reinforcement and inspiration have made this document possible.

I would like to acknowledge my fantastic collaborators over the years. At the BC Cancer Agency I would like to thank Dr. Connie Eaves; her incredible passion, intellect and insight into stem cell biology has elevated my research. Thank you Dr. Melanie Kardel and Dr. Michael O'Connor for giving me access to countless resources at the TFL and for all of your experimental advice. Special thanks to Dr. David Kent for our long-lasting friendship, our scientific discussions, your wisdom on navigating academia and for the numerous Canucks games you have dragged me out to. Many thanks to Dr. Peter Gray and Dr. Trent Munro for access to your dual-reporting CHO line, which has been fantastic to work with. I wish to also acknowledge NSERC, MSFHR and CIHR for the

much appreciated funding and research support. In addition, thanks to MabNet, the Stem Cell Network and all of their members for additional support and for allowing me to attend numerous conference proceedings and communicate my research findings.

Finally, I would like to thank my vast network of dear friends and family whose love and encouragement over the years have empowered me to complete this insurmountable task. Sid, Rosa, Vick, Christine, Rob, Kate, Travis and Kelly thank you for your lifelong friendships and your continuous support despite the long distance that separates us. Thank you Dan, Adam, Corey, Jason and Coplen for all of the fantastic visits I have when I go home. Mike, Lisa, Scot, Jay, Jenn, Kyle and Beth from the first mountain we summited together to our last ski run, thank you for getting me out of the lab and exploring this beautiful province with me. Special thanks to the Ellis family for adopting me and giving me a place to work on my thesis outside of the lab. Sincere thanks to Gabriel and Jennifer for all that you have done for me over the years, it will take a lifetime to pay back what you have given me. Nick and Verna, I also give you special thanks as your support, help and reinforcement have meant the world to me. Thank you Ron for all of your encouragement and never letting me give up, I will always treasure our friendship. I also thank Kingsley for being a great mentor, friend and introducing me to the business world. Additionally, Jill and Sally, you have been my family away from home and your love and encouragement over the years are reflected many times over in this work. To my siblings Jenna, Brad, Katie, Adriana and Patrick, you have always been there through thick and thin and for that I am eternally grateful. Lastly, I thank my parents who have never given up on me and always push me to strive for excellence.

Chapter 1 Introduction

1.1 Thesis Outline

The first observation of a cell by Robert Hooke in 1665 led to the concept of cells as the basic units of life¹. Subsequent understanding of cells, including their intra and intercellular interactions, has led to whole classes of medical breakthroughs including pharmaceutical small molecules that regulate gene expression², biologic proteins produced by cells³ and most recently cellular immunotherapies⁴. By nature, populations of mammalian cells are genotypically and phenotypically heterogeneous, often complicating the treatments of a variety of diseases^{5,6}. Even genetically identical cells display considerable functional diversity^{7,8,9}, a trait that is observed frequently in clonal cell lines^{10,11,12}. Since cell lines are ubiquitously used to produce biologics, model disease and study gene regulatory networks, understanding phenotypic variations in clonal populations is needed for their effective use as well as of fundamental biological importance.

The field of microfluidics is particularly applicable to clonal analysis and offers numerous advantages over conventional methods such as scalability, high cell or template concentrations in small volumes, higher-throughput and parallelization^{13,14}. In particular, microfluidic cell culture platforms provide the ability to examine the clonal responses *in situ* through the use of live-cell imaging and dynamic fluidic control¹⁴. While mammalian cells have been cultured *in vitro* using microfluidics, the cell culture of single clones in small volumes has yet to accurately match results achieved at larger scales for a variety

of cell types¹⁵. This thesis describes how scalable cell culture techniques can be used to accurately assess clonal populations in small volumes.

The following chapter reviews microfluidic technology in the context of mammalian cell culture and clonal analysis. It also introduces two cell types whose clonal analysis is of great importance and reviews recent work to assess these populations clonally.

The second chapter develops a technique to mimic bioreactor conditions by re-suspending small volumes cultures of Chinese Hamster Ovary cells in conditioned media from large-scale fed-batch cultures. This technique is tested and validated on multiple clones and cell lines in 24-well deep well plates and finally applied in a microfluidic setting.

The third chapter presents a microfluidic magnetic bead assay capable of detecting antibody titers in nanoliter volumes. The assay is then combined with microfluidic cell culture and the conditioned medium re-suspension technique of the second chapter to make productivity assessments of Chinese Hamster Ovary cells at the clonal level.

The fourth chapter applies microfluidic cell culture to the clonal analysis of adherent mammalian cells. In this case, clonal populations of human embryonic stem cells are cultured in a microfluidic device and their responses to self-renewing and differentiating conditions are analyzed in terms of growth kinetics, morphology and transcript expression.

The final chapter describes the significance of the work done while concluding the thesis. Recommendations for subsequent experiments and approaches to carry on this work are also described.

1.2 Recombinant Protein Production in Mammalian Cells

The cost of developing a new drug was estimated in 2010 to be from 0.8 and 1.8 billion USD¹⁶. To reduce costs, microbial systems are often preferred for the production of simple recombinant proteins such as insulin¹⁷. However, most recombinant proteins must be synthesized with post-translational modifications such as mammalian types of glycosylations^{18,19}. Mammalian cell culture systems are needed for the production of recombinant proteins (referred to as biologics) due to their ability to perform complex protein synthesis, folding and post-translational modifications^{20,21}. Recombinant proteins produced by mammalian cells are being used for the treatment of many diseases including many forms of cancer^{22,23,24}, arthritis²⁵ and autoimmune disorders^{26,27}; valued at 100 billion dollars in sales with many more biologics undergoing clinical trials^{28,29}.

Chinese Hamster Ovary (CHO) cells have been widely used to produce top selling biologics³⁰. In order to meet the market demand, biologics produced in the CHO cell system undergo a long, costly and complex cell line and culture process development to ultimately scale-up production³¹. The process as well as the recombinant protein must pass rigorous regulatory approval requirements to ensure the safety and efficacy of treatments³². Accelerating the development of promising biologics in the CHO cell system should yield both commercial and public health benefits (e.g. effective drugs reach the market sooner to provide more successful treatments).

1.2.1 Chinese hamster ovary cells

In 1957 Theodore Puck successfully established the first CHO cell line in culture by isolating an ovary from a female *Cricetulus griseus* specimen³³. Although initially isolated for genetic purposes, favorable metabolism, growth characteristics and performance in bioreactors during *in vitro* culture established CHO cells as a model host cell line³⁴. Early mutagenic studies performed on the original CHO cell line were particularly successful at isolating auxotrophic behavior (for proline in particular)³⁵. Ensuing experiments with CHO cell mutants lacking the dihydrofolate reductase (DHFR) gene demonstrated dependence on thymidine and glycine, providing the foundation for a widely used genetic selection methodology³⁶. In the DHFR CHO expression system, transfection with a vector containing DHFR prevents methotrexate (MTX), a DHFR inhibitor, from poisoning transfected cells (with selection occurring in the absence of glycine and thymidine)³⁷. Another widely used CHO cell expression vector system makes use of glutamine synthetase (GS) with methionine sulfoximine (MSX) based selection³⁸. Since GS is responsible for the synthesis of glutamine from ammonium and glutamate, transfection of CHO cells with a GS vector (while inhibiting endogenous GS activity with MSX) can allow for selection in the absence of glutamine^{39,40}. The ease of integrating genetic selection coupled with their familiarity and adaptability to varied culture conditions have since established CHO cell lines as the preferred system for recombinant protein manufacturing.

Several CHO cell variants such as CHO-S and CHO-K1 have been easily adaptable to suspension culture and serum free media for the purpose of manufacturing biologics⁴¹. The first lines used for recombinant protein production included those

capable of secreting human interferon^{42, 43} and tissue-type plasminogen activator (tPA)⁴⁴. Many more manufactured proteins used the CHO cell system, producing glycoforms similar to those found in humans³⁴; an example of this can be found in the consistency between CHO produced and human Immunoglobulin G1 (IgG1)⁴⁵. In the case of immunoglobulins, variations in species-specific glycosylation can substantially impact biological activity^{46,47}. Today the CHO expression system is used in the production of the majority of top selling biologics including Humira (Abbvie)²⁵, Rituxan (Roche/Biogen)^{22,48}, Enbrel (Amgen/Pfizer)⁴⁹, Avastin (Roche)²³ and Herceptin (Roche)²⁴. The majority of new target recombinant proteins are also produced using CHO cells⁵⁰. With the expectation that the CHO expression system remains the primary producer of blockbuster pharmaceuticals, improving the efficiency and efficacy of cell line selection and scale-up is of utmost importance⁵¹.

1.2.2 Selection of high-producing cell lines

The large-scale production of a biologic requires the selection of a high-producing, stable cell line that reaches a high viable cell number that can be maintained for an extended period of bioreactor culture to achieve a high product yield⁵². The process of going from a transfected CHO cell pool to selecting the clone for full-scale biologic production can involve the screening of up to thousands of clones⁵³. Cell line selection is normally the slowest step in the overall process development, with a duration of ~6 months to ~1 year^{54,55}. Thus, the efficient selection of high-producing, stable cell lines is crucial for the rapid and cost-effective scale-up of biologics production.

Typically, cell line development begins by transfecting cells with a gene of interest and performing limiting dilutions on the transfected pool in order to isolate single

clones^{56,57}. An initial productivity assessment is usually performed on hundreds to thousands of clones in static 96-well plates (grown in cloning medium) followed by an initial clone ranking^{58,59}. Selected clones are then expanded into successively larger volumes (such as 24- and 6-well plates, shake flasks and then bioreactors that are meant to simulate large-scale biologic fed-batch production)^{60,61}. It is not uncommon for the manufacturing of biologics to reach scales of up to 20000 L⁶². A representative schematic outlining typical cell line selection process is described in Figure 1.1.

During scale up, the number of cell lines examined at each stage is reduced as high-producing clones are selected while low-producing clones are discarded⁶³. Unstable productivity is often witnessed as high producing clones are scaled-up. This can be due to expression instability or poor adaptation to suspension culture, production medium or fed-batch culture⁵³. In the case of expression instability, the losses in productivity are often due to epigenetic transcriptional silencing from DNA methylation in the cDNA promoter region or due to the loss of recombinant gene copies as the cells proliferate^{10,64,65,66,67}. Gene amplification procedures have been shown to increase cell line instability as well as increase clonal productivity as much as 400-fold^{10,68}.

In addition to cellular stability issues, the clonal microenvironment is continuously changing during scale up; starting from static cloning in medium designed to promote clone survival in dilute conditions, to a suspension fed-batch medium designed to maximize productivity^{69,70}. Thus, the changing culture conditions from cloning to scale-up result in a poor predictability of early productivity measurements⁷¹. Porter *et al.* examined the rankings of 175 individual clones in 96-well plate, 24-well plate, 125 mL batch and 125 mL fed-batch cultures and found that the top 10 highest

producing clones at the fed-batch stage were variably ranked throughout each of the previous stages⁷¹, such that the highest-performing clones can easily be rejected early during the screening process⁷². Providing a more accurate assessment of how a clone will perform in a large-scale fed-batch bioreactor would be most valuable at the cloning stage⁷³. Such a process would ideally screen candidate clones in fed-batch conditions at the single-cell level. However, fed-batch evaluation in small volumes can be challenging due to limitations such as assay sensitivity⁷⁴, evaporation from small volumes⁷⁵ and conditioning effects when working at limiting dilutions^{76,77}.

1.2.3 Fed-batch culture and small volume evaluation

Fed-batch cultures are processes in which nutrients are added (fed) over the course of the cultivation⁷⁸, either discretely (e.g. daily feeds) or continuously. These feed additions cause substantial changes in volume, osmolality as well as product, nutrient and cell concentrations⁷⁹. Nutrient consumption and waste accumulation are considered when designing feed strategy, to maximize the overall process productivity⁸⁰. The result is a culture ideally suited to processes where productivity and cell growth are sensitive to the limiting nutrient⁸¹.

Large-scale fed-batch culture technology has advanced substantially over the past few decades and is now considered to be quite robust and reliable⁸². Nonetheless, there is increasing pressure to speed up fed-batch process development and reduce costs due to pipeline concerns, patent expiry and competition⁸³. A variety of small-volume bioreactors have become available to provide accurate simulations of production conditions down to μL volumes^{84,85,86,87}. For example, Legmann *et al.* used hundreds of 700 μL micro-bioreactors to mimic a 3L bioreactor system and reported excellent correlations between

the two scales for pH, dissolved oxygen (dO₂), viability, and product titer over a 14-day fed-batch⁸⁶. The introduction of deep-well microtiter plates (ranging from 6 to 96 wells per plate) coupled with robotic fluid handling have simulated larger bioreactors in volumes ranging from 0.1 – 10 mL^{84,88,89}. However, at these volumes control over parameters such as pH, dO₂ and osmolarity are more difficult due to differences such as limited feedback control and increased evaporation^{90,91,92}. Potential solutions to these limitations include optical sensors to measure dO₂ *in situ* and re-designing the plate lid^{93,94}. Nonetheless, parallel small-scale systems still have the potential to accelerate the development pipeline by providing early fed-batch evaluation of promising clones⁸⁴. In these systems the fed-batch should ideally be performed clonally to identify the clones that will ultimately perform the best in fed-batch bioreactors^{20,95,96}.

1.2.4 Heterogeneity in CHO cell lines

To make predictive productivity assessments early in the scale-up process, it is important to understand the causes of variations in productivity. For example, intrinsic mammalian cell heterogeneity causes cells to display a range of performances and growth characteristics⁵³. Between cell lines, differences in specific productivity have been noted for varying gene copy number, promoter/enhancer type, cell type/sub-type and expression vector construction^{97,98,99,100}. However, even within a genetically homogeneous cell line, variations can be expected due to at least the cell cycle^{101,102,103,104}. A report by Pilbrough *et al.* found no productivity dependence on cell cycle, although the half life of the fluorescent molecules used were longer than the typical generation time thereby limiting the readout to greater than one division time¹⁰⁵. Other inherent effects may also cause higher or lower producing sub-populations to arise within cell lines, such as genetic

heterogeneity^{106,107,108,109}. Due to the large variability observed, all mammalian cell lines that produce recombinant proteins are required to be clonal¹¹.

Stochastic fluctuations in gene expression have also been shown to contribute to observed protein expression changes^{110,111,112,113}. By using a dual reporter, intra-clonal variations in protein expression (of as much as 70% of the mean) have been shown to contribute to expression instabilities over time^{105,114}. Such variations were dynamic, when the highest and lowest 5% producing sub-clones were isolated, these sub-populations returned to the original productivity distribution after 18 days¹⁰⁵. Thus, they represent a temporary high/low-expression state resulting from random fluctuations, unlike epigenetic silencing where there is a greater and more permanent decrease in productivity^{67,110}. The difference between stochastic variations and expression instability will therefore be dependent on both the amplitude and the persistence of the fluctuation and any technology seeking to precisely evaluate clones will ultimately have to address these fluctuations over their respective timescales. Whatever the causes of productivity measurement variability, a reliable productivity assessment at early stages will need to select the highest fed-batch performance clones, despite both genetic and environmental sources of variability.

1.2.5 Single CHO cell measurements and limitations

Cloning at limiting dilutions in multiwell plates has been the most widely used method to evaluate populations arising from single cells^{52,53}. In traditional multiwell plate formats, the earliest productivity measurement on a clonal population are usually feasible 2 – 3 weeks post-transfection (due to limited sensitivity) in the form of an enzyme-linked immunosorbent assay^{71,115}. Fluorescence activated cell sorting (FACS) has also been used

prior to depositing clones into microwells, however this only provides a rough assessment of productivity, based on membrane associated recombinant protein^{116,117,118,119}. Using fluorescent reporters analyzed by FACS, an indirect measurement of single cell productivity can be obtained. However, the reporter levels are not always indicative of recombinant protein secretion rates and the reporter expression may also influence productivity as well as clonal stability such that cell lines of this type are generally not used in manufacturing^{105,114,117}.

Recently, techniques that make use of semi-solid media have been developed to increase the throughput and efficiency of clone selection^{120,121}. Some of these procedures make use of cell-surface affinity matrices wherein the secreted recombinant product is captured on or near the surface of the producing cell, labeled with a fluorescent marker and FACS sorted^{58,122}. When combined with automation and robotics, semi-solid medium techniques such as the ClonePix FL have the ability to replace limiting dilution cloning while enriching for high performing clones^{59,123,124}. However, fluorescence measurements using the ClonePix FL often do not correlate well to later productivity assessments⁵⁹. In addition, the methodology and automation of ClonePix FL type systems is often quite stringent and costly^{125,126}.

An additional limitation is that clone selection using limiting dilution and automated systems (eg. ClonePix FL) is generally done under static batch conditions, that are known to correlate poorly with later suspension fed-batch productivity measurements⁷¹. Current early productivity assessments also are performed at low seeding concentrations, much lower than the cell concentrations and thus medium conditioning in a manufacturing setting⁵³. Other operational parameters such as the O₂,

pH and osmolarity levels may also be drastically different due to the difficulty in quantifying them at the clonal level. Consequently, there is a strong motivation to develop technologies capable of precisely quantifying productivity at the single cell level in conditions that are more representative of large-scale bioreactors.

1.3 Human Embryonic Stem Cells

1.3.1 Stem cell potential and pluripotency

In human development, the zygote and the blastomere are the only structures known to be totipotent, with the ability to form all tissue types in an organism including extra-embryonic tissues such as the placenta¹²⁷. This level of potency has yet to be fully harnessed *in vitro*¹²⁸. The discovery and isolation of human embryonic stem cells (hESCs) by James Thomson in 1998 from the inner cell mass of blastocysts did demonstrate the ability to propagate human pluripotent cells indefinitely as immortalized cell lines^{129,130}. hESCs are a quintessential pluripotent cell and are characterized by their ability to differentiate into all 3 germ layers, proliferate extensively *in vitro*, form teratomas and demonstrate telomerase activity¹³¹. Due to their potency, hESCs hold vast therapeutic potential in the form of cell replacement and transplantation therapies but this potency also adds to the risks of any hESC-derived cell therapy¹³². Since most medical applications will require specific lineages and pluripotent cells have the potential to produce all cells in an organism, directed differentiation of hESCs into multipotent and unipotent cells will be needed¹²⁸.

Several approaches have been used to assess the self-renewal potential and differentiation capacity of putative pluripotent cells; these include but are not limited to:

growth capacity, morphology, specific antigen and transcription factor expression as well as a variety of functional assays^{129,133,134}. When in culture, hESCs are known to have a high nucleus-to-cytoplasm ratio, a compact colony morphology and doubling times between 24 and 48 h¹³⁵. hESCs also express molecular markers including Octamer binding protein (OCT) 3, OCT4 (also known as POU5F1), Stage Specific Embryonic Antigen (SSEA) 3, SSEA4, NANOG, teratocarcinoma related antigen (TRA)-1-60, TRA-1-81 and alkaline phosphatase^{136,137,138}. Based on their specific expression patterns in pluripotent cells, OCT4, SOX2 and NANOG in particular have been found to be essential in maintaining pluripotency^{139,140}, with OCT4 functioning as a heterodimer with SOX2¹⁴¹. The necessity of a core set of highly expressed transcription factors regulating pluripotency was highlighted by the ability to derive induced pluripotent murine and human cells via the ectopic expression of only 4 factors: NANOG OCT4, SOX2 and C-MYC^{142,143,144,145}. During early differentiation hESCs have been shown to lose their pluripotency-associated properties at different rates^{146,147}. Thus, in order to gain a full understanding of cell state, the use of both molecular markers and functional assays is necessary.

1.3.2 Heterogeneity in ESC populations

A major obstacle preventing the proper characterization of any cell potential is that cell populations rarely act as a homogenous entity^{148,149}. ESCs in particular display considerable inherent heterogeneity at the molecular level and manifest sub-populations with functionally distinct phenotypes^{150,151,152,153}. As an example, the transcription factor NANOG is only expressed in roughly 80% of ESCs in a typical population^{154,155}. When NANOG⁺ and NANOG⁻ populations are isolated and propagated, both fractions were

able to reestablish the original expression pattern, suggesting that NANOG expression is dynamic even though NANOG⁻ populations demonstrate bias towards differentiation¹⁵⁶. In addition to molecular variations, ESCs also demonstrate heterogeneity at the functional level as dynamic sub-populations have been found within OCT4⁺ undifferentiated cells that exhibit distinct behaviors *in vitro* and *in vivo* when differentiation is induced¹⁵³. Such fluctuations have the potential to destabilize the pluripotent state and make them more susceptible to differentiation without making a lineage commitment¹⁵⁷. The dynamic nature of these results suggest that pluripotent cells may move between different states due to stochastic fluctuations in transcription factor gene expression⁷.

The stochastic nature of gene expression implies that chance may play a role in hESC fate decisions and the heterogeneity observed in hESC populations^{8,9,158,159,160}. Alternatively, heterogeneity could infer the co-existence of several stable states within the hESC populations, each with a specific molecular expression pattern^{152,161,162}. Heterogeneous transcription factor expression could also be a fundamental component of future cell fate decisions where a factor reaching an expression threshold could impose a specific differentiation outcome¹⁶³. Examples have already been seen in the hematopoietic system where multilineage gene expression has been observed to precede commitment¹⁶⁴. Thus, distinguishing between these causes of variation is needed for the proper understanding of cell potency¹⁶⁰. In order to determine whether the variations observed in hESC populations are reversible, the ability to analyze multiple dynamic clonal cultures is vital.

1.3.3 Clonal analysis of hESCs

The ability to assess clonal cells is critical when attempting to understand cell population heterogeneity¹⁶⁵. The clonal analysis of hESCs has not yet become widespread due to difficulties in effectively isolating subsets of clonogenic populations^{166,167}. One complication is that stem cells often reside in complex microenvironments involving many niche interactions^{168,169}. Moreover, pluripotent stem cells have extremely low survival and plating efficiencies when re-suspended as single cells during passaging^{130,170,171}. Several methods to circumvent this poor survival have included modifying signaling pathways such as Rac-Rho¹⁷² and IGF-AKT¹⁷³ or plating cells onto murine or human derived fibroblasts¹⁷⁴. Sub-lines of hESCs have also been adapted to culture at low densities while still retaining the fundamental pluripotent properties including normal karyotype, pluripotency marker expression, and the ability to differentiate into all three germ layers¹⁷⁵. However, such cell lines are also associated with forms of neoplastic progression (e.g. amplification on chromosome 20) that may provide a selective advantage^{176,177,178}. Regardless of the drawbacks, use of the above hESCs can provide functional readouts of stem cell renewal capacity¹⁷⁹.

When successful, clonal interrogation has the ability to uncover the cellular hierarchies that exist within hESC populations¹⁶⁵. For example, the isolation of SSEA3⁺ and SSEA3⁻ cells demonstrated that they both had the ability to initiate further pluripotent cultures, but retained differing levels of core transcription factors, clonogenic capacities and cell cycle properties¹⁷⁴. Similarly, retroviral marking of individual cells has allowed for the *in situ* observation of the propensity of single hESCs to commit to different lineages and functional assay results¹⁸⁰. When clonal tracking was used on single hESCs,

it revealed two self-renewing sub-populations: one that lacked clonogenic ability but contributed to *in vitro* embryoid body (EB) differentiation and another with high clonogenic capacity that contributed substantially in teratoma formation yet was less frequently observed to contribute towards EB differentiation¹⁸¹. These studies highlight the need to examine hESCs clonally through the *in situ* tracking and imaging of single cells and clonal populations¹⁸².

1.4 Microfluidics

1.4.1 Microfluidic large scale integration

Today's information age results from the invention of integrated circuits and microchips, which owe their existence to the application of microfabrication to the electronics industry¹⁸³. Virtually all integrated circuits are now made using photolithographic microfabrication; this technology is also being applied to produce fluidic circuits with impressive results as well^{184,185}. When coupled with a technique called soft lithography, replica molding of photolithographic features provides a low-cost, rapid prototyping method of manufacturing microstructures for the purpose of addressing biological problems^{186,187}. For this process, patterns are drawn using computer assisted design (CAD) and then printed (via high resolution photoplotting) to create a photolithographic mask¹⁸⁸. This mask is placed between a UV light source and a thin layer of photoreactive polymer known as a photoresist (usually coated on a silicon wafer). Exposure of the photoresist to UV light then transfers the mask pattern to the wafer with the exposed photoresist crosslinking and becoming insoluble in a developing solution (for a negative photoresist such as SU8)¹⁸⁹. Finally, unexposed photoresist is

washed off in developer solution leaving a patterned silicon wafer. Repeating the above process with more photoresist layers produces three-dimensional structures, with the height of each feature determined by the thickness of the corresponding photoresist layer¹⁹⁰.

A single silicon wafer with photolithographic features can serve as a master for replica molding via soft lithography, to produce hundred of copies. In this procedure a liquid elastomer called polydimethylsiloxane (PDMS) is poured onto the master and thermally cured at 65 to 80°C. After curing, the solid polymer layer of PDMS (containing the inverse photolithographic pattern) can be peeled off the wafer. When sealed against a surface, the topographical features in the PDMS act as chambers and channels, facilitating the rapid prototyping of microfluidic systems¹⁸⁷.

A significant advancement in the area of soft lithography occurred in 2000 when Stephen Quake demonstrated the off-ratio bonding of multiple layers of PDMS¹⁹¹. This technique, termed multilayer soft-lithography (MSL), made way for the incorporation of intricate flow mechanisms into PDMS devices including valves, multiplexers, pumps and mixers¹⁹². The basic microfluidic valve unit consists of two perpendicular channels stacked one on top of another and separated by a thin membrane of PDMS; by applying a positive pressure to one of the channels, the thin membrane is deflected, thereby blocking flow in the second channel¹⁹³. Coupling replica molding with the scale-up of valve density allows for large-scale integration of microfluidic platforms that, though with much larger features, are analogous to current integrated circuits (i.e. contain thousands of control components and valves)¹⁹⁴. Integrated fluidic circuits are now used in many

areas of chemistry and biology and provide numerous advantages including impressive parallelization, multiplexing, automation and scalability¹⁹⁵.

1.4.2 Single cells and microfluidic chips

The ability of microfluidics to precisely control picoliter sample volumes has facilitated an entire new field of small volume single cell manipulation^{14,196,197}. For example, the physical trapping of individual cells can now be performed through a variety of means^{198,199,200,201,202}. As a result, integrated fluidic platforms have been able to demonstrate outstanding capacity to precisely quantify DNA and RNA levels in single cells^{203,204,205,206}. Measurement sensitivity has even been extended into the range of single molecule resolution when coupled with techniques such as digital PCR^{203,207,208,209}. Such microfluidic measurements have also been applied to single cell whole genome and transcriptome analysis^{205,210,211,212,213,214}.

At the translational level, intracellular and secreted proteins have also been measured on single cells in microfluidic devices^{211,215,216,217}. By confining cells in small volumes, protein concentrations around single cells can reach detectable levels orders of magnitude sooner than would be attainable by conventional methods¹⁴. For example, microfluidic antibody bead capture assays developed by Singhal, *et al.* confirmed detection sensitivities on the order of 8×10^4 molecules secreted from single hybridoma cells²¹⁶. Similarly, microfluidic droplet encapsulation has facilitated the quantification of secreted proteins in single T cells²¹⁸ and tumor cells²¹⁹, and paracrine signaling effects have been quantified by co-encapsulating multiple cells in droplets or beads²²⁰. Thus, ultrasensitive protein detection methods have established microfluidics as a technology for the molecular characterization of single cells²²¹.

When coupled with live-cell imaging, microfluidics additionally offers the potential to assess single cells *in situ* with advantages of compartmentalization, parallelization as well as dynamic and spatial control over medium conditions¹⁴. The properties of PDMS are such that microfluidic devices can be gas permeable, optically transparent, elastomeric and biocompatible, thus making them suitable for cell culture^{13,222,223}. Recent reports of microfluidic cell culture devices have examined important biological responses in prokaryotes (*E. coli*)²²⁴ and simple eukaryotes (*S. Cerevisiae*)^{225,226}. For example, Falconnet *et al.* were able to discern that variable phenotypic responses of yeast to pheromone were not by chance but due to genetic and non-genetic heritability²²⁶. Moreover, the use of spatial or temporal gradients and combinatorial screening in microfluidic devices allow for investigations of gene expression and regulation responses that would be extremely difficult, if not impossible to reproduce otherwise^{227,228,229,230}. Overall, the above reports exploit the significant advantages of microfluidic cell culture, including clonal analysis, high cell concentrations, dynamic stimulus control, ease of automation, live-cell imaging and lineage tracing.

1.4.3 Challenges of microfluidic mammalian cell culture

Many reports have examined heterogeneous responses in mammalian cell populations using microfluidic cell culture^{14,15}. To date, the mammalian cell types that have been propagated using microfluidic platforms include but are not limited to: neurons²³¹, neural stem cells²³², embryonic stem cells^{233,234,235,236,237}, endothelial cells²³⁸, hepatocytes²³⁹, mesenchymal stem cells²⁴⁰ and hematopoietic stem cells²⁴¹; with some of these studies performing single cell culture^{241,242,243,244}. However, the challenges of

mammalian cell culture have restricted most microfluidic reports to high perfusion rates and relatively large chamber volumes^{233,234,235,238,240,245,246,247,248}. Also, when cultured in microfluidic systems the cell doubling times are often reported to be significantly lower than in large-scale cultures and often not even measured^{233,234,247,248,249}.

Although the high working concentrations of cells in small microfluidic chambers allows for greater cell medium conditioning, due to the permeability of PDMS these small chambers are very sensitive to evaporation and the resulting increase in osmolarity^{223,250}. Significant increases in osmolarity have been shown to inhibit the growth of mammalian cells due to evaporation through PDMS²⁵¹. Additionally, diffusion of small molecules between the PDMS and the microfluidic chamber allows for toxins to leach into and nutrients to be absorbed out of the medium, and this can affect cell growth^{252,253}. To buffer such effects and grow mammalian cells robustly, many groups have resorted to the use of osmotic baths and reservoirs located in geometrical proximity to culture chambers^{241,250,254,255}.

Numerous accounts have outlined the ability of microfluidic platforms to control O₂, CO₂, Temperature and pH conditions on chip for the purpose of robust cell culture^{256,257,258,259,260,261,262}. However, microfluidic osmotic baths coupled with sufficient perfusion can maintain the osmotic and other conditions needed in the culture chambers to mimic larger-scale *in vitro* concentrations of nutrients and wastes, without a need for on-chip pH/O₂/CO₂ sensors^{241,254,255}. As a result, high-throughput microfluidic platforms can approximate larger and more complex bioreactors simply by continuously perfusing fresh or conditioned medium at high enough rates^{263,264}. With the preliminary successes of the above platforms to cultivate sensitive cell types (such as hematopoietic and

embryonic stem cells) using precise microenvironmental control, there is little doubt that the culture of CHO clones (that proliferate well under a wide range of conditions) and individual hESCs should be successful^{241,265}.

1.5 Thesis Objectives

Effective clonal analysis of mammalian cells is essential for understanding the states of heterogeneous populations and for identifying important clonal and sub-populations¹⁶⁵. Traditional methods of clonal expansion are often restricted to techniques such as limiting dilution, which lack sensitivity and differ greatly from the microenvironments found *in vivo*¹⁶⁹ and eventual large-scale bioreactors⁷¹. Microfluidic cell culture systems offer numerous advantages including scalability, parallelization, high effective concentrations in small volumes and dynamic stimulus control^{13,14}. This thesis aims to develop small volume cell culture techniques to assess clonal populations of mammalian cells in microenvironments that mimic large-scale cultures.

The thesis addresses the following specific objectives:

1. Use perfusion and re-suspension in conditioned media along with the effective high concentrations and increased survival of small volume culture to mimic large-scale conditions, allowing for predictive clonal measurements.
2. Establish a microfluidic assay capable of dynamic detection of IgG titers in nL volumes.
3. Develop a microfluidic cell culture platform capable of live-cell imaging, growth measurement, dynamic fluidic control, cell recovery, and

transcript/protein quantification of clonal populations. Apply the technology to the culture and dynamic assessment of CHO clones.

4. Use microfluidic cell culture technology to perform clonal measurements on hESC clones during early differentiation conditions.

The integration of microfluidic cell culture with dynamic perfusion conditions, sensitive assays and cell recovery will allow for hundreds of clones to be analyzed in parallel. Thus, through the combination of sensitivity and precision in mimicking complex microenvironments, microfluidic cell culture represents a significant contribution to the field of clonal interrogation.

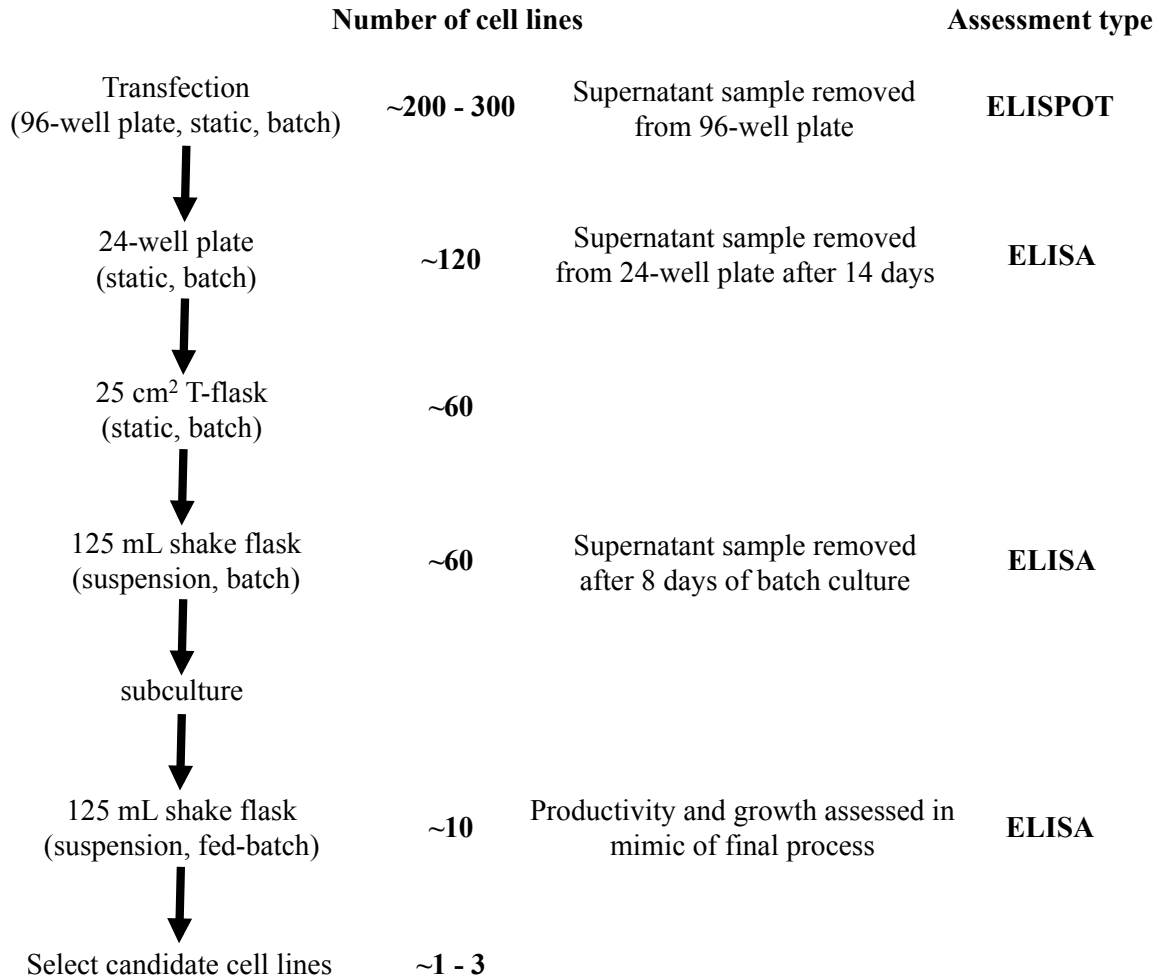


Figure 1.1 Schematic of typical cell line selection

In a typical cell line selection process the initial transfected pool is cultured under selective pressure to prevent non-transformed cells from proliferating. Approximately 200 – 300 clones are then examined in a static 96-well plate format via an ELISPOT assay with the top ~120 clones being scaled up to 24-well plates for a static ELISA evaluation⁷¹. The top ~60 clones from the 24-well plate stage are then scaled up to 125 mL shake flasks, subcultured and a batch performance evaluation is made. The top ~10 clones from the batch assessment are then evaluated under fed-batch conditions with a few top clones being selected for large-scale (3+ L) bioreactor assessment⁶².

Chapter 2 Simulating Fed-batch CHO Cell Cultures using Conditioned Medium for Clonal Analysis

2.1 Introduction

Chinese Hamster Ovary (CHO) cells are ubiquitously used for the production of recombinant therapeutics³⁰. However, scale up of CHO cells from transfected pools commonly requires the screening of hundreds to thousands of clones to select those with favorable attributes²⁶⁶. The clones selected for large-scale biologic production ideally demonstrate high specific productivity, growth rate, expression stability and product quality⁵³. Identifying robust clones and constructing an industrially relevant cell line can take up to ~1 year; this is labor intensive, costly and the process development step that most delays the market launch of valuable new therapeutics⁸². A major challenge in this process is that clones with promising characteristics at initial screening stages often do not maintain their performance in a bioreactor setting or when tested over 50 doublings (40 – 45 days)³⁴. These drops in cell line performance are attributed to intrinsic properties of the clones and only partially understood⁶⁵.

Transfected CHO cell pools exhibit considerable transfection site and copy number heterogeneity due to the indiscriminate nature of transgene integration^{267,268,269}. Losses in transgene copy number over time have historically been linked to decreases in cell specific productivity^{10,67}. Recently, powerful targeted integration site transfection methods have been developed, such as using clustered regularly interspaced short

palindromic repeats (CRISPR)²⁷⁰ and zinc-finger endonucleases^{271,272}, in an effort to yield more homogeneous populations but are limited to a single integration locus leading to lower productivities when compared to random integration²⁷³. Expression changes have also been known to occur without the loss of the transgene due to epigenetic silencing^{274,275,276,277}. Additionally, gene expression can be stochastic in nature, so even a fully functional transgene that is not silenced may be expressed at varied levels over time^{105,111,113}. Numerous innate factors thus contribute to temporal CHO cell performance, adding to environmental pressures that also play a role.

A major extrinsic cause of changing clonal performance between culture scales is the changing bioprocess medium conditions⁶². For the initial productivity assessment, clones are often screened at limiting dilution in a batch culture and static medium environment, vastly different from the eventual suspension based fed-batch production medium conditions⁵⁹. Clones that perform well under static conditions may not do so in suspension and fed-batch culture while, conversely, others that may perform well in a large-scale bioreactor may not perform well in a static batch culture⁷². For example, in Porter *et al.* major changes in clone rankings were observed between batch and fed-batch cultures⁶². Thus, static batch selection can often not select the clones that would have the highest performance in fed-batch bioreactor conditions. A consequence of this is that many clones need to be tested at least under small-scale fed-batch conditions after a first screening in batch cultures.

Many types of scale-down culture systems have been developed for the evaluation of clones under medium conditions more similar to large-scale production^{14,84,85,86,87,88,278}. Recently, deep well microtiter plates (DWPs) have demonstrated an ability to culture

cells in suspension fed-batch, with similar gas exchange rates and shear forces as greater volume bioreactors^{89,90,91,92,279}. Such culture systems do have drawbacks such as the absence of pH and oxygen feedback control as well as high evaporation rates due to their high surface to volume ratios^{90,91,92,279}. Small scale pH and oxygen controlled bioreactors have also been used to evaluate clonal performance, but are limited by throughput and high cost²⁸⁰. At far smaller nL scales, integrated microfluidic cell culture systems have the potential to advance scale-down screening by providing single cell sensitivity for large numbers of clones^{13,14,241,244}. The ability to screen clones accurately early during process scale up should make more use of technologies to accurately reproduce the manufacturing scale medium conditions.

If scale-down technologies are to properly screen for large-scale clonal performance, they will need to examine culture parameters such as medium conditioning. Medium conditioning has long been used to culture primary mammalian cell types^{281,282} where conditioned media have been found to contain a range of cytokines and growth factors^{283,284,285,286}. In the recombinant protein expression field, investigation into cell-conditioned medium components has been used to identify additives to improve defined single-cell cloning media²⁸⁷. Although advances have been made in CHO cell medium conditioning analysis, individual components are not always completely defined, resulting in inconsistencies during cloning and scale-up^{288,289}. Nevertheless, the use of conditioned medium provides a means to improve early stage productivity assessments by allowing clones to be evaluated in cultures that more closely resemble large-scale production.

In this work semi-automated methods for simulating bioreactor conditions in small volumes were developed by exposing clonal populations to larger-scale fed-batch conditioned medium. Conditioned media harvested daily from 125 mL parental CHO cell fed-batch cultures were either used to re-suspend clones in 3 mL deep well plate cultures or perfused in microfluidic cultures. Deep well plates using conditioned media were compared to shake flask fed-batch cultures while optimizing protocols to improve the similarity of the culture outcomes. This was tested with several clonal cell lines and then in a microfluidic device. The use of this system to analyze clonal performance in small volumes under simulated production conditions should accelerate the scale-up of biologic manufacturing by improving the assessment of clones earlier in the process.

2.2 Materials and Methods

2.2.1 Cell lines and cell culture

Several CHO cell types were used for this study including CHO-S clones D2 and D4, derived from CHO-K1 (ATCC CCL61), secreting human IgG1 (containing a VL Kappa chain) while proportionally expressing EGFP and mCherry intracellularly¹¹⁴. In these cell lines an hMet IIA promoter drives expression of the heavy or light chain of a recombinant IgG while an attenuated internal ribosomal entry site promotes cap-independent translation of EGFP and mCherry reporters; vector information for the cell lines can be found in Sleiman *et al.*¹¹⁴. Clones D2 and D4 were cultured in CD FortiCHO medium (Thermo-Fisher Scientific, Waltham, MA) supplemented with 25 μ M L-methionine sulfoximine (Sigma-Aldrich, St Louis, MO), 20 μ g/mL puromycin (Thermo-Fisher Scientific, Waltham, MA) and 4X anti-clumping agent (Thermo-Fisher Scientific,

Waltham, MA). These cells were passaged at either 1.25×10^5 or 2.5×10^5 cells/mL (for either 4 or 3 days of culture respectively), in 125 mL shake flasks (Dow Corning, Midland, MI), 50 mL shake tubes (TPP, Leeds, UK) or 10 mL round bottomed 24-well DWPs (VWR, Radnor, PA).

An untransfected parental CHO-S line, derived from CHO-K1¹¹⁴, was cultured in CD CHO (Thermo-Fisher Scientific, Waltham, MA) or CD FortiCHO medium that was supplemented with 4 mM L-glutamine (Sigma-Aldrich, St Louis, MO) and 4X anti-clumping agent. These cells were passaged at either 0.75×10^5 or 1.5×10^5 cells/mL (for 4 or 3 days of culture respectively) in 50 mL shake tubes or 500 mL shake flasks (Dow Corning, Midland, MI).

The final cell type used was the CHOm56 clone (derived from CHO-K1SV) that expresses a human IgG1 monoclonal antibody named 4A1 (Pfizer, St. Louis, MO) containing VH Gamma and VL Lambda chains⁵⁷. CHOm56 was maintained in CD CHO medium supplemented with 4 mM L-glutamine and 4X anti-clumping agent. The cells were passaged at either 1.25×10^5 or 2.5×10^5 cells/mL (for 4 or 3 days of culture respectively) in 50 mL shake tubes or 10 mL round bottomed 24-well DWPs.

All CHO cell lines were maintained in orbital shaking incubators (Kuhner, Basel, Switzerland) at 37°C, 5% CO₂, 85% relative humidity and either 125 rpm (125 or 500 mL shake flasks) or 225 rpm (50 mL shake tubes, 24-well DWPs) with a 5 cm shaking diameter. All cell concentrations and viabilities were measured using Trypan Blue (Thermo-Fisher Scientific, Waltham, MA) exclusion in a Cedex automated cell counter (Roche Innovatis, Bielefeld, Germany). Prior to cell counting, culture samples were diluted with an equal amount of 0.25% trypsin/EDTA (Thermo-Fisher Scientific,

Waltham, MA) and topped up to 1 mL with 1X PBS (Thermo-Fisher Scientific, Waltham, MA) followed by incubation for 15 min at 37°C to break up cell aggregates.

2.2.2 Fed-batch culture

CHO-S clone (D2 & D4) fed-batch cultures were inoculated at 2.5×10^5 cells/mL in CD FortiCHO medium supplemented with 25 μ M L-methionine sulfoximine, 20 μ g/mL puromycin and 4X anti-clumping agent. CHO-S parental line fed-batch cultures were inoculated at 0.9×10^5 cells/mL in either CD CHO or CD FortiCHO medium depending on whether medium was harvested for the CHOm56 or CHO-S (D2 & D4) clones, respectively. CHOm56 clone fed-batch cultures were inoculated at 2.5×10^5 cells/mL in CD CHO medium.

Starting volumes for fed-batch cultures were 3 mL (24-well DWP), 25 mL (50 mL tube or 125 mL flask) or 125 mL (500 mL flask). Fed-batch cultures in flasks (125 mL & 500 mL) and tubes (50 mL) were sampled daily starting on day 3 with 0.5 mL taken for automated cell counting (Cedex, Roche Innovatis, Bielefeld, Germany) at a 1:2 dilution with 0.5 mL of 0.25% trypsin/EDTA while another 0.25 mL was taken for supernatant analysis (ELISA, glucose, lactate, osmolarity, etc.). Deep well plate fed-batch cultures were also sampled daily with 0.05 mL taken for automated cell counting (Cedex, Roche Innovatis, Bielefeld, Germany) at a 1:20 dilution with 0.05 mL of 0.25% trypsin/EDTA and 0.9 mL of 1X PBS while another 0.25 mL was taken for supernatant analysis (ELISA, glucose, lactate, osmolarity, etc.). Starting on day 3, cultures were fed daily (after sampling) with CD EfficientFeed A (Feed A) or CD EfficientFeed C (Feed C) AGT (adjusted to a pH of 7.02) (Thermo-Fisher Scientific, Waltham, MA) at a rate of 6.7% of the initial culture volume. For pH controlled cultures, 6% NaHCO₃ was added

when the pH dropped below 6.8. Fed-batch cultures were run for up to 14 days (minimum 8 days) until cell viabilities dropped below 70%. 3 mL scale-down fed-batch cultures in 24-well DWPs were run using the Duetz Microflask system^{90,290}.

To adjust for dilution caused by cell removal and feed addition, the following formulae were used to calculate the adjusted viable cell density (VCD_{adj}) in all fed-batch cultures:

$$VCD_{Adj} = VCD_x \times DF_x \quad (2.1)$$

where VCD_x is the viable cell density on day x and DF_x is the cumulative dilution factor defined as:

$$DF_x = DF_{x-1} \times \left(1 + \frac{V_{feed}}{V_x}\right) \quad (2.2)$$

where DF_{x-1} , is the previous day's dilution factor, V_{feed} is the feed volume and V_x is the volume on day x expressed as:

$$V_x = V_{x-1} - V_{evap} - V_{sample} + V_{feed} \quad (2.3)$$

where V_{x-1} , V_{evap} , and V_{sample} are the volume on day $x-1$, the evaporated volume and the sampled volume respectively.

2.2.2 Conditioned medium harvesting and re-suspension

Conditioned medium (CM) was harvested daily (starting on day 3) from parental CHO cell fed-batch cultures in 500 mL flasks and then re-suspended in 3 mL DWP cultures. After sampling and feeding the parental flask, the CM (3 mL x number of DWP wells + 5 mL) was harvested and transferred into 50 mL centrifuge tubes (Thermo-Fisher Scientific, Waltham, MA). Harvested medium was then spun down at 1000 rpm for 7 min (to remove cells) in a Beckman GS-6 series centrifuge (Beckman Coulter, Brea, CA)

followed by supernatant removal and filtration through a 0.22 μm filter (Dow Corning, Midland, MI). CM was kept at 4°C until later use. As relatively large volumes were removed from the 500 mL flask cultures, feed volumes were adjusted down to the new decreased volume. Thus for parental cultures where media harvesting occurred, the adjusted feed volume on day x ($V_{feed,Adj}$) can be described by:

$$V_{feed,Adj} = 0.067 \times (V_0 - \sum_i^x V_{h,i}) \quad (2.4)$$

where V_0 is the initial culture volume and V_h is the volume of CM harvested daily.

Following harvesting and storage, 24-well DWP cultures were re-suspended daily in CM starting on day 3. All DWP cultures were inoculated at 3×10^5 cells/mL with a starting volume of 3 mL/well. In the case that less than 24 wells per plate were used for cell culture, the remaining wells were filled with CD FortiCHO to buffer against evaporation loss. Beginning on day 3, DWPs were sampled daily with 0.05 mL taken for automated cell counting (Cedex, Roche Innovatis, Bielefeld, Germany) at a 1:20 dilution with 0.05 mL of 0.25% trypsin/EDTA and 0.9 mL of 1X PBS. Next, DWPs were spun down at 1000 rpm for 7 min (to remove cells) in a Beckman GS-6 series centrifuge, followed by either automated or manual supernatant removal for downstream analysis (ELISA, glucose, lactate, osmolarity, etc.). Finally cell pellets in each well were re-suspended in 3 mL of CM from the corresponding parental flask cell concentration. Control batch and fed-batch wells in DWPs on the same plate were re-suspended in their original medium to ensure that centrifugation was not responsible for differences between culture methods.

2.2.3 Cell culture and assay automation

A Microlab NIMBUS instrument (Hamilton Robotics, Reno, NV) equipped with a 1 mL 96-CORE pipetting head and 4 independent variable span 1 mL channels was set up for automated liquid handling. To increase the pipetting precision (and thus experimental reproducibility) all aspiration, dispensing, mixing and trituration steps were automated with fixed volumes and pipetting speeds. All steps were programmed using custom algorithms generated through Hamilton Method Editor (**Appendix A**).

2.2.4 ELISA

Antibody titers for CHO-S clones were measured according to previously reported ELISA methodologies¹¹⁴. Supernatant samples were collected by spinning down culture samples for 3 min at 1000 rpm in a Spectrafuge 16M microcentrifuge (Labnet International, Edison, NJ); the resulting supernatant was collected and stored at -20°C prior to analysis. Nunc-Immuno 96-well Maxisorb plates (Sigma-Aldrich, St Louis, MO) were coated with a goat anti-human IgG Fc γ -specific primary antibody (Jackson ImmunoResearch, Baltimore, MD) and incubated overnight at 4°C. The next day, plates were washed 3 times with wash buffer (1X PBS, 0.1% Tween-20) followed by blocking with a blocking solution (1X PBS, 0.02% Tween-20, 0.5% skim milk) for 1 h at room temperature prior sample loading. Measurements were standardized to IgG1 from human serum (Sigma-Aldrich, St Louis, MO) loaded at concentrations ranging from 2.5 ng/mL to 10 μ g/mL. Once all standards and samples were loaded, wells were incubated with a sheep anti-kappa light chain HRP-conjugated secondary antibody (The Binding Site, Birmingham, UK). Bound antibodies were quantified by incubating with 3,3',5,5'-

Tetramethylbenzidine substrate (Sigma-Aldrich, St Louis, MO) for 8 min at room temperature in the dark. The reaction was terminated with 2 M H₂SO₄ followed by plate reading at 450 nm using a microplate reader. Titer measurements were adjusted for dilution caused by feed addition by multiplying the cumulative dilution factor by the measured titer.

2.2.5 Microfluidic cell culture

Microfluidic cell culture arrays were fabricated according to Lecault *et al.* protocols and contained 4 arrays of 2048 chambers for a total of 8192 microbioreactors per device; all microfluidic platforms also contained an iso-osmotic bath to buffer against osmolarity changes due to evaporation during culture²⁴¹. Protocols for fabricating the microfluidic cell culture platforms can be found in **Appendix B**.

Prior to each experiment, a newly fabricated, sterile device was mounted onto an Axiovert 200 inverted microscope (Carl Zeiss, Oberkochen, Germany) then dead-end filled with filter-sterilized 1% FBS and incubated overnight at 37°C in humidified 5% CO₂ to prime the channels and chambers for cell culture. The osmotic bath was then filled with CD FortiCHO medium supplemented with 25 µM L-methionine sulfoximine, 20 µg/mL puromycin and 4X anti-clumping agent to equilibrate the osmotic strength throughout the device. The next day, a sterile solution of fresh CD FortiCHO medium supplemented with 25 µM L-methionine sulfoximine, 20 µg/mL puromycin and 4X anti-clumping agent was incubated in the culture chambers for 45 min at room temperature. A single-cell suspension (at 10⁶ cells/mL) of CHO-S D2 clones¹¹⁴ was then stochastically loaded into the device. Once microscopic monitoring of the microfluidic array indicated that it was filled, the cells were allowed to settle for 5 – 10 min (to prevent wash out

during subsequent flushing steps). The chambers were then flushed again for 7 – 10 min with fresh CD FortiCHO medium supplemented with 25 μ M L-methionine sulfoximine, 20 μ g/mL puromycin and 4X anti-clumping agent to remove any leftover cells in the channels. This process was repeated as many times as necessary until the desired number of single clones was obtained. Devices were then incubated in a custom designed incubator (described in Chapter 4) at 37°C in humidified 5% CO₂ overnight next to several 22 mm dishes filled with water to maintain humidity. Cell growth was subsequently monitored for 96 – 192 h depending on when chambers became confluent. During this period, the entire system (including the Axiovert 200 inverted microscope) was contained in a custom environmental chamber heated to 37°C and supplied with humidified 5% CO₂ at a rate of 46 mL/min to maintain this CO₂ level in the device. Custom Labview (National Instruments, Austin, TX, USA) software was used to image the cells in each chamber with a 10 \times objective every 24 h using differential interference contrast (DIC) microscopy. The medium in each chamber was replaced daily with either fresh CD FortiCHO medium supplemented with 25 μ M L-methionine sulfoximine, 20 μ g/mL puromycin and 4X anti-clumping agent or parental CHO cell line CM corresponding to the day of culture harvested under pressure driven flow.

2.2.6 Statistical analysis

Pooled two-sample t-tests were used to identify whether maximum viable cell densities, specific productivities and antibody titers were significantly different from positive (25 mL fed-batch) and negative (batch) controls. Bonferroni's method was used to ensure an overall confidence of >95% when multiple t-tests were performed. This resulted in each test being performed with $(100 \times (1 - 0.05/n))$ %-confidence where n is

the number of comparisons made, implying that p must be less than $0.05/n$ for a response to be deemed significantly different from a control with 95% confidence²⁹¹.

2.3 Results

2.3.1 Feed screening and pH control

Prior to simulating fed-batch conditions with CM, feed strategies were explored in an attempt to improve CHO cell fed-batch performance and maximize harvested CM quality. The CHO-S D2 clone was evaluated under fed-batch conditions using Feed A or Feed C. With Feed C, the need for pH control was also tested by comparing the addition of NaHCO_3 when the pH dropped below 6.8 to non-pH controlled cultures. The viable cell densities (VCDs) and viabilities for all feed conditions were analyzed over 13 days of fed-batch culture and compared to batch culture (Figure 2.1A and B). No significant difference ($p \sim 0.4$) was observed in the peak viable cell densities achieved by the fed-batch cultures at $\sim 20 \times 10^6$ viable cells/mL, at double the peak batch culture cell concentration. However, the viability of the Feed A cultures dropped significantly ($p = 0.004$) after day 7 when compared to the Feed C cultures. After day 7 the Feed C cultures (1.85 pg/cell/day) maintained a higher specific productivity than the Feed A culture (1.58 pg/cell/day) (Figure 2.1C). The human IgG1 titers at the end of the Feed C cultures were 0.41 g/L and 0.39 g/L with and without pH control respectively, and both were higher than the Feed A titers (0.35 g/L) and significantly higher than the batch titers (0.12 g/L, $p = 0.0001$). In the Feed A cultures the pH dropped below 6.8 on day 5 and did not recover, while the Feed C cultures without pH control maintained their pH above 6.8 (Figure 2.1D). The controlled pH Feed C cultures dropped below 6.8 once, only requiring base

addition on day 4. Since the Feed C cultures had greater pH stability and high specific productivity, the Feed C without pH control process was chosen for the subsequent fed-batch studies.

2.3.2 Automating conditioned medium re-suspension

To use CM in DWP fed-batch cultures the cells needed to be centrifuged and re-suspended. Preliminary experiments on 3 mL DWP batch cultures demonstrated no significant difference in the peak VCD between uncentrifuged (4.9×10^6 cells/mL) and daily-centrifuged (4.1×10^6 cells/mL) DWPs ($p = 0.5$) (Figure 2.2A). However, over days 6 – 8 the centrifuged plates demonstrated lower VCDs suggesting that there may be some acceptable cell losses due to cumulative re-suspension over 7+ days of culture. Additionally, the 25 mL shake flask batch control reached a higher maximum VCD of 8×10^6 cells/mL) than the 3 mL batch cultures, indicating differences between these culture scales.

The next experiments proceeded to determine whether re-suspended CM DWP cultures would match the performance of 3 mL DWP and 25 mL shake flask fed-batch cultures. When compared to 25 mL shake flask fed-batch cultures, viable cell densities for manually re-suspended CM DWP cultures were significantly lower ($p = 0.016$) but not significantly different from the 3 mL DWP fed-batch ($p = 0.85$) or 25 mL batch ($p = 0.51$) cultures. The 25 mL fed-batch cultures reached a maximum VCD of $\sim 18 \times 10^6$ cells/mL whereas the other cultures had significantly lower ($p = 0.016$) maxima at $7 - 8 \times 10^6$ cells/mL (Figure 2.2B). Bonferroni's method was used to ensure an overall confidence of >95% for the 3 simultaneous t-tests being performed (resulting in each test requiring 98.33% confidence, or $p < 0.017$ for a response to be deemed significant)²⁹¹.

The viabilities were similar, with the exception of the 25 mL batch culture that had a greater viability drop on day 8 (Figure 2.2C) and all specific productivities were similar (Figure 2.2D). The observed difference between 3 mL and 25 mL fed-batch cell concentrations revealed the need for optimization at the DWP scale.

In an effort to improve 3 mL DWP culture performance plate sampling, CM harvesting and re-suspension was automated using robotic fluid handling (Figure 2.3). Using 4 pipettes at one time, 4 DWP wells were handled simultaneously. This enabled more rapid as well as more accurate and reproducible sampling and re-suspension, through programmed aspiration, dispensing, mixing and trituration. After sampling, the DWPs were centrifuged followed by removal of 85% of the initial volume and re-suspension in CM. In addition, the fed-batch cultures were reduced to 8 days from 14 to double the experimental throughput (such that they could be performed weekly rather than biweekly).

2.3.3 Effect of cell concentration on conditioned medium re-suspension

The automation of DWP sampling, feeding and re-suspension resulted in the automated DWP fed-batch cultures achieving a peak VCD of 16×10^6 cell/mL (Figure 2.4A) whereas the initial manual protocol only achieved 8×10^6 cell/mL (Figure 2.2B). However, even after fed-batch culture optimization the CHO-S D2 clone cultures re-suspended in CM reached less than half of the maximum cell concentrations compared to the 3 mL DWP ($p = 0.01$) and 25 mL fed-batch ($p = 0.05$) cultures.

It was realized that the parental cell line medium conditioning was more rapid because the parental CHO cell line ($\mu_{\max} = 0.033 \text{ h}^{-1}$) grew at a higher rate than the CHO-S D2 clone ($\mu_{\max} = 0.025 \text{ h}^{-1}$) (Figure 2.4A and B). Thus, the protocol was changed to re-

suspend the clonal cells in CM from the parental culture at the same cell concentration rather than the same day of culture. Using this method, the DWP cultures re-suspended in CM had cell growth profiles (Figure 2.4B) and viabilities (Figure 2.4C and D) that much more closely matched the 25 mL fed-batch, and these cultures reached a maximum of 20×10^6 viable cells/mL. This was significantly greater than the 3 mL DWP fed-batch culture (14×10^6 viable cells/mL, $p = 0.003$) and the 3 mL batch control (5×10^6 viable cells/mL, $p = 0.0004$). Again, to ensure an overall confidence of >95% for the multiple t-tests being performed, Bonferroni's method was used (resulting in each test requiring 98.75% confidence across 4 tests, or $p < 0.013$)²⁹¹. This result suggests that the CM may contain factors that promote cell growth as the CM re-suspended CHO-S D2 clones were observed to reach peak VCD at the same time as the parental line when cell concentrations were matched (Figure 2.4B). However, exposing clones to CM from high VCD cultures too early during culture could also have an inhibitory effect on growth (Figure 2.4A), which could be due to the buildup of waste products in the medium. Consequently, when re-suspending clones in CM the cell concentrations from both the harvested CM and the re-suspended clone should be monitored closely to ensure that clones achieve a high VCD and maximize specific productivity over the course of the culture.

2.3.4 Conditioned medium re-suspension applied to other clones and cell lines

This CM cell concentration matching method was then tested on a lower productivity CHO-S D4 clone and produced the same overall result (Figure 2.5A and C) as did a biological replicate for the D2 clone (Figure 2.5B and C). The 3 mL CM re-

suspended CHO-S D4 cell culture reached a maximum VCD of $\sim 18 \times 10^6$ cells/mL, not significantly different from the 25 mL CHO-S D4 and 125 mL parental fed-batches ($\sim 20 \times 10^6$ cells/mL, $p = 0.1$) while significantly outperforming the 3 mL batch control (5×10^6 cells/mL, $p = 0.002$) but not the 3 mL DWP fed-batch (12×10^6 cells/mL, $p = 0.03$). In this case, each test again required 98.75% confidence across 4 tests, or $p < 0.013$ to achieve an overall confidence of $>95\%$ ²⁹¹. Specific productivities were analyzed for both clones to determine if the CM re-suspension protocol could distinguish their IgG productivities (Figure 2.5D). Specific productivities for all CHO-S D2 cell cultures (3 mL CM re-suspended, 3 mL batch, 3 mL fed-batch and 25 mL fed-batch) varied between 1.5 and 2.5 pg/cell/day. The CHO-S D4 cell specific productivities for all cultures varied from 0.4 to 1 pg/cell/day (differences between CHO-S D4 cultures were not significant), which was significantly lower ($p = 3 \times 10^{-12}$) than the range for the CHO-S D2 clone (in FortiCHO based medium). The reproducibility of this method was also demonstrated further on the CHO-S D2 clone across 3 independently replicated experiments (Figure 2.6A and B).

To test a different medium and cell line, the CM re-suspension technique was tested with CD CHO medium and a CHO K1SV derived cell line, CHOm56 (Figure 2.6C and D). As in previous experiments, the peak VCD for the 3 mL CM re-suspended CHOm56 clone ($\sim 18 \times 10^6$ cells/mL) significantly outperformed the 3 mL DWP fed-batch and batch controls ($\sim 10 \times 10^6$ cells/mL, $p = 0.004$ and $\sim 7 \times 10^6$ cells/mL, $p = 0.002$ respectively) with $p < 0.013$ required to achieve an overall confidence of $>95\%$ across 4 tests²⁹¹. However, the 3 mL CM re-suspended CHOm56 clone growth even somewhat outperformed the 25 mL CHOm56 and 125 mL parental fed-batch flasks (with peak

VCDs of $\sim 14 \times 10^6$ cells/mL and $\sim 15 \times 10^6$ cells/mL respectively) but the differences were not significant ($p = 0.06$ & $p = 0.08$ respectively). Overall, the ability of this technique to simulate large-scale (25+ mL) fed-batch conditions across multiple cell lines and media types suggests a robust protocol that could be widely applicable.

2.3.5 Microfluidic conditioned medium perfusion

Though CM re-suspension has been demonstrated at the 3 mL scale, an ideal system would first screen clones at the single cell level in CM followed by scale up to DWPs. However, single cell culture can be challenging due to poor growth observed at low seeding density, which is further exacerbated by high evaporation rates in small volumes. Microfluidic cell culture offers the advantage of more rapid product accumulation and high cell seeding density through the use of nanoliter sized chambers. Thus, to demonstrate its applicability to clone selection and single cell culture, the CM re-suspension technique was tested in microfluidic perfusion cultures (Figure 2.7). However, it should be recognized that microfluidic cell culture systems are static and normally fixed in volume so that simple addition of feeds or CM re-suspension during single cell culture are not feasible. These systems are ideally suited for perfusion culture such that CM could be introduced periodically via perfusion to simulate a larger scale fed-batch. For this procedure, PDMS microfluidic devices were fabricated according to Lecault *et al.* and contained 4 arrays of 2048 culture chambers, each 4 nL in volume ($160 \mu\text{m} \times 160 \mu\text{m} \times 100 \mu\text{m}$)²⁴¹. An “iso-osmotic bath” was also included above the individual culture chambers to minimize evaporation and enable robust culturing of CHO clones^{224,241,250}. Culture chambers were designed with an inverted geometry so that the flow velocity was minimal at the bottom of the chambers; this allowed for near complete

medium exchange without perturbing the cells²⁴¹. Environmental control was achieved using a custom heated enclosure (described in Chapter 4).

In this procedure CHO-S D2 clones were loaded onto a microfluidic cell culture device and either fresh FortiCHO or CM from a 125 mL parental CHO cell line fed-batch culture (as performed in Figure 2.5 and Figure 2.6) was perfused through the device daily. A batch culture was set up beside the microfluidic chip to provide a control. The cells cultured with the CM perfusion technique significantly outgrew both the fresh medium perfusion condition ($p = 0.01$) as well as the batch plate control ($p = 0.01$) over several days of culture (Figure 2.7A and B). A comparison to batch plate controls was used over these timescales since both fed-batch and CM re-suspended cultures are not fed/re-suspended until day 3. Additionally, phase contrast images taken of the microfluidic cultures also showed a noticeable difference between the fresh medium and CM conditions, with the former undergoing more apoptosis (Figure 2.7C and D). This result demonstrates that our CM re-suspension technique can readily be scaled down and adapted to culture clones in perfusion conditions that mimic a large-scale fed-batch environment. At the end of Chapter 3 this technique will be combined with a microfluidic secretion assay in order to furthermore make clonal productivity assessments under simulated bioreactor conditions.

2.4 Discussion

In summary, the feasibility of a conditioned medium re-suspension/perfusion technique to simulate large-scale production at the 3 mL DWP and microfluidic culture scales was demonstrated. By using CM harvested to equal the cell concentration of a parental fed-batch, the CM perfusion and re-suspension cultures matched the VCDs and

specific productivities of larger cultures (25 and 125 mL). DWP CM re-suspension was demonstrated to be feasible across multiple clones (CHO-S D2 & D4), cell lines (CHO-S & CHOm) and media types (CD CHO and FortiCHO). When applied to a microfluidic system, the perfused CM growth rates were greater than both static microfluidic and batch controls. Thus, methods for simulated fed-batch of prospective candidate clones or transfected pools have been developed. The coupling of microfluidic CM perfusion with single cell secretion assays (Chapter 3) will allow for the screening of hundreds to thousands of individual clones under simulated fed-batch conditions, thereby vastly accelerating the window to discover high-producing clones that are of manufacturing relevance. Beyond CHO cells, this capability might also be useful for the analyses of and selection from other populations of cells where simulated larger-scale medium screening conditions are required.

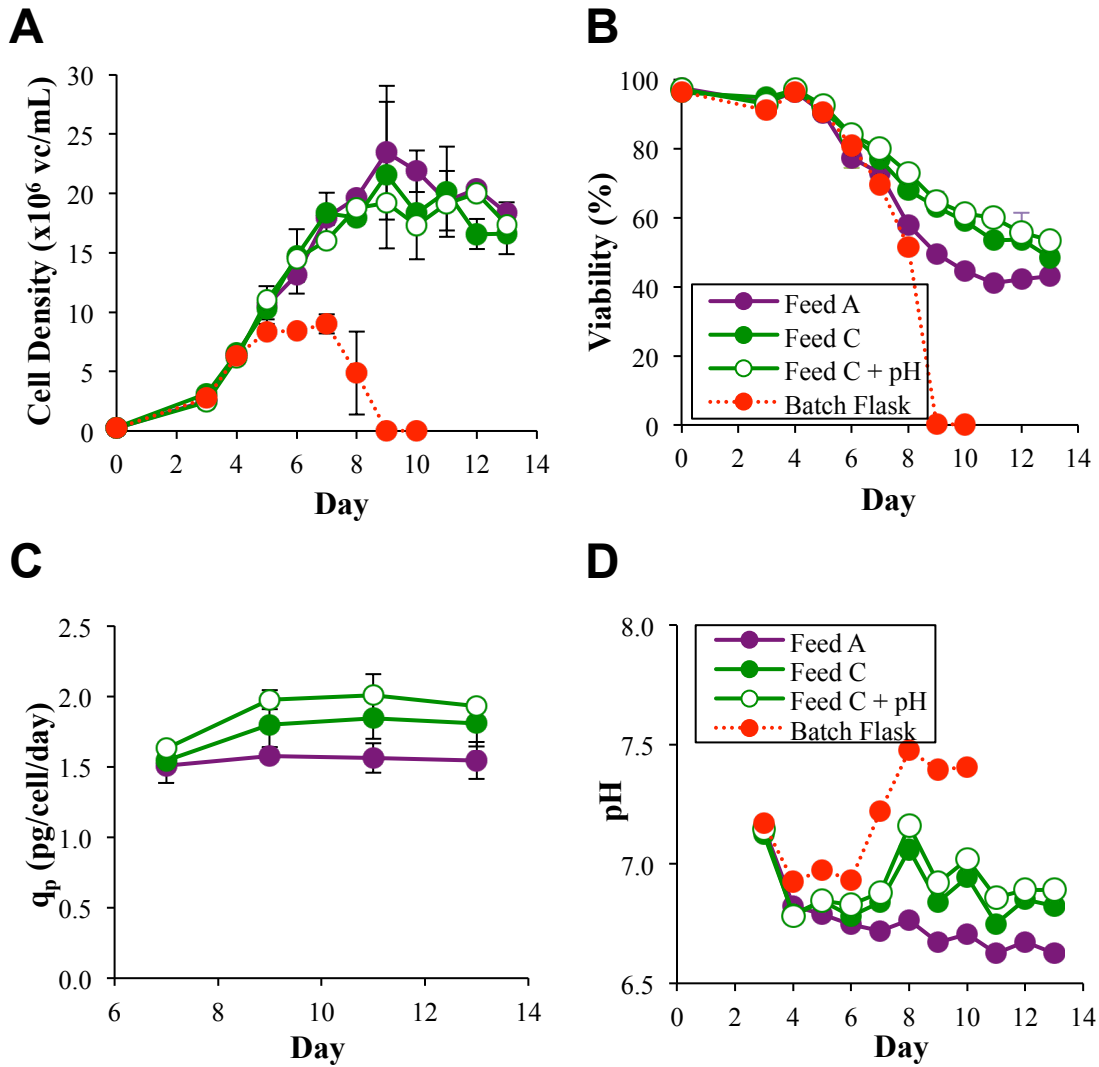


Figure 2.1 CHO-S D2 performance comparison for different feed strategies

(A) VCDs for CHO-S D2 clones in 25 mL flask cultures over a 14 day fed-batch experiment. (B) Viabilities for all conditions (Feed A, Feed C, Feed C with pH control and batch) over 14 days of culture. (C) 48 h specific productivities for the 3 different feed strategies (Feed A, Feed C and Feed C with pH control). (D) pH profiles for all conditions (Feed A, Feed C, Feed C with pH control and batch) over 13 days of culture.

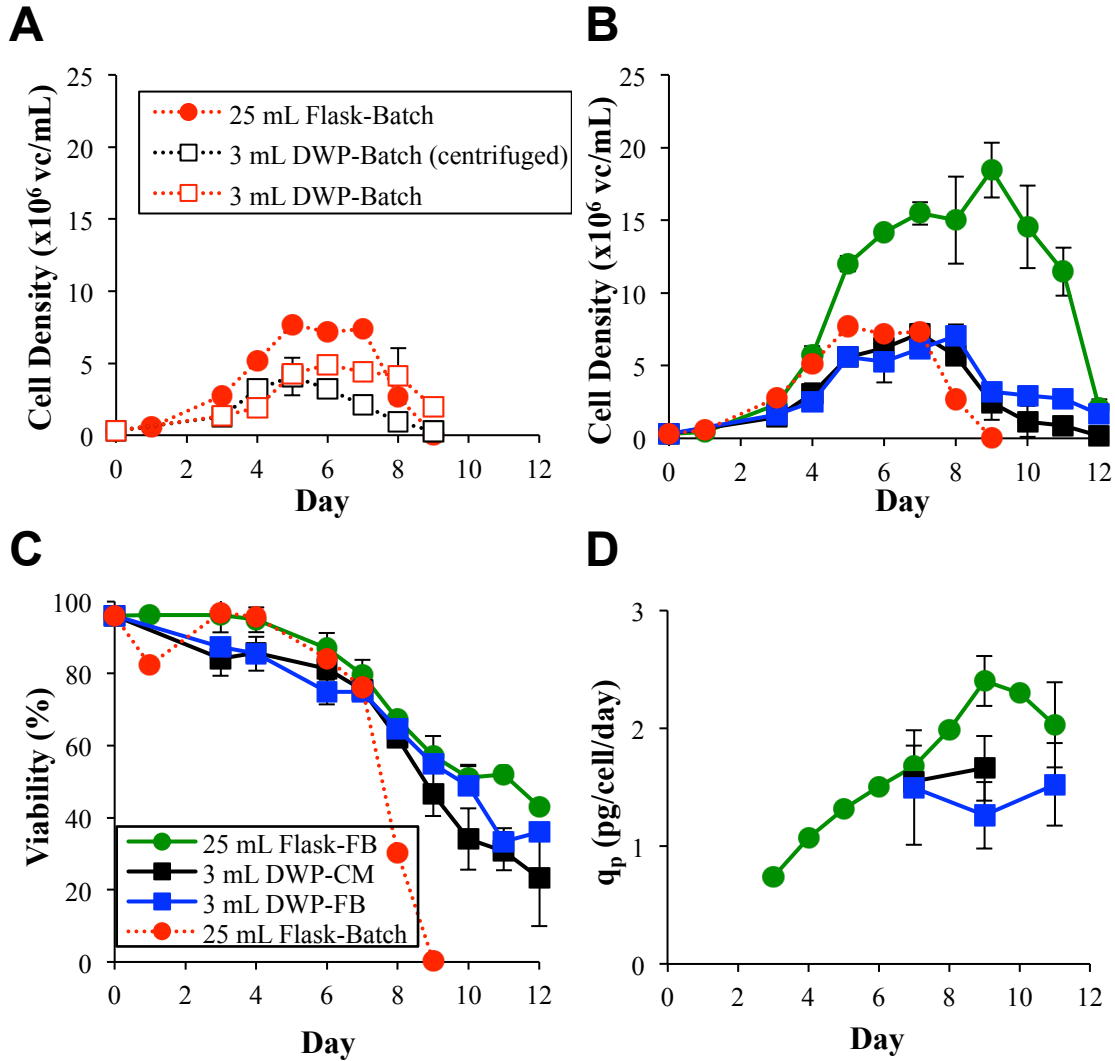


Figure 2.2 3 mL deep well plate and 25 mL shake flask CHO-S D2 performance comparison

(A) VCD profiles for centrifuged and uncentrifuged CHO-S D2 clone batch controls. (B) VCDs for all conditions (CM re-suspension, FB and batch) for 12 days of culture. (C) Viabilities for all conditions (CM re-suspension, FB and batch) over 12 days of culture. (D) 24 h specific productivities for 3 mL CM re-suspension cultures compared to 3 and 25 mL FB cultures.

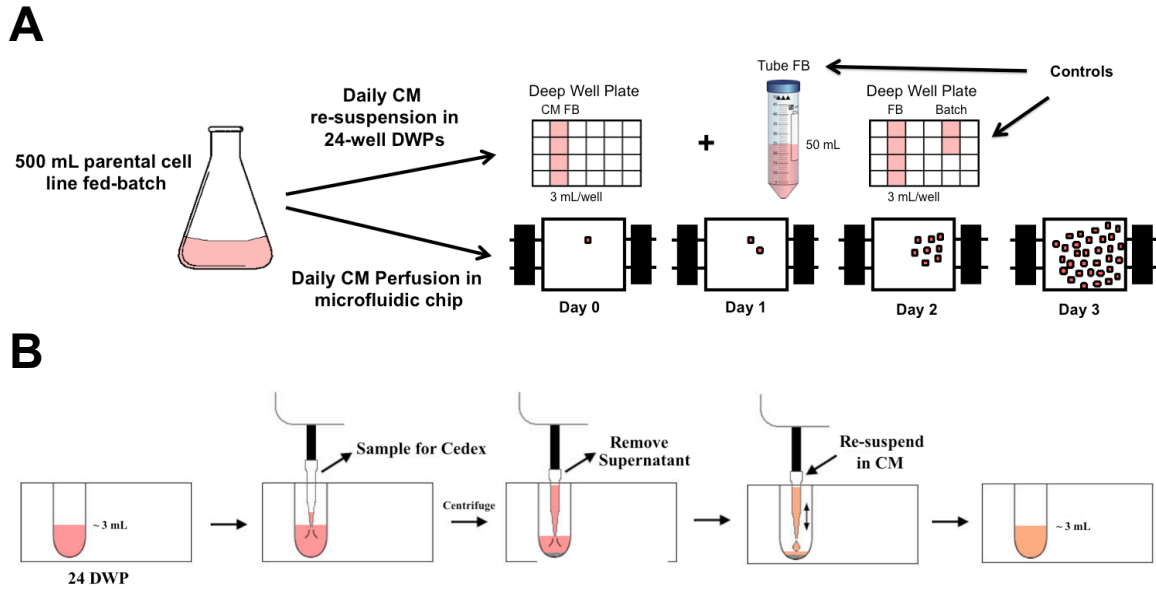


Figure 2.3 Schematic for automated conditioned medium perfusion/re-suspension

(A) Schematic of CM sampling and perfusion/re-suspension process. Daily samples are first retrieved from a parental fed-batch in a 500 mL flask. For microfluidic cultures, nL volume wells are perfused daily using the harvested CM. In the case of DWPs, 3 mL cultures are pelleted and re-suspended in harvested CM according to the automated protocol in (B). (B) Schematic for robotic sampling and cell pellet re-suspension of 3 mL DWP cultures using Hamilton NIMBUS instrument.

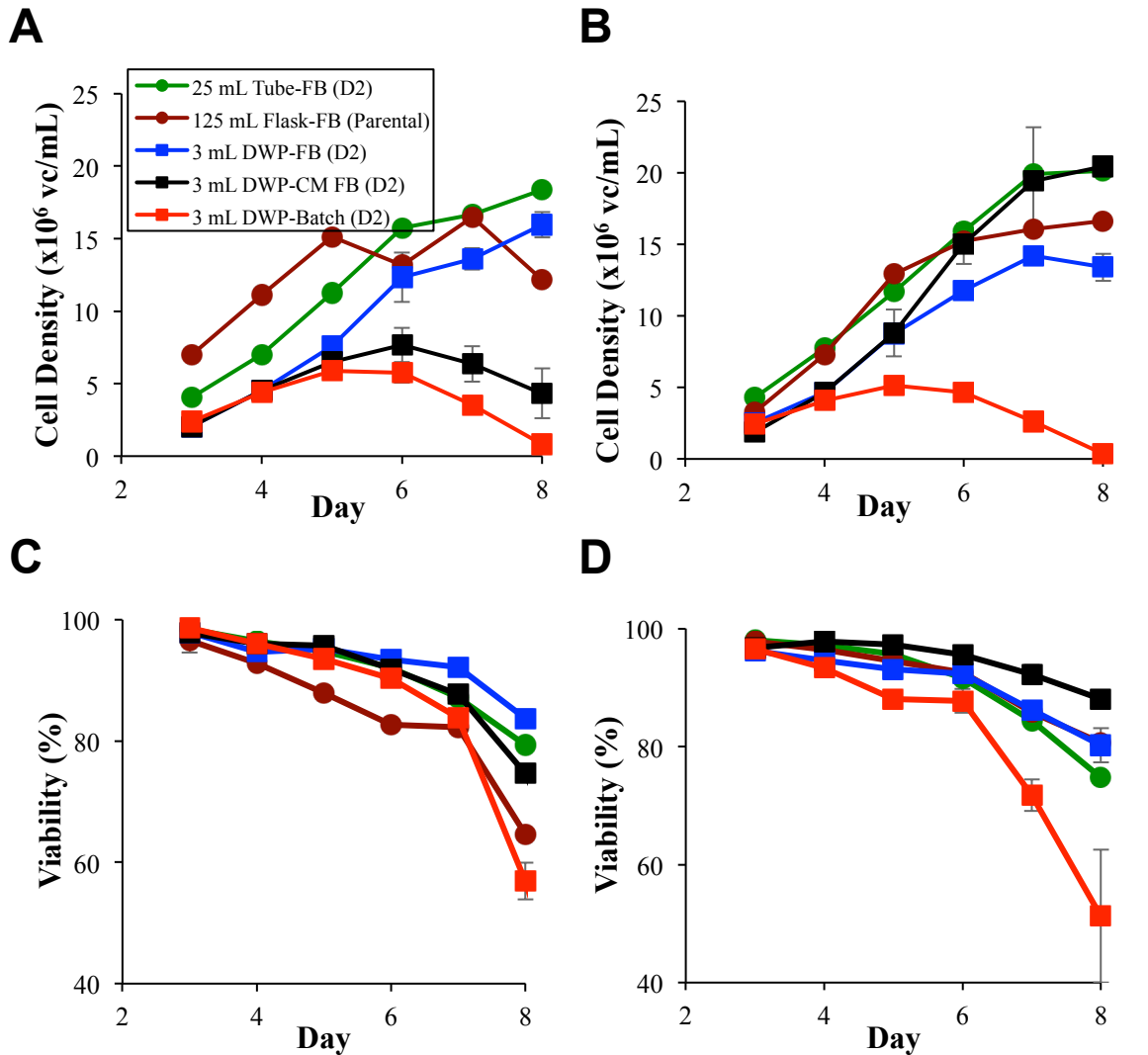


Figure 2.4 Concentration matching for conditioned medium re-suspension

method

(A) VCD profiles for CHO-S D2 clones with CM cultures re-suspended in harvested CM from the same day of culture. (B) VCD profiles for CHO-S D2 clones with CM cultures re-suspended in harvested CM with a matching cell concentration. (C) Viabilities for all conditions (CM re-suspension, FB and batch) over 8 days of culture for the matching day of culture experiment. (D) Viabilities for all cultures (CM re-suspension, FB and batch) over 8 days of culture for the matching cell concentration experiment.

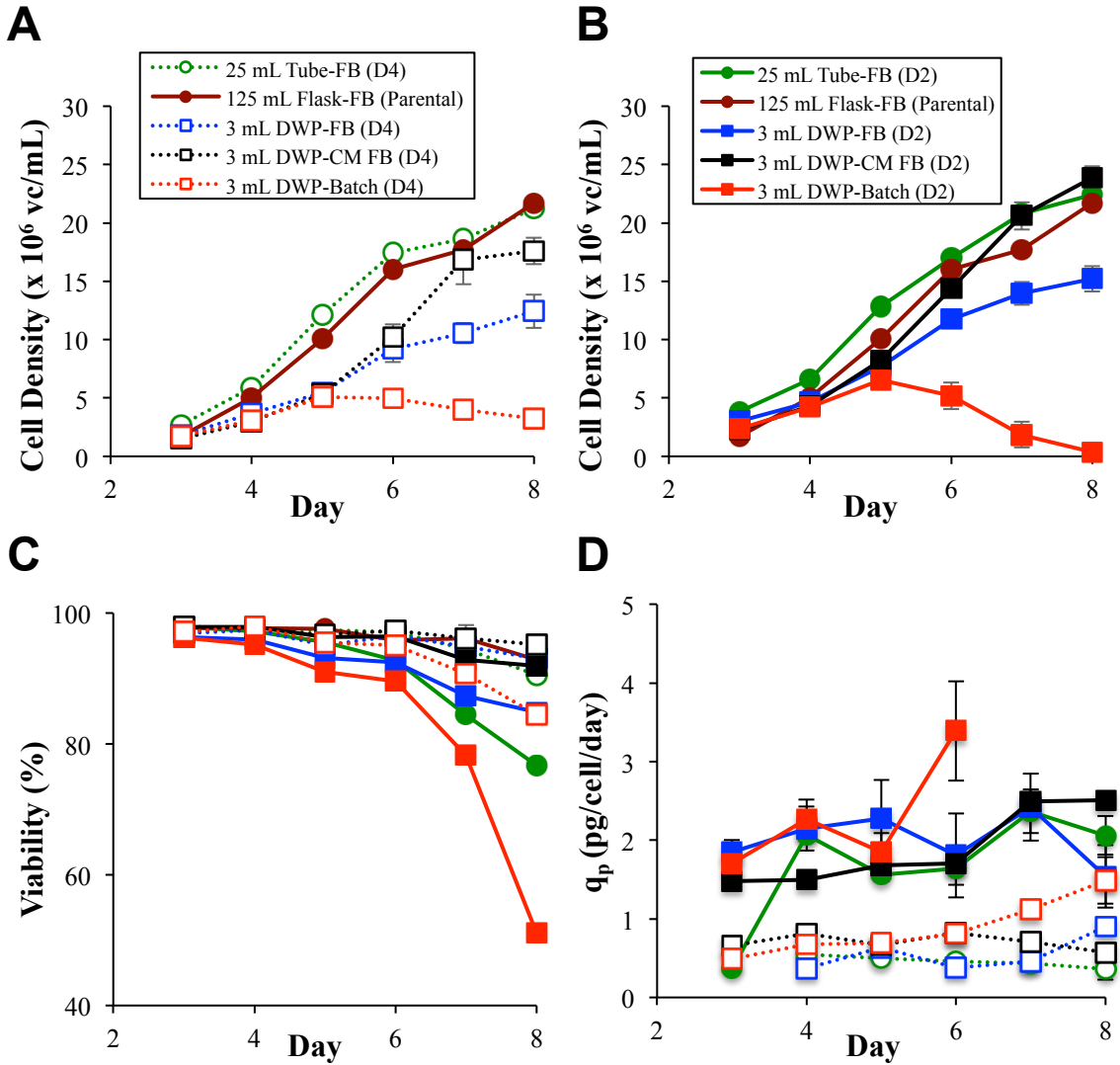


Figure 2.5 Conditioned medium re-suspension performance for multiple clones

(A) VCD profiles for CHO-S D4 clones over an 8-day fed-batch experiment. (B) Independently replicated VCD profiles for CHO-S D2 clones over an 8-day fed-batch experiment. (C) Viabilities for all clones (D2 & D4) over 8 days of culture. (D) Specific productivities for all clones (D2 & D4) over 8 days of culture.

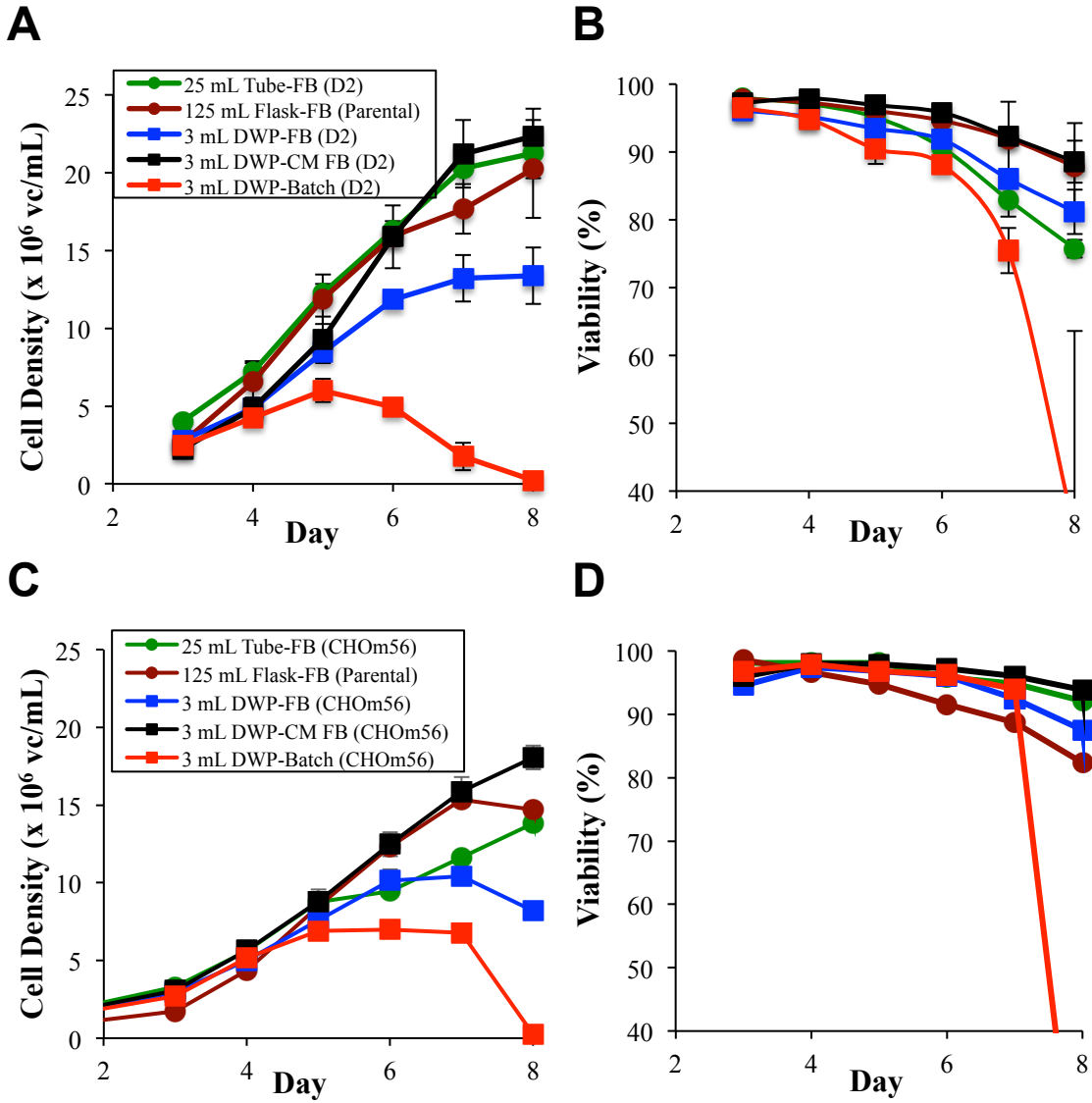


Figure 2.6 Conditioned medium re-suspension reproducibility for CHO-S D2 and applicability to CHOM56 cell line.

(A) VCD profiles for CHO-S D2 clones for 8 days of culture across 3 independently replicated experiments. (B) Viabilities for CHO-S D2 clones for 8 days of culture across 3 independently replicated experiments. (C) VCD profiles for CHOM56 clones over an 8-day fed-batch experiment. (D) Viabilities for CHOM56 clones over 8 days of culture.

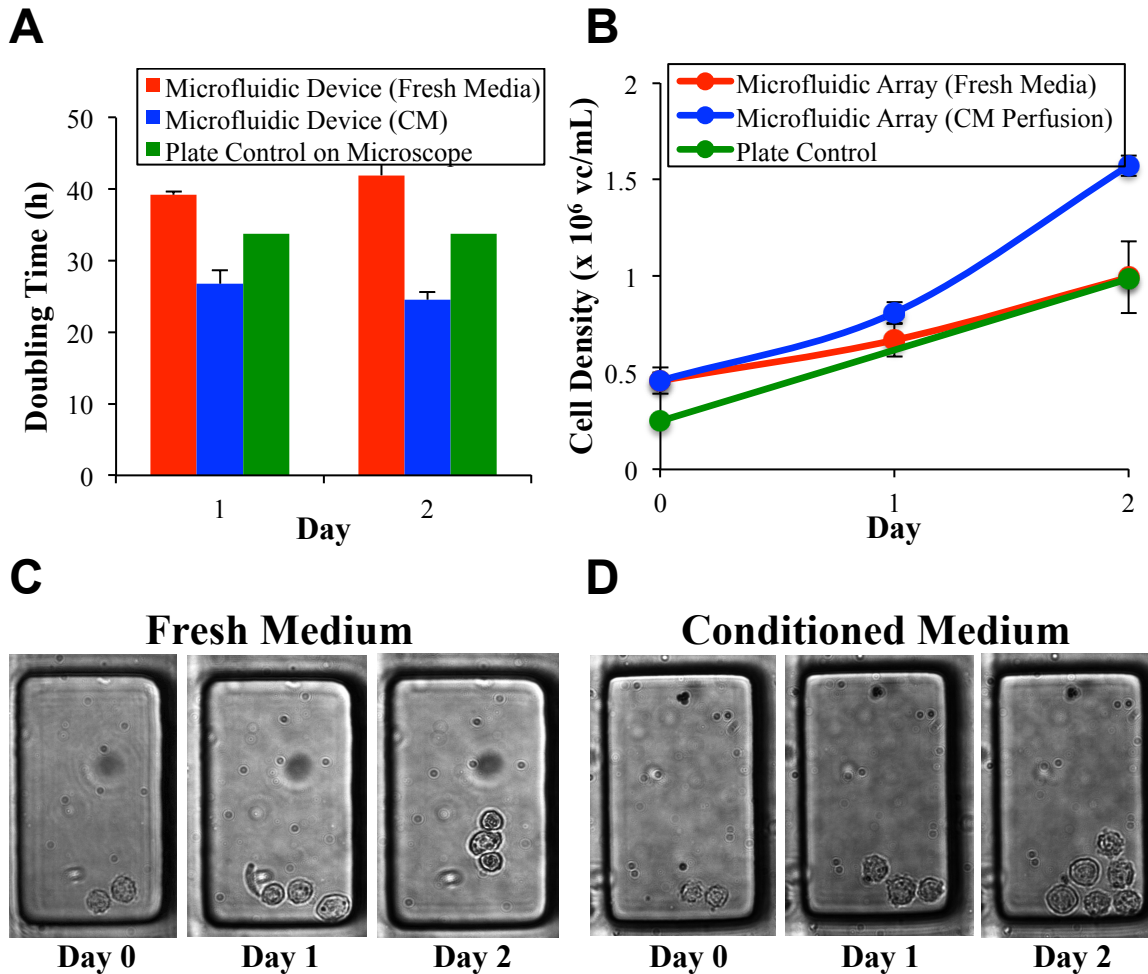


Figure 2.7 Conditioned medium perfusion in microfluidic CHO-S cultures.

(A) Doubling times for microfluidic cultures perfused in either conditioned medium or fresh medium compared to batch plate controls. (B) Average VCD profiles across all chambers for CHO-S D2 microfluidic cultures perfused in either conditioned medium or fresh medium compared to batch plate controls. (C) Phase contrast images of typical CHO-S D2 clones grown in daily fresh medium perfusion conditions. (D) Phase contrast images of typical CHO-S D2 clones grown in daily conditioned medium perfusion conditions.

Chapter 3 A Dynamic Microfluidic Bead Assay to Detect IgG in nL Volumes

3.1 Introduction

The use of Chinese Hamster Ovary (CHO) cells is of fundamental importance to the production of recombinant therapeutics due to their ability to generate high titers of molecules that contain complex post-translational modifications as well as for reasons of bioprocess convention and regulatory precedent^{20,21}. During scale-up, clones are selected for model characteristics such as high growth rate, stability, specific productivity, and product quality⁵³. However, the scale up of CHO lines from transfected pools commonly requires the screening of hundreds to thousands of clones and is nontrivial in nature⁵². Some of the challenges associated with clonal screening include limited assay sensitivity⁷⁴, evaporation from small volumes⁷⁵, and conditioning effects at limiting dilutions^{76,77}. Thus, when clones are screened as early as possible during scale-up, they are not always evaluated in the most effective manner and many clones drop off in performance as they progress to larger culture scales^{71,72}.

The drop off in clonal productivity between culture scales can be traced to a variety of microenvironmental causes as well as innate genetic or epigenetic changes⁷¹. For example, simply changing from batch to fed-batch culture has been shown to significantly affect productivity⁶². Initial clonal screening conditions at limiting dilution in static batch medium differ greatly from the final fed-batch bioreactor environment⁵⁹. However, even in identical medium conditions, CHO pools are very heterogeneous due to

the randomness of transgene integration^{292,293,294}. Intrinsic causes of decreased CHO performance include changes in transgene copy number^{10,65,67} and epigenetic silencing^{295,296,297}. Moreover, stochastic fluctuations of a fully functional and unsilenced transgene have been known to result in dynamic protein expression^{105,111,113}. Specifically, temporary states of high and low antibody expression have been observed to relax back to the population mean over time¹⁰⁵. Thus if a technology is to be able to precisely quantify secretion at the clonal level it should be sensitive enough to detect dynamic fluctuations while doing so in a microenvironment reflective of large-scale culture as clones with reduced protein expression will have a selective advantage.

Another obstacle to successful early clonal performance evaluations is the imprecision of single-cell measurements. Traditionally, the first productivity measurement during scale-up is performed a few weeks post-transfection via enzyme-linked immunosorbent spot (ELISPOT) assay; prior to this point there are not enough cells to generate a detectable level of antibody by conventional enzyme-linked immunosorbent assay (ELISA) methods^{71,74,115}. Semi-solid medium techniques have recently increased the throughput of clone selection by making use of cell-surface affinity matrices; clones are ranked based on the level of secreted recombinant product that is captured by the matrix on the cell surface^{58,120,121,122}. This technique can be combined with automated systems such as Clonepix FL to replace limiting dilution cloning and enrich for high producers but issues of fluorescence correlation to later productivity measurements still remain^{59,123,124}. These measurements are also performed in a low concentration static environment that differs greatly from the medium conditions they will experience later during scale-up⁵³. In any case, highly sensitive technologies that are

able to dynamically measure protein titers in small volumes will likely form the basis for advances in early CHO clone screening.

Microfluidic technology allows for the manipulation of picoliter sized volumes thereby increasing biological measurement sensitivity while reducing the time, labor and cost of analysis^{14,194,195}. Single cells can now be manipulated in microfluidic settings through a variety of means facilitating genomic, transcriptomic and proteomic analysis^{13,200,203,204,206,207,208,209}. At the protein level, microfluidic technology has simplified the detection of both secreted and intracellular proteins, achieving sensitivities down to 8×10^4 molecules secreted from single hybridoma cells^{215,216,217,221}. More advanced techniques such as droplet encapsulation have allowed for the analysis of secreted proteins from T-cells²¹⁸ and tumors cells²¹⁹ with paracrine signaling even being quantified in the case of co-encapsulation²²⁰. Although microfluidic secretion measurements have been performed on single cells²¹⁶, they have yet to be combined with robust long-term microfluidic cell culture²⁴¹ to accurately assess single high performing clones under large-scale production conditions. The unification of small volume cell culture with microfluidic assay sensitivity offers the potential to assess clonal variations in protein expression *in situ* while possessing the advantages of increased throughput, parallelization, automation and reduced reagent consumption^{224,225,226,240,241,242,243,244}.

A semi-automated, dynamic, microfluidic assay is presented to detect human Immunoglobulin G secreted from single CHO clones in nanoliter volumes under conditions similar to large-scale bioreactors. Through the use of magnetic beads, the assay is used to assess fixed quantities of Immunoglobulin G in microfluidic volumes over multiple days. This assay is also coupled with automated bead segmentation

algorithm to speed up image analysis. Microfluidic measurements on CHO-S clones were performed to test the applicability of the microfluidic assay for therapeutic screening under conditioned medium perfusion. The microfluidic assay combined with automated imaging and bead segmentation has the potential to streamline the process of clone selection by allowing productivity assessments at the single cell level in a simulated bioreactor production environment.

3.2 Materials and Methods

3.2.1 Dynamic microfluidic bead assay protocol

CD FortiCHO medium (Thermo-Fisher Scientific, Waltham, MA) supplemented with 25 μ M L-methionine sulfoximine (Sigma-Aldrich, St Louis, MO), 20 μ g/mL puromycin (Thermo-Fisher Scientific, Waltham, MA) and 4X anti-clumping agent (Thermo-Fisher Scientific, Waltham, MA) was used for the duration of the magnetic bead assay. Magnetic protein-G coated beads with an average diameter of \sim 3 μ m (ProActive® Microspheres, Bangs Laboratories) were washed 2 times with PBS followed by re-suspension in CD FortiCHO medium. The beads were aliquoted at a concentration of 1 mg/mL and immediately loaded into the device at a flow rate of 10 μ L/min from PTFE tubing maintained in an upright position. Once a concentration of \sim 100 – 200 beads per chamber was achieved for the majority of the array (after approximately 7 – 10 min of flow), the flow was stopped and the beads were allowed to settle at the base of chambers via gravity. The remaining beads in channels between chambers were washed away with CD FortiCHO for 7 min at 10 μ L/min. Chambers were then isolated by closing all valves on the device. For microfluidic clonal productivity measurements beads were incubated

with cells at 37°C for 2 h. Otherwise, microfluidic arrays were loaded with standard concentrations (between 0 and 100 µg/mL) of purified human IgG1 (Thermo-Fisher Scientific, Waltham, MA) diluted in CD FortiCHO medium for 7 min at 10 µL/min; then incubated at 37°C for 2 h.

Following incubation with primary or secreted antibody, the array was flushed with CD FortiCHO for 7 min at 10 µL/min. Next, arrays were loaded with 2 µg/mL of labeled secondary antibody (Dylight 594-conjugated AffiniPure F(ab')₂ fragment of rabbit anti-human IgG (H+L) (Jackson ImmunoResearch) diluted in CD FortiCHO medium for 7 min at 10 µL/min. Secondary antibody was incubated at 37°C for 15 min, followed by a washing step with CD FortiCHO for 7 min at 10 µL/min prior to imaging. The final step of the assay consisted of magnetic removal of beads whereby a magnet was held 2 – 5 mm above the device while the entire array was flushed with CD FortiCHO for 15 – 20 min at 10 µL/min (until the majority of beads were visibly removed).

3.2.2 Image acquisition and assay automation

The microfluidic platform and environmental enclosure were fixed onto an inverted Axiovert 200 microscope (Carl Zeiss, Oberkochen, Germany). Custom software developed using Labview (National Instruments, Austin, TX, USA) was used to image the cells/antibody in each chamber with a 10× objective lens and an Orca ER CCD camera (Hamamatsu, Naka-ku-Hamamatsu, Japan) prior to incubation, after incubation and after magnetic bead removal. The entire microfluidic device was scanned automatically with a ProScan II motorized XY stage (Prior Scientific, Rockland, MA); temporal resolution for imaging was 20 min for each image set (~1024 chambers). All

flushing, washing and incubation steps were also automated and controlled through the use of custom Labview software.

3.2.3 Bead segmentation

All bead segmentation algorithms were written in MATLAB (MathWorks, Natick, MA) and can be found in **Appendix C**. Beads segmentation sought to achieve 3 main things: background subtraction, noise reduction and thresholding to produce a binary mask. First, the starting image was morphologically opened to get an estimate of the background noise. The resulting image was then subtracted from the original to generate a more uniform background. Next, a 10 x 10 median filter was applied to remove additional particulate noise and enhance edge detection of the beads. This filtered image was then contrast enhanced. Finally, a threshold (empirically determined) was applied to produce a binary mask and small objects (<50 pixels) were removed. The final mask was then applied to the original image so that only regions containing beads were taken into account when summing the pixel intensity across the image. The summed pixel intensity for each image (after the binary mask was applied) was taken as the total bead intensity and automatically exported into a spreadsheet. The summed pixel intensity value prior to incubation was subtracted from the post incubation image to determine the total change in bead intensity due to incubation with antibody and divided by the total bead area to result in a mean bead pixel intensity output.

3.2.4 Cell culture

Several CHO cell types were used for this study. CHO-S clones D2 and D4 (derived from CHO-K1 ATCC CCL61), secreting human IgG1 (containing a VL Kappa

chain) while proportionally expressing EGFP and mCherry intracellularly¹¹⁴, were maintained in CD FortiCHO medium supplemented with 25 μ M L-methionine sulfoximine, 20 μ g/mL puromycin and 4X anti-clumping agent. In these cell lines an hMet IIA promoter drives expression of the heavy or light chain of a recombinant IgG while an attenuated internal ribosomal entry site promotes cap-independent translation of EGFP and mCherry reporters; vector information for the cell lines can be found in Sleiman *et al.*¹¹⁴. Clones were propagated by seeding every 72 – 96 h with either 1.25×10^5 or 2.5×10^5 cells/mL (for either 4 or 3 days of culture respectively) in either 10 mL round bottomed 24-well DWP wells (VWR, Radnor, PA), 50 mL shake tubes (TPP, Leeds, UK) or 125 mL shake flasks (Dow Corning, Midland, MI).

An untransfected parental CHO-S line (derived from CHO-K1 ATCC CCL61) that does not secrete any product¹¹⁴, was maintained in CD FortiCHO medium that was supplemented with 4 mM L-glutamine (Sigma-Aldrich, St Louis, MO) and 4X anti-clumping agent. The parental CHO-S line was propagated by seeding every 72 – 96 h with either 0.75×10^5 or 1.5×10^5 cells/mL (for either 4 or 3 days of culture respectively) in either 50 mL shake tubes or 500 mL shake flasks (Dow Corning, Midland, MI).

All CHO lines were maintained in orbital shaking incubators (Kuhner, Basel, Switzerland) at 37°C, 5% CO₂, 85% relative humidity and either 125 rpm (125/500 mL shake flask) or 225 rpm (50 mL shake tube, 24-well DWP) with a 5 cm shaking diameter. All cell concentrations and viabilities were measured via Trypan Blue (Thermo-Fisher Scientific, Waltham, MA) exclusion in a Cedex automated cell counter (Roche Innovatis, Bielefeld, Germany). Prior to cell counting, culture samples were diluted with an equal amount of 0.25% trypsin/EDTA (Thermo-Fisher Scientific, Waltham, MA) and topped

up to 1 mL with 1X PBS (Thermo-Fisher Scientific, Waltham, MA) followed by incubation for 15 min at 37°C to break up cell aggregates.

3.2.5 Parental cell line fed-batch culture

CHO-S parental line fed-batch cultures in 500 mL shake flasks were inoculated with 100 mL at 0.9×10^5 cells/mL in CD FortiCHO medium supplemented with 4 mM L-glutamine and 4X anti-clumping agent. Flasks were sampled daily starting on day 3 with 0.5 mL taken for automated cell counting (Cedex, Roche Innovatis, Bielefeld, Germany) at a 1:2 dilution with 0.5 mL of 0.25% trypsin/EDTA while another 0.25 mL was taken for supernatant analysis (ELISA, glucose, lactate, osmolarity, etc.). Starting on day 3, cultures were fed daily (after sampling) with CD EfficientFeed C AGT (adjusted to a pH of 7.02) (Thermo-Fisher Scientific, Waltham, MA) at a rate of 6.7% of the initial culture volume. Parental fed-batch cultures were run for up to 14 days (minimum 8 days) until cell viabilities dropped below 70%. To adjust for dilution caused by cell removal and feed addition, viable cell densities were adjusted according to Equations 2.1 - 2.4.

3.2.5 Conditioned medium harvesting

Conditioned medium was harvested daily (starting on day 1) from parental CHO line fed-batch cultures in 500 mL flasks for the purpose of perfusing microfluidic cultures. After sampling and feeding the parental flask, the necessary volume of CM (1 mL per day of culture on the device) was harvested and transferred into 1 mL microcentrifuge tubes (Thermo-Fisher Scientific, Waltham, MA). Harvested medium was then spun down at 1000 rpm for 7 min (to remove cells) in a Beckman GS-6 series centrifuge (Beckman Coulter, Brea, CA) followed by supernatant removal and filtration

through a 0.22 μm filter (Dow Corning, Midland, MI). CM was kept at 4°C (for up to 2 weeks) until later use.

3.2.6 ELISA

Antibody titers for CHO-S clones were measured according to previously reported ELISA methodologies¹¹⁴. Supernatant samples were collected by spinning down cell culture samples for 3 min at 1000 rpm in a Spectrafuge 16M microcentrifuge (Labnet International, Edison, NJ); the resulting supernatant was collected and stored at -20°C prior to analysis. First, Nunc-Immuno 96-well Maxisorb plates (Sigma-Aldrich, St Louis, MO) were coated with a goat anti-human IgG Fc γ -specific primary antibody (Jackson ImmunoResearch, Baltimore, MD) and incubated overnight at 4°C. The next day, plates were washed 3 times with wash buffer (1X PBS, 0.1% Tween-20) followed by blocking with a blocking solution (1X PBS, 0.02% Tween-20, 0.5% skim milk) for 1 h at room temperature prior sample loading. Measurements were standardized to IgG1 from human serum (Sigma-Aldrich, St Louis, MO) loaded at concentrations ranging from 2.5 ng/mL to 10 $\mu\text{g/mL}$. Once all standards and samples were loaded, wells were incubated with a sheep anti-kappa light chain HRP-conjugated secondary antibody (The Binding Site, Birmingham, UK). Bound antibodies were quantified by incubating with 3,3',5,5'-Tetramethylbenzidine substrate (Sigma-Aldrich, St Louis, MO) for 8 min at room temperature in the dark. The reaction was terminated with 2 M H₂SO₄ followed by plate reading at 450 nm using a microplate reader. Titer measurements were adjusted for dilution caused by feed addition by multiplying the cumulative dilution factor by the measured titer.

3.2.7 Flow cytometry

All CHO samples were washed 2 times with PBS followed by re-suspension in PBS + 10% FBS solution for flow cytometry. Positive live (propidium iodide-negative, PI-; Sigma-Aldrich, St Louis, MO) cells were gated using an untransfected CHO-1 (a non-reporting cell line) sample as a negative control using FlowJo software (Tree Star, Ashland, OR, USA).

3.2.8 Microfluidic cell culture

Microfluidic cell culture arrays were fabricated according to Lecault *et al.* protocols and contained 4 arrays of 2048 chambers for a total of 8192 microbioreactors per device; all microfluidic platforms also contained an iso-osmotic bath to buffer against osmolarity changes due to evaporation during culture²⁴¹. Protocols for fabricating the microfluidic cell culture platforms can be found in **Appendix B**.

Prior to each experiment, a newly fabricated, sterile device was mounted onto an Axiovert 200 inverted microscope then dead-end filled with filter-sterilized 1% FBS and incubated overnight at 37°C in humidified 5% CO₂ (in a custom enclosure described in Chapter 4) to prime the channels and chambers for cell culture. The osmotic bath was then filled with CD FortiCHO medium supplemented with 25 µM L-methionine sulfoximine, 20 µg/mL puromycin and 4X anti-clumping agent to equilibrate the osmotic strength throughout the device. The next day, a sterile solution of fresh CD FortiCHO medium supplemented with 25 µM L-methionine sulfoximine, 20 µg/mL puromycin and 4X anti-clumping agent was incubated in the culture chambers for 45 min at room temperature. A single-cell suspension (at 10⁶ cells/mL) of CHO-S D2 clones, secreting

human IgG1 (containing a VL Kappa chain) while proportionally expressing EGFP and mCherry intracellularly¹¹⁴, was then stochastically loaded into the device (with microscopic monitoring). Once the microfluidic array appeared to be filled, cells were allowed to settle to the bottoms of chambers for 5 – 10 min (to prevent wash out during subsequent flushing steps). The chambers were then flushed again for 7 – 10 min with fresh CD FortiCHO medium supplemented with 25 μ M L-methionine sulfoximine, 20 μ g/mL puromycin and 4X anti-clumping agent to remove any leftover cells in the channels. This process was repeated as many times as necessary until the desired number of single clones was obtained. Devices were then incubated at 37°C in humidified 5% CO₂ overnight next to several 22 mm dishes filled with water to maintain humidity. Cell growth was subsequently monitored 96 – 192 h depending on when chambers became confluent. During this period, the entire system (including the Axiovert 200 inverted microscope) was contained in an environmental chamber heated to 37°C with a smaller microfluidic enclosure being supplied with humidified 5% CO₂ at a rate of 46 mL/min to maintain this CO₂ level in the device (described in Chapter 4). Custom software developed using Labview (National Instruments, Austin, TX, USA) was used to image the cells in each chamber with a 10 \times objective lens every 24 h using differential interference contrast (DIC) microscopy. The medium in each chamber was replaced daily with either fresh CD FortiCHO medium supplemented with 25 μ M L-methionine sulfoximine, 20 μ g/mL puromycin and 4X anti-clumping agent or parental CHO line CM corresponding to the day of culture harvested under pressure driven flow.

3.3 Results

3.3.1 Microfluidic secretion assay development

Prior to setting up a robust bead assay protocol, various assay parameters were explored. Starting from previous reports using polystyrene beads, the incubation time, objective lens, and bead type were varied in an attempt to improve sensitivity and assay throughput (Figure 3.1)^{14,216}. All preliminary bead measurements were performed off-chip with bead intensities acquired by manually drawing line profiles through images and recording the maximum fluorescence amplitude of each bead (Figure 3.1A). This method was chosen to ensure that analysis times were reasonable and it has been shown to be reliable in previous reports²¹⁶. For example, taking the mean intensity over the entire projected area of the bead would have required manually outlining each bead individually and this could have caused greater technical variation if not performed systematically or in an automated fashion. To obtain an adequate sample size, a minimum of 10 line profiles were recorded for each field of view with at least 4 fields of view analyzed per condition. Initial observations on 10 μm Protein A coated polystyrene beads incubated for 2 h showed saturation above 10 $\mu\text{g}/\text{mL}$ human FITC IgG with a dynamic range of roughly 2 orders of magnitude (0.1 – 10 $\mu\text{g}/\text{mL}$) (Figure 3.1B). This dynamic range was also compatible with the intended cell line (CHO-S D2) which would be expected to generate titers of ~ 0.04 $\mu\text{g}/\text{mL}$ in 2 h (assuming a mean specific productivity of 2 pg/cell/day in 4 nL). No significant difference was observed between objective lenses and exposure times suggesting a lower magnification objective and shorter exposure could be used for the assay to reduce imaging time.

Next, the feasibility of a shorter incubation time was tested; 10 μm polystyrene beads were exposed to fixed concentrations of human FITC IgG (0.001 – 100 $\mu\text{g}/\text{mL}$) for 15 min (Figure 3.1C). With the shorter incubation time decreased sensitivity was observed along with less saturation at higher concentrations suggesting that a shorter incubation time would be more suitable screening for higher producing clones (eg. a clone producing at a rate of ~ 20 $\text{pg}/\text{cell}/\text{day}$ would generate a titer of ~ 0.05 $\mu\text{g}/\text{mL}$ in 15 min in 4 nL and be detectable by the assay). The shorter incubation time would not be suitable for the intended cell line (CHO-S D2) which would only be expected to generate ~ 0.005 $\mu\text{g}/\text{mL}$ in 15 min (assuming a mean specific productivity of 2 $\text{pg}/\text{cell}/\text{day}$ in 4 nL). In addition, although the 10 μm polystyrene beads proved to be sensitive enough for the assay, bead recovery for repetitive assays proved to be non-trivial, resulting in magnetic bead removal being explored.

3 μm Protein G coated magnetic beads were then compared to Protein A coated polystyrene beads of similar size (4 μm) by incubating for 2 h with either human IgG (followed by 15 min incubation with Alexa-594 secondary antibody) or rabbit FITC IgG (Figure 3.1D). Similar sensitivity for both types of beads was observed (~ 0.1 $\mu\text{g}/\text{mL}$), however the magnetic beads had a slightly higher background autofluorescence. In both cases negative controls, whereby beads were incubated for 2 h with 1% BSA containing no antibody followed by 15 min incubation with Dylight 594-conjugated AffiniPure F(ab')₂ fragment of rabbit anti-human IgG (H+L), produced signal in the same range as incubating with 0.001 – 0.01 $\mu\text{g}/\text{mL}$ of human IgG for 2 h (Figure 3.1D). While the concentration of secondary antibody was sufficient to generate a robust dilution series, the higher background bead autofluorescence could be due to non-specific binding of the

F(ab')₂ secondary antibody fragment to Protein G on the magnetic beads. Thus, modifying the secondary antibody type, concentration or incubation time could further improve the assay. Nevertheless, the advantage of being able to magnetically separate beads from cells in microfluidic chambers far outweighed the drawback of higher autofluorescence. Thus, the assay was developed using 3 μm Protein G coated magnetic beads whereby clones (CHO-S D2) were incubated with the beads for 2 h followed by incubation with secondary antibody for 15 min and magnetic removal (Figure 3.2).

The microfluidic bead assay incorporated elements from previous high sensitivity measurements of single cell secretion²¹⁶ and combined them with robust microfluidic cell culture practices²⁴¹. In particular, a method was sought after whereby clones could be left to proliferate in microfluidic chambers while beads were repeatedly brought into chambers to perform a productivity measurement and removed magnetically when complete. By incorporating magnetic removal into the assay, the beads could be separated from the cells simply by introducing a magnet to the system. This key step offers the potential for multiple productivity assessments to be performed during cell culture while minimally disturbing the cells. For this procedure, CHO-S D2 clones were loaded into the array at a concentration of 10⁶ cells/mL with high aspect ratio chambers allowing cells to be sequestered to the bottom of chambers via gravity (Figure 3.2A). Chambers were then flushed thoroughly with FortiCHO medium to remove excess antibody, and 3 μm Protein G coated magnetic beads in fresh FortiCHO were introduced and allowed to settle to the bottom of chambers (Figure 3.2B). FortiCHO medium was then used to wash away excess beads in the channels between chambers, and cells were isolated and incubated for 2 h in order to capture secreted antibody (Figure 3.2C).

Subsequently, chambers were again washed with FortiCHO to remove unbound antibody (Figure 3.2D). A secondary antibody (labeled with Alexa-594) was then loaded into chambers and incubated for 15 min (Figure 3.2E). Finally, the chamber array was washed with FortiCHO to remove unbound secondary antibody and all chambers were imaged (Figure 3.2F). For imaging, a custom Labview algorithm was used to focus the beads while taking DIC and fluorescent images of the entire chamber array. All imaging was performed using an Axiovert 200 inverted microscope under a 10× objective lens. Following the assay, a magnet was then used to pull the beads to the chamber roof and flushed away with FortiCHO medium (Figure 3.2G). New beads could then be reintroduced into the chamber array to repeat the measurement (Figure 3.2H). This assay could theoretically be performed several times daily under physiological conditions with the only bottleneck being the speed with which images could be manually processed.

3.3.2 Automated bead segmentation

In an attempt to further increase assay sensitivity and throughput an automated bead segmentation algorithm was developed (Figure 3.3). The motivation for automation was the labor-intensive nature of manual bead intensity analysis, which would not be feasible for analyzing hundreds to thousands of clones. Several image processing steps were performed to produce a mask which could be applied to the original image including morphological opening, background subtraction, median filtering, contrast enhancement and thresholding (code can be found in **Appendix C**). When applied to fixed concentrations of human IgG on chip, the algorithm achieved a segmentation efficiency of 82% (n = 2048 chambers), which was defined as the percentage of total chambers that were segmented correctly. The algorithm was also found to be sensitive to

the number of beads in the chamber with the likelihood of improper segmentation increasing when the number of beads in the chamber dropped below ~50. Since the laminar flow through the microfluidic chip resulted in faster flow through the center of the chamber array, the majority of the improperly segmented images were chambers containing little to no beads at the edges of the array; segmentation efficiency could thus be increased by omitting the last few columns of the microfluidic array. Additionally, extremely high signal was observed when the algorithm failed to segment the beads due to the summation of pixel intensities across the masked image (improperly segmented masks included both the area of the beads as well as the entire background of the image producing an abnormally high value); the simple application of a threshold to omit chambers containing artificially high signal prior to antibody incubation solved this issue. Overall, the bead segmentation algorithm greatly increased the speed and efficiency of image analysis, reducing analysis time down to minutes from hours or days of manual labor.

3.3.3 Dynamic precise measurements of IgG in nL chambers

Subsequently, the microfluidic assay was validated on fixed quantities of human IgG (0.001 – 100 $\mu\text{g/mL}$) and manually analyzed images were compared to the results of the automated bead segmentation algorithm (Figure 3.4A and B). Unlike the manual case described above, mean bead intensity (using the segmentation algorithm) was calculated by dividing the total intensity of all the beads in the chamber by the total bead area. This method produced a much smaller standard deviation and higher signal to noise than the manual intensity analysis (Figure 3.4B). Although superior to manual intensity analysis the automated result could be due to the different metric used to assess bead intensity;

regardless, automation of bead segmentation significantly reduced image analysis time. Similar to previous manual results off chip (Figure 3.1), the assay with automated segmentation was observed to have a dynamic range of ~ 3 orders of magnitude (0.01 – 10 $\mu\text{g}/\text{mL}$) with the ability to detect as little as $\sim 10^6$ molecules of IgG (0.06 $\mu\text{g}/\text{mL}$ in 2 h) (Figure 3.4B). Again, this dynamic range was compatible with the intended cell line (CHO-S D2 which would generate ~ 0.04 $\mu\text{g}/\text{mL}$ in 2 h in 4 nL).

The ability to reproducibly detect the same quantity of antibody across multiple measurements was also tested on chip by alternating fixed concentrations of IgG in the same microfluidic chambers over multiple days. This test alternated high (10 $\mu\text{g}/\text{mL}$) and low (0.1 $\mu\text{g}/\text{mL}$) concentrations of antibody daily over 4 days to ensure that a high antibody titer measured on one day did not bleed over into or cross contaminate the subsequent measurement (Figure 3.4C). During these measurements it was observed that the introduction of high (10 $\mu\text{g}/\text{mL}$) antibody concentration into a microfluidic chamber did not significantly affect subsequent low (0.1 $\mu\text{g}/\text{mL}$) antibody measurements and vice versa. Additionally, concentrations of high and low antibody matched values obtained in previous experiments, further validating the reproducibility of the assay. Negative control chambers (whereby 0 $\mu\text{g}/\text{mL}$ was incubated with beads daily) also did not differ significantly across 4 days of measurements (Figure 3.4D). On top of this, the magnetic bead removal efficiency during all experiments was found for be $>99\%$ (measured by counting the number of beads initially loaded in the chamber and comparing that to the number remaining after magnetic removal). Leftover beads also did not significantly affect subsequent measurements (Figure 3.4C), further demonstrating the robustness of the magnetic removal process. This ability of the microfluidic assay to discriminate

between fixed antibody concentrations across multiple measurements demonstrates its technical precision and applicability to clonal screening.

3.3.4 Evaporation considerations and cell culture optimization

Following assay validation on fixed antibody quantities, the microfluidic system was adapted so that the assay could be performed on live clones in culture. First, the entire microscope setup was contained in a custom heated enclosure (to maintain the temperature at 37°C) while the microfluidic device was surrounded in a secondary enclosure supplying the platform with humidified 5% CO₂ (described in Chapter 4). A major design feature allowing for the culture of single clones was the inclusion of an “iso-osmotic bath” above the microfluidic array; an approach previously found to work for the clonal culture of hematopoietic cells^{224,241,250}. Without the use of the osmotic bath CHO clones did not proliferate in the microfluidic setting with growth significantly underperforming larger scale cultures (in agreement with previous mammalian cell reports)²⁴¹. The lack of proliferation during preliminary growth testing was traced to the substantial evaporation occurring in the enclosure (Figure 3.5A). Substantial osmolarity changes were observed when cell culture dishes or the osmotic bath containing medium or PBS were left uncovered in the enclosure. When covered, the osmotic strength of the bath was maintained within the physiological range of 285 - 295 mOsm/kg (Figure 3.5A). As the osmotic bath was only separated from the cell culture chambers by a thin permeable PDMS membrane, any osmotic changes in the bath should reflect similar changes in the osmotic strength of medium in the microfluidic array. Thus, for all subsequent experiments the osmotic bath remained covered so as to buffer any osmotic changes in the microfluidic chambers due to evaporation.

Next cell culture under magnetic bead assay conditions was attempted and it was discovered that clones did not proliferate when chambers were loaded with the bead concentration (1 mg/mL) used in the fixed IgG concentration experiments (Figure 3.5B). Increased apoptosis per cell was observed at higher bead concentrations with beads aggregating around the cells suggesting that physical contact with the beads could be a possible cause of increased cell death (eg. cell surface proteins interacting with the protein G coating of beads). When bead concentrations were reduced to 0.1 mg/mL less cell death was observed and cells proliferated normally compared to large-scale batch controls (Figure 3.5B). This result was repeated when the full assay was performed under physiological conditions (37°C, 90% RH, 5% CO₂) on cells in the device suggesting that the microfluidic setting should be ideal for assessing single cell productivity.

3.3.5 Microfluidic productivity assessment of CHO-S D2 clones

To demonstrate applicability to clone selection, the assay was tested on CHO-S D2 clones under simulated fed-batch conditions using the conditioned medium perfusion technique developed in Chapter 2 (Figure 3.5C). Under this process CHO-S D2 clones were loaded onto the microfluidic device and CM from a 125 mL parental cell line fed-batch culture (from the day of culture corresponding to the matching cell concentration) was perfused into the device daily with the microfluidic assay being performed on day 1 and 3 of culture. Due to the bead toxicity observed at 1 mg/mL, beads were loaded at a concentration of 0.1 mg/mL for all experiments to ensure robust cell growth. The reduced bead concentration was observed to be too low for the bead segmentation algorithm to properly segment the beads. Thus all images in the cell experiments were analyzed manually (the same method used in previous reports) by drawing line profiles through the

beads and taking the maximum bead intensity²¹⁶. Although manual analysis was proven to be less precise in the earlier titer measurements, it has still been proven to be sufficient²¹⁶ for a proof-of-concept demonstration of titer measurements on single cells. Titers were calculated using this method by comparing bead intensities to a standard curve generated by incubating fixed concentrations (0 – 100 µg/mL) of IgG in microfluidic chambers and analyzing images manually (Figure 3.6A).

Using the above manual bead segmentation method, the specific productivities of 27 clones (with 5 blank chamber controls containing no cells) were calculated across 2 days of measurements (Figure 3.6B). All negative chamber controls (located in proximity to chambers containing cells) were observed to have no detectable amount of antibody present suggesting that there was no cross-contamination between chambers or bleed over from chambers containing cells. For the chambers containing cells, specific productivities varied widely across multiple measurement days signifying that clonal production could be dynamic and highlighting the need to assess clones over multiple days. Close attention was paid to the number of cells in each chamber before and after each assay was performed to ensure that differences in specific productivities across multiple measurements were not due to cells being washed away during the flushing steps of the assay. Although chambers were designed to be deep enough (>100 µm) such that once settled cells could not be washed away²⁴¹, when chambers became confluent or clones grew on top of each other this broke down and there was the potential for the top cells to enter the flow streamlines near the roof of the chamber. All situations where some clones were washed away during one of the assays were omitted from analysis. Even when no washing away was observed, some clones were observed to drop off production

by the second measurement. This could be due to inherent changes in productivity/expression stability, technical variation or possible apoptosis during the measurement (potentially artificially causing a higher first measurement). Similarly, clones were observed that increased productivity between the first and second measurements. These could be low producers that aren't detectable until enough subclones are generated in the chamber or evidence of dynamic clonal expression. In either case, the results from these measurements demonstrate the importance of evaluating clones more than once over the course of culture as many factors could cause expression to change between measurements.

Next microfluidic clonal q_p results were compared to bulk population productivity and intracellular mCherry expression (Figure 3.6C). The combined specific productivity across all microfluidic chambers containing CHO-S D2 clones was found to be 2.8 ± 1.4 pg/cell/day through the use of the magnetic bead assay. This was not significantly different than the bulk fed-batch CHO-S D2 specific productivity which was found to be 1.7 ± 0.7 pg/cell/day ($p = 0.30$). Similarly, 17/27 clones (63%) were observed to produce quantities of antibody above the detectable limit. This was again in agreement with FACS profiles of bulk populations of CHO-S D2 where ~64% of clones were observed to express mCherry and EGFP at levels above the negative control (Figure 3.6C). Lastly, a determination of how closely individual intracellular mCherry expression correlated to clonal specific productivity was attempted by recording the mean fluorescence intensity of all subclones in each chamber in the 594 nm channel. A positive correlation between Day 1 specific productivity and mean intracellular mCherry expression was observed demonstrating the usefulness of using a reporter cell line in this study (Figure 3.6D)¹¹⁴.

While this observation was noteworthy, it should be added that the half-life of the mCherry molecules is greater than the division time of the cells¹⁰⁵ so the specific productivity at the time of the assay would change more rapidly than the reporter fluorescence. Thus, the microfluidic assay has the added capability to measure clonal changes in productivity on timescales shorter than on cell division. As the observed microfluidic clonal specific productivities matched those of bulk populations across multiple temporal measurements this technique demonstrates a precise method to screen CHO clones in conditions similar to large-scale bioreactors.

3.4 Discussion

In summary, proof of concept functionality of a magnetic bead assay that dynamically detects IgG secretion from single CHO clones in nL volumes has been demonstrated. The assay was specifically designed to make multiple temporal titer measurements over the course of clonal culture by combining removable magnetic beads with a microfluidic cell culture system capable of time-lapse microscopy and programmable medium exchange under physiological conditions. The design was combined with an automated bead segmentation algorithm providing a quick and reproducible method of daily IgG titer quantification in 4 nL volumes. When validated on fixed concentrations of IgG, the semi-automated assay (coupled with automated bead segmentation) repeatedly demonstrated sensitivity down to 10^6 molecules. When the bead assay was combined with CHO clones, clonal growth did not significantly differ from batch controls in CM perfusion conditions however bead toxicity was observed above 1 mg/mL. The clonal dual reporter CHO line (CHO-S D2) was found to be very heterogeneous when repeated measurements were performed over multiple days. Clones

evaluated in the microfluidic setting matched bulk productivity measurements made at larger scales while specific productivity correlated positively to intracellular mCherry fluorescence, which was in agreement with previous reports^{105,114}. Thus, the combination of clonal microfluidic cell culture and *in situ* measurement of secretion product provides a technique to assess single cell productivity that would not be possible via other methods such as the collection and analysis of supernatant from microfluidic wells due to the limited sample size from single cells and the lack of sensitivity of traditional off-chip ELISA methods⁷⁴.

This study addresses the need for early clonal evaluation during the scale-up of production cell lines. The coupling of microfluidic CM perfusion with a single cell secretion assay provides the potential to screen hundreds to thousands of clones in conditions similar to the large-scale fed-batch microenvironment, thus fast-tracking the ability to uncover high-performing clones that could be used in a manufacturing setting. The combination of single cell resolution and a dynamic secretion assay should provide great potential for screening transfected pool population dynamics in simulated bioreactor conditions. Additionally, this single cell screening capability is also applicable to other populations of cells that secrete valuable products in conditions where precise microenvironmental control is needed.

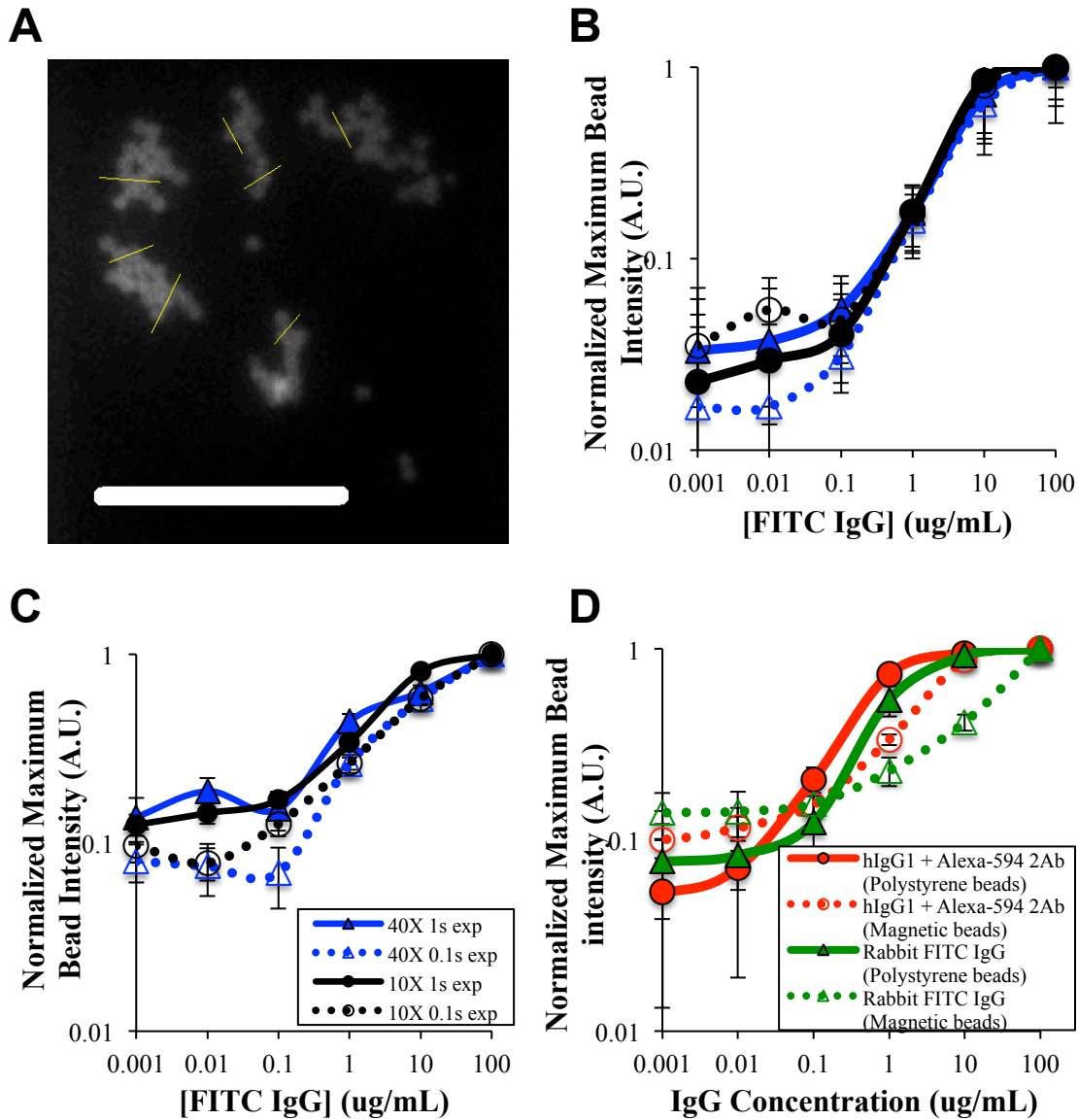


Figure 3.1 Bead assay development

(A) Typical bead image with line profiles (yellow) manually drawn through beads to calculate maximum bead intensity (scale bar = 100 μm). (B) Isotherm of maximum bead intensities for 10 μm protein A coated polystyrene beads incubated with human FITC labeled IgG for 2 h using different objective lenses (10 \times and 40 \times) and camera exposures (0.1 s and 1 s). (C) Isotherm of maximum bead intensities for 10 μm protein A coated polystyrene beads incubated with human FITC labeled IgG for 15 min using different

objective lenses (10× and 40×) and camera exposures (0.1 s and 1 s). **(D)** Isotherm of maximum bead intensities for 4 μm protein A coated polystyrene beads and 3 μm protein G coated polystyrene beads incubated with either rabbit FITC labeled IgG for 2 h or human IgG for 2 h followed by 15 min incubation with Alexa-594 labeled secondary antibody.

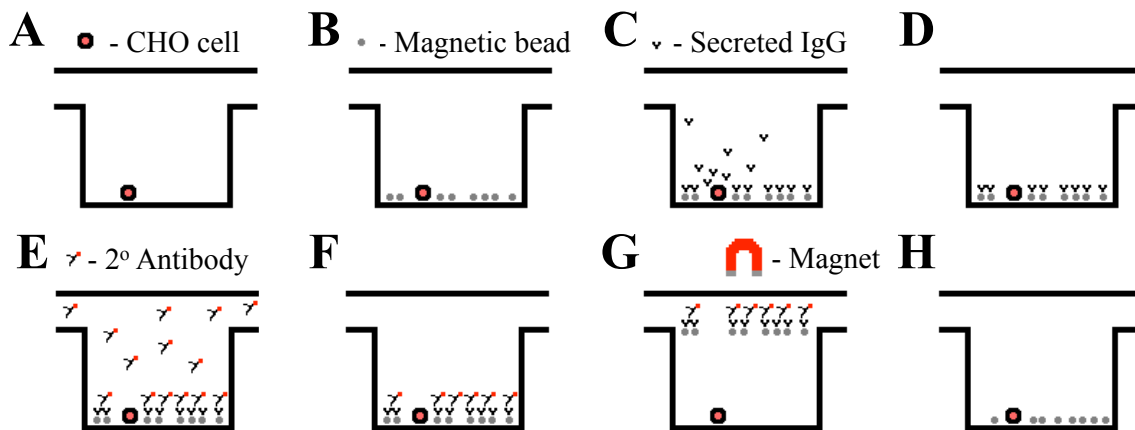


Figure 3.2 Schematic for dynamic microfluidic bead assay

(A) Cells are initially loaded into microfluidic chambers. (B) Magnetic Protein-G coated beads are loaded into chambers and array is imaged to obtain background fluorescence level. (C) Beads are incubated for 2 h to capture human IgG secreted from clones. (D) Chamber array is washed with medium to clear unbound antibody. (E) Clones are incubated for 15 min with Alexa-594 labeled secondary antibody. (F) Chamber array is washed with medium to clear unbound secondary antibody and chambers are imaged to obtain fluorescence readout. (G) Beads are raised with magnet and washed away with medium. (H) New magnetic beads are loaded and assay is repeated as necessary.

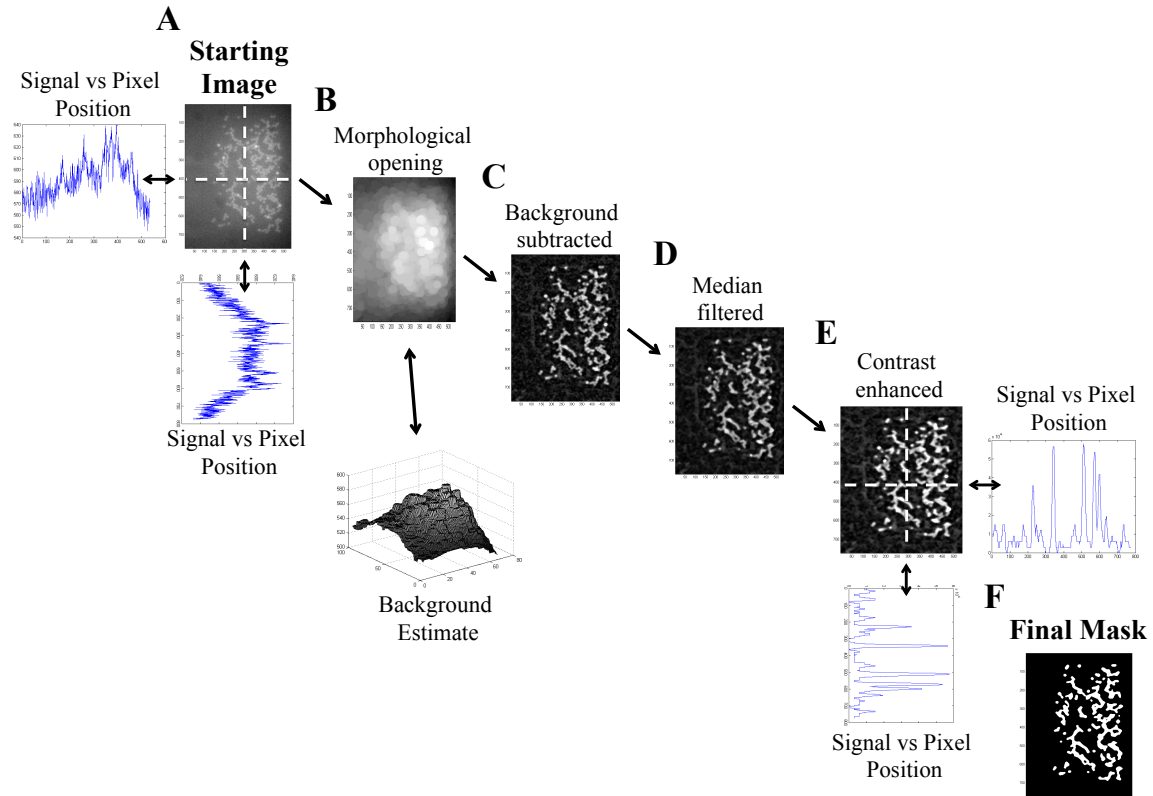


Figure 3.3 Automated bead segmentation

(A) Original unfiltered image and typical signal and noise levels. (B) Image is morphologically opened to estimate background noise. (C) Background is subtracted from morphologically opened image. (D) A 10 x 10 pixel median filter is applied to further reduce noise. (E) The contrast of the filtered image is enhanced for the purpose of thresholding. (F) Threshold is applied to the image and small objects (<50 pixels) to produce the final mask. The final mask is then applied to the original to segment the beads.

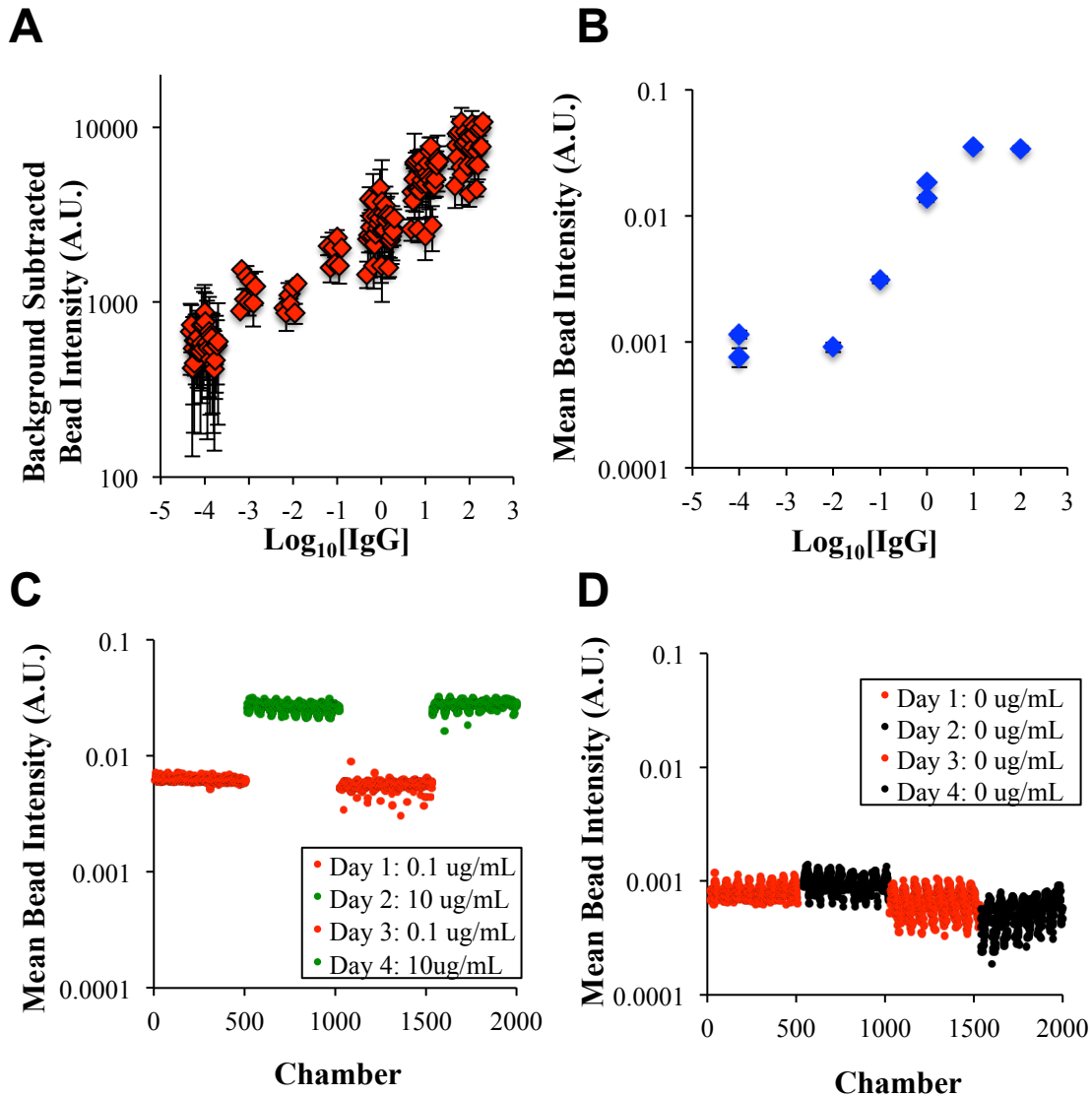


Figure 3.4 Magnetic bead assay validation on fixed IgG concentrations

(A) Distribution of manually calculated background subtracted bead intensities for 0.0001 – 100 $\mu\text{g/mL}$ of IgG. (B) Isotherm of mean bead intensities using the automated bead segmentation algorithm (0.0001 – 100 $\mu\text{g/mL}$ of IgG). (C) Bead intensities for the same chambers exposed to alternating concentrations of human IgG (0.1 and 10 $\mu\text{g/mL}$) over 4 daily assays. (D) Bead intensities for the same chambers exposed to 0 $\mu\text{g/mL}$ of human IgG over 4 daily assays.

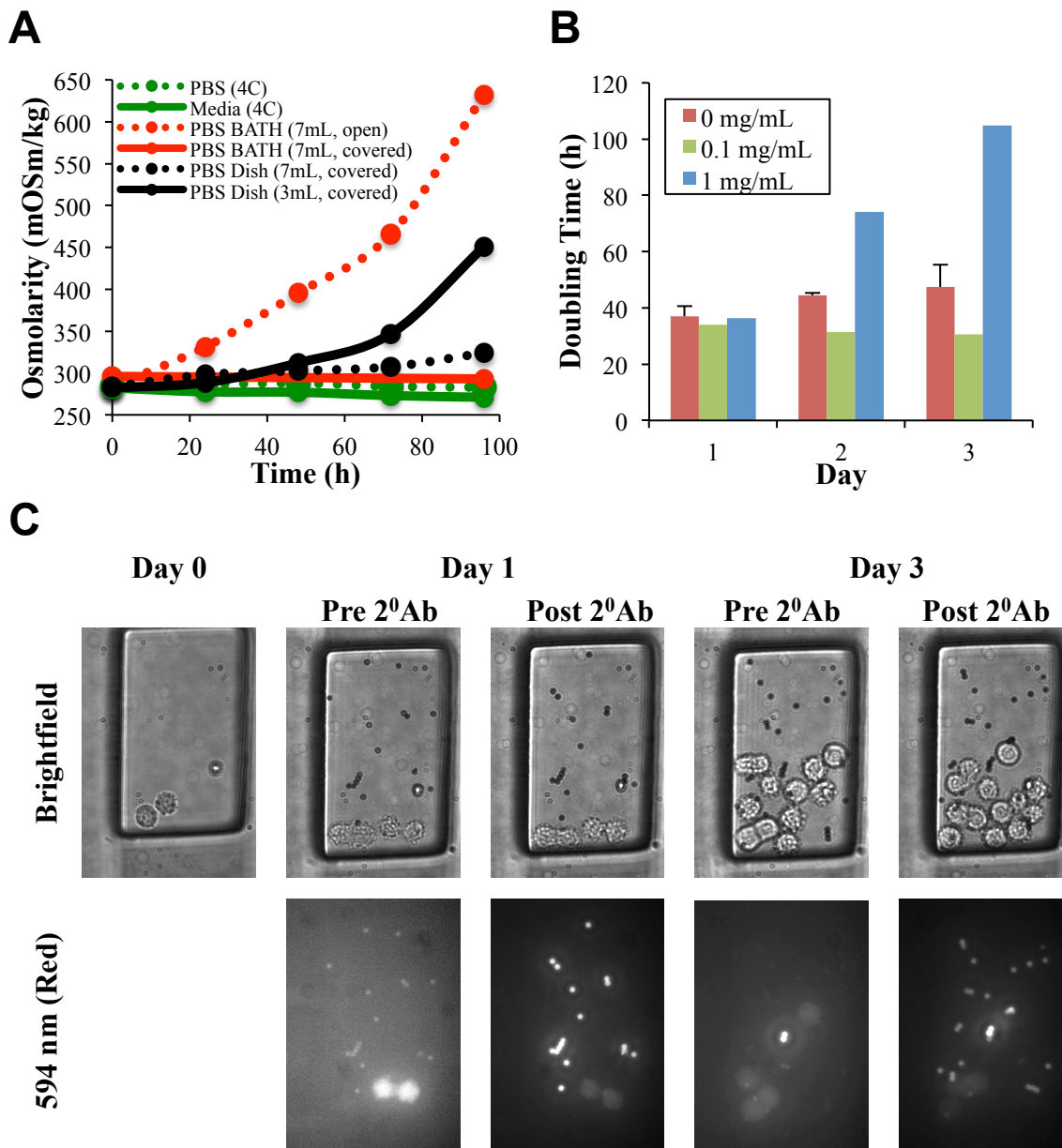


Figure 3.5 Microfluidic productivity assessments during clonal CHO culture

(A) Osmolarity of batch pate controls and osmotic bath over 4 days of microfluidic cell culture under varying conditions. (B) CHO-S D2 doubling times during microfluidic cell culture with varying concentrations of magnetic beads (0 – 1 mg/mL). (C) Brightfield and fluorescent images over 3 days of clonal cell culture in conditioned medium.

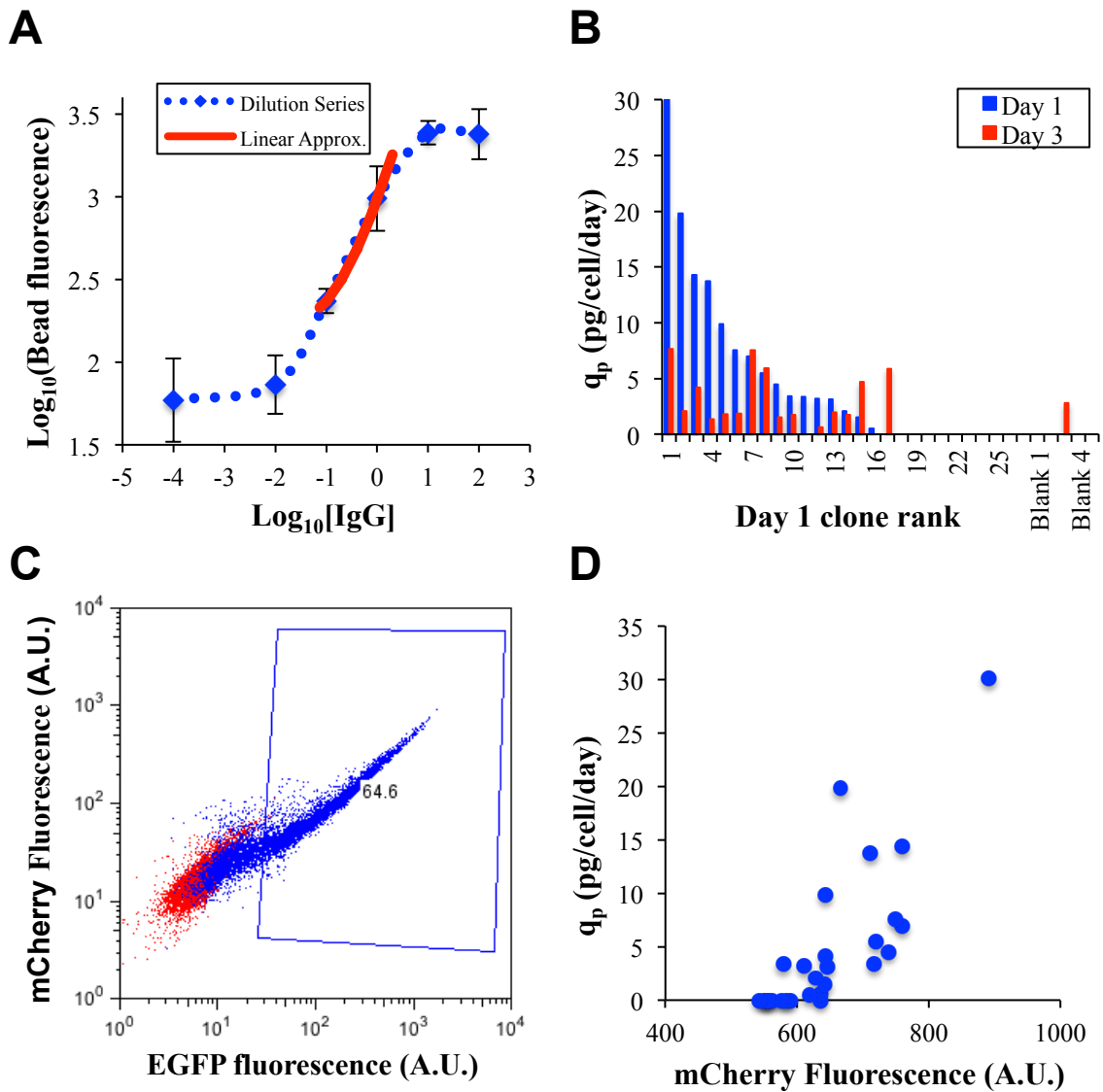


Figure 3.6 Microfluidic clone ranking in fed-batch conditioned medium

(A) Manual bead intensity analysis for fixed IgG concentrations in microfluidic chambers. Linear approximation is used to calculate titers in linear region of isotherm. (B) 27 clones grown in microfluidic chambers ranked by day 1 q_p via manual bead intensity analysis. (C) Intracellular fluorescence flow cytometry profile of dual reporting (Heavy Chain = EGFP, Light Chain = mCherry) CHO-S D2 clone. (D) Correlation

between measured q_p and intracellular fluorescence on day 1 for CHO-S D2 clones in microfluidic device.

Chapter 4 Microfluidic Cell Culture for the Clonal Analysis of hESC Populations

4.1 Introduction

Human embryonic stem cells (hESCs) are defined by their ability to generate precursors of all three germ layers as well as undifferentiated progeny with the same potentialities¹²⁹. The self-renewal property of hESCs allows them to serve as an essentially unlimited source of cells for research and therapeutic purposes. hESCs and their derivatives also display heterogeneity in their outputs as they expand in microenvironments or specialized niches that induce their differentiation^{168,169,298}, and this heterogeneity is also seen when hESCs are induced to differentiate *in vitro*. Heterogeneity within hESC cultures also affects the fate of their progeny^{149,152,181}, and this can result in the manifestation of diverse self-renewal and differentiation capacities at a clonal level^{151,174,299}. For clinical applications, such heterogeneity is a significant issue, as incompletely differentiated cells carry a risk of tumorigenesis³⁰⁰. Thus there is a real need for an improved understanding of the determinants of hESC heterogeneity, and analytical methods to analyze their extent and control^{165,301,302,303}.

The very low survival and plating efficiency of isolated hESCs (<1%) has historically posed a significant obstacle to assessing their growth and differentiation at a clonal level^{130,170,171}. Typical hESC protocols have thus involved passaging cells in clumps, and averaging results from many colonies³⁰⁴. Attempts to circumvent conventional passaging techniques or improve plating efficiencies tend to promote

chromosomal abnormalities such as trisomy 12 and 17^{305,306,307}. Culturing cells with Y-27632 Rho-associated kinase inhibitor (ROCK inhibitor) has been shown to increase plating efficiencies, but can also be accompanied by other effects that compromise the usefulness of this approach^{172,308,309,310}. A subline of CA1 hESCs (CA1S) was recently isolated that had been adapted to grow efficiently at low densities to enable colony formation from approximately 25% of plated cells, while still retaining essential hESC properties, including a normal karyotype, expression of standard pluripotency markers, and the ability to generate cells of all three germ layers¹⁷⁵. However, detailed genome analysis did reveal that the increased plating efficiency was associated with the duplication of a 3.8MB segment of chromosome 20, a known hESC mutation hotspot previously associated with enhanced hESC survival^{176,177,178}. Nevertheless, the high plating efficiency of this cell line and its generally preserved hESC properties make it very useful for clonal studies of the heterogeneous growth patterns displayed by the progeny of individual hESCs.

Integrated microfluidic systems have been widely recognized for their utility in implementing large numbers of single-cell cultures while providing enhanced control over medium conditions, and minimizing reagent costs, time and labor^{13,14,206,311,312}. These features have been exploited in the design of various types of cell culture devices for analyzing the growth of single bacteria²²⁴, yeast²²⁵ and various types of mammalian cells^{237,240,241,249,313}, including mouse ESCs that are normally passaged as single cells²⁴³. However, the use of microfluidic devices to analyze hESC growth has been largely restricted to devices containing small numbers of relatively large chambers (>1 mm² in

area)^{233,234,235,248,314,315,316,317,318}, with limited reports of single hESC colony cultures in <650 nL volumes^{234,248,315}.

The design and use of a semi-automated microfluidic device capable of culturing and analyzing up to 160 clonal CA1S hESCs in 25 nL chambers at single-cell resolution is now described. This device includes an automated Matrigel coating step, manual loading of hESCs in single-cell suspensions, dynamic and automated scheduling of medium perfusion, recoverability of cells for downstream analyses, and live-cell imaging of the cultures over a one week period of incubation. The use of this device to analyze the clonal growth of CA1S hESCs¹⁷⁵ demonstrates its ability to reveal the heterogeneity of differentiation patterns displayed by clonally tracked hESC.

4.2 Materials and Methods

4.2.1 Microfluidic device design and operation

A 160-chamber microfluidic device (Figure 4.1A) was fabricated out of polydimethylsiloxane (PDMS) (RTV 615, GE Advanced Materials, Wilton, CT) using standard multilayer soft lithography techniques^{191,194} and the push-up valve geometry; it included a 3 cm by 1.5 cm iso-osmotic bath (to accommodate ~2 mL of medium)²⁴¹. Microfluidic channels were 200 μm wide and 25 – 30 μm high with a rounded profile (for valving) made by re-reflowing the photoresist layer. This channel height allowed for the unrestricted flow of single hESCs (~17 μm in diameter measured using an automated cell counter) (Cedex, Roche Innovatis, Bielefeld, Germany) into the culture chambers. Six fluidic inputs (connected to a binary tree multiplexer) enabled single cells (or other reagents) to be delivered to 16 columns of 10 culture chambers. The multiplexer valves

were also connected to a binary tree at the waste end of the device to keep reagents from reaching any of the other chambers via backflow during switches in valve actuation. Inclusion of a series of 10 row selector valves along the right side of the device allowed individual chambers to be separately addressed. A peristaltic pump, consisting of three valves in series located above the waste outlet, controlled the separate delivery of materials into each chamber. Pump dosage was restricted using the number of pump actuation cycles and the flow speed (given by the pressure drop across the system, usually 10 psi). Typically, the pump delivered ~0.4 nL per cycle, with each cycle lasting 100 – 1000 milliseconds.

4.2.2 Cell culture

CA1S cells¹⁷⁵ were maintained in mTESR1 basal medium (STEMCELL Technologies, Inc., Vancouver, BC, Canada) with added penicillin (100 U/mL), streptomycin (100 µg/mL) and amphotericin B (0.25 µg/mL) (Invitrogen, Carlsbad, CA, USA). As in previous reports, ROCK inhibitor^{172,319} was not used for the culture of CA1S cells¹⁷⁵. For passaging, the cells in 4 – 8 day cultures were washed with PBS prior to being detached with TrypLE Express (Invitrogen, Carlsbad, CA, USA) at 37°C for 10 min, counted and transferred into new tissue culture dishes containing a pre-coated layer of 1:30 diluted Matrigel (Becton Dickinson, San Jose, CA, USA) and mTeSR1. To induce differentiation, the mTeSR1 medium was replaced 24 or 72 h later with Dulbecco's Modified Eagle Medium Nutrient Mixture F-12 (DMEM/F12) (Invitrogen, Carlsbad, CA) supplemented with 10% fetal bovine serum (FBS; Sigma, St Louis, MO) and the same antibiotics.

4.2.3 Microfluidic hESC culture

Prior to each experiment, a newly fabricated (**Appendix B**), sterile device (chips were cured at 80°C for a minimum of 3 days) was dead-end filled with filter-sterilized PBS and incubated overnight at 37°C in humidified 5% CO₂ in a custom incubator system to prime the channels and chambers for substrate coating (Figure 4.1B). The osmotic bath was then filled with mTESR1 to equilibrate the osmotic and gaseous content throughout the device. The next day, a sterile solution of Matrigel (1:30 diluted in DMEM/F12; Becton Dickinson, San Jose, CA, USA) was incubated in the culture chambers for 45 min at room temperature while the separate cell inoculation channels were flushed with mTESR1. The chambers were then also flushed with mTESR1 to prevent the Matrigel from solidifying in the chambers. A single-cell suspension of 10⁶ CA1S cells/mL was then manually seeded into the separate inoculation channels (with microscopic monitoring), one chamber at a time to achieve the deposition of a single cell into each chamber. The channels were then flushed again with mTeSR1 to remove any leftover cells in the channels and the microfluidic device then incubated at 37°C in humidified 5% CO₂ overnight to allow for the cells to attach. Cell growth was subsequently monitored for 96 – 192 h depending on when chambers became confluent. During this period, the entire system (including the Leica DMI6000B microscope [Leica Microsystems GmbH, Wetzlar, Germany] equipped with a motorized X-Y stage used to image the cells) was contained in an environmental chamber heated to 37°C and supplied with humidified 5% CO₂ at a rate of 46 mL/min to maintain this CO₂ level in the device. Custom software developed using Labview (National Instruments, Austin, TX, USA) was used to image the cells in each chamber with a 10× objective every 3 h using differential

interference contrast (DIC) microscopy. The medium in each chamber was replaced 4 times daily with ~100 nL of medium via peristaltic pumping under the control of custom Labview software. At the end of each experiment, cells in the device were incubated with 5 µg/mL Hoechst 33342 dye for 10 min at room temperature to stain the nuclei and obtain a final cell count. Hoechst stained colonies were imaged using DIC and fluorescence microscopy. Individual nuclei were manually counted using ImageJ software (NIH, Bethesda, MD, USA) to determine the final cell count for each chamber image. Specific growth rates were calculated using the initial cell count (a single cell), the final Hoechst stained cell count, and the time of culture. Colony areas were derived from DIC images by manually tracing out each colony using ImageJ software, returning a value in pixels. The areas in pixels were converted to µm² by using the channel width (200 µm) in each image as a reference. Final area per cell was calculated by dividing the colony area in the final DIC image by the final cell count for that chamber (calculated via Hoechst 33342 staining).

4.2.4 Colony recovery and RT-qPCR

To recover live cells from the device, the chambers were first flushed with PBS to remove floating (dead) cells or extra-cellular debris. The adherent cells were then detached using TrypLE (30 min at 37°C) and eluted with mTeSR1 through the outlet port into PTFE tubing connected to a 2 mL syringe. The contents of each syringe were then expelled into a well of a 24-well plate (pre-coated with Matrigel and containing 0.5 mL of mTESR1) and the cells expanded further for 7 days for additional analyses.

For RT-qPCR analyses, the cells in all chambers were lysed simultaneously in the device using a chemical lysis buffer (100 µL lysis re-suspension buffer + 10 µL lysis

enhancer solution) from the Cells Direct kit (Invitrogen, Carlsbad, CA, USA). The lysis reaction was performed with the device at room temperature for 10 min, followed by heat inactivation of the lysis reagent at 70°C for 10 min (on a flatbed thermocycler). Extracts from each chamber were then eluted through the outlet port into individual 0.5 mL microcentrifuge tubes using 7 – 10 μ L Ultrapure H₂O with thorough flushing between separate chamber harvests to minimize chamber cross-contamination.

OCT4 and GAPDH transcript levels were measured in a one-step RT-qPCR reaction using the Cells Direct kit in 25 μ L reactions and cycles of 20 min at 50°C for RT, followed by a hot-start at 95°C for 2 min, and 50 cycles of 15 s at 95°C and 45 s at 60°C. GAPDH transcripts were measured using Assay: Hs02758991_g1 from ABI (kit primer sequences were proprietary and not disclosed). OCT4 (POU5F1) primer sequences (obtained from RTPrimerDB* and synthesized by Biosearch Technologies) were ACC CAC ACT GCA GCA GAT CA (forward) and CAC ACT CGG ACC ACA TCC TTC T (reverse), the detection probe was Quasar670-CCA CAT CGC CCA GCA GCT TGG-BHQ-2 and the RT primer was TTG TGC ATA GTC GCT GCT TGA T. OCT4 transcript levels were normalized to GAPDH values using the $\Delta\Delta$ CT method³²⁰ where the mean Δ CT (OCT4 CT – GAPDH CT) for recovered clones grown in mTESR1 was taken to be Δ CT_{ctrl} and any chambers with GAPDH CT values greater than 23.6 (i.e., 2 SDs below the mean no template control (NTC) cycle threshold) were considered below the noise level of the assay and omitted from further analysis (Figure 4.2A and B). It should be noted that the OCT4 primer sequences were found to bind to multiple genomic sequences suggesting that non-specific amplification may have occurred during this assay. Control experiments omitting the reverse transcription step would be able to

determine the magnitude of non-specific amplification. However, a previous report has measured 988 ± 368 copies of the OCT4 mRNA in undifferentiated CA1S cells, so any non-specific amplification would be ~ 2 orders of magnitude lower than the signal observed from the assay²⁰⁶. Off-chip dilution series for both GAPDH (Figure 4.2A) and OCT4 (data not shown) mRNA demonstrated detection sensitivity down to single-cell equivalents, and material recovered from different chambers showed little to no evidence of cross-contamination (Figure 4.2C-F).

4.2.5 Immunostaining

Cells in the device were washed with PBS, fixed in 4% paraformaldehyde for 10 min at room temperature and then blocked with a solution of 10% FBS, 1% BSA, 0.1% Triton X-100 in PBS for 45 min. Primary antibodies used were anti-OCT3/4 (2 $\mu\text{g}/\text{mL}$ Rat IgG; R&D systems, Minneapolis, MN, USA), anti-SSEA3 (4 $\mu\text{g}/\text{mL}$ Rat IgM; R&D systems, Minneapolis, MN, USA) and anti-TRA-1-60 (4 $\mu\text{g}/\text{mL}$ Mouse IgM; Abcam, Cambridge, MA, USA) diluted in PBS and incubated with cells overnight at room temperature. These were then detected using appropriate secondary antibodies (Cy5, Goat Anti-Rat IgG, 10 $\mu\text{g}/\text{mL}$; Cedarlane Laboratories, Burlington, NC, USA; Alexa 488, Goat Anti-Mouse IgM, 4 $\mu\text{g}/\text{mL}$; Invitrogen, Carlsbad, CA, USA; and Alexa 488, Goat Anti-Mouse IgM, 4 $\mu\text{g}/\text{mL}$; Invitrogen, Carlsbad, CA, USA) diluted in PBS and incubated with the cells in the dark for 2.5 h at room temperature. The primary antibody was omitted as a negative control. Cell nuclei were stained with 1 $\mu\text{g}/\text{mL}$ of DAPI (Invitrogen, Carlsbad, CA, USA) for 10 min at room temperature in the dark. Samples were imaged using DIC and fluorescence microscopy.

4.2.6 Flow cytometry

Cells were incubated with anti-SSEA3 (10 µg/mL Rat IgM; R&D systems, Minneapolis, MN, USA) or anti-TRA-1-60 (10 µg/mL Mouse IgM; Abcam, Cambridge, MA, USA) and then Alexa-488, Goat Anti-Mouse IgM (4 µg/mL; Invitrogen, Carlsbad, CA, USA) and positive live (propidium iodide-negative, PI-; Sigma-Aldrich, St Louis, MO) cells gated using CA1S cells that had been induced to differentiate for 3 weeks on gelatin in FBS as a negative control using FlowJo software (Tree Star, Ashland, OR, USA).

4.2.7 Statistical analysis

Data are reported as mean ± standard deviation unless otherwise noted. Statistical comparison of the cloning efficiency between microfluidic devices and reported values compared 143 clones over 2 microfluidic experiments to published results performed in triplicate; a two-tailed t-test was used to determine significance. Comparison of the OCT4 expression data included a Kruskal-Wallis test to see if there was a significant difference between all groups, followed by a Dunn test to find significant pairwise comparisons. Multiple comparisons were accounted for by using Bonferroni's method²⁹¹. 143 clones (2 experiments) in mTESR1 conditions were compared to 22 and 4 clones exposed to 110 and 134 h of 10% FBS respectively. Validation of microfluidic growth rates was performed in triplicate when comparing with plate controls in mTESR1 conditions; a single experiment comparing plate controls to the microfluidic chip was also performed under DMEM/F12 + 10% FBS conditions for 72 h (Figure 4.3A).

4.3 Results

4.3.1 Design features and clonal culture performance

A multilayer soft lithography PDMS microfluidic device was designed with 160 culture chambers, each 25 nL in volume (500 μm x 500 μm x 100 μm). To enable scalable and robust culturing of hESC clones that would display comparable proliferation kinetics and plating efficiencies to those seen in macro-scale cultures, several additional design elements were incorporated. This included an “iso-osmotic bath” above the individual culture chambers that mimicked a strategy that was previously found to work for primary hematopoietic cells^{224,241,250}. Separate flow channels were designated for Matrigel coating and cell loading to prevent upstream cell attachment in channels during inoculation. Integrated microvalves were also used to control a fluidic de-multiplexer to allow each chamber to be individually supplied with up to 6 different reagents during an experiment, and a peristaltic pump to allow precise flow control. Finally, environmental control during cell culture was achieved using a custom heated enclosure, used to maintain the entire microscope at 37°C, and a secondary enclosure, surrounding only the microfluidic device, through which humidified 5% CO₂ in air was passed (Figure 4.1B).

Using this device, growth rates of CA1S could be obtained that consistently matched those measured in 6-well plates under both maintenance (mTESR1) and differentiating conditions (DMEM/F12 + 10% FBS) (Figure 4.3A). Immunostaining results further showed that undifferentiated cultures of CA1S cells grown in the device

maintained expression of OCT4, SSEA3 and TRA-1-60 at levels typical of conventional cultures and previous microfluidic reports (Figure 4.3B)^{236,237}.

The device was then used to compare the clonal growth potential of CA1S cells maintained in mTESR1 medium for 165 and 190 h with that of cells maintained in parallel (in the same microfluidic device), but exposed for the last 134 and 110 h, respectively to DMEM/F12 supplemented with 10% FBS to induce CA1S cell differentiation¹⁷⁵. Cells initially settled and spread on the Matrigel coated surface of each chamber; within 72 h $48 \pm 10\%$ of the cells had produced at least two progeny (143 clones in 2 devices). Notably, this was significantly ($p = 0.04$, t-test) higher than the $24 \pm 4\%$ cloning efficiency of these cells measured after 24 h in conventional cultures¹⁷⁵. Single input cells proliferated to form colonies in both mTESR1 and after FBS exposure (Figure 4.4A and B). While tracking colonies throughout the experiment, DIC images were analyzed to calculate colony areas at multiple time points and this was used as a quantitative measure for tracking cellular growth²³⁴. Figure 4.4C also shows the evolution of colony area for clones under both maintenance and differentiating conditions.

4.3.2 Quantification of cell proliferation and colony morphology

Upon reaching confluence in the mTESR1 cultures, final cell numbers were determined by introducing Hoechst 33342 dye to count individual nuclei, and this was used with end-point DIC images to calculate the final average area per cell for each chamber (Figure 4.4D). For cells cultured in only mTESR1, the average cell area was $511 \pm 351 \mu\text{m}^2$, whereas after 110 or 134 h in FBS, the average cell area was increased to $1240 \pm 540 \mu\text{m}^2$ and $1100 \pm 770 \mu\text{m}^2$, respectively. Most colonies that formed in undifferentiated mTESR1 conditions had a well-defined border surrounding the colony

and reached confluence after 7 to 8 days (Figure 4.4A, Figure 4.5A). Colonies that formed in the FBS-containing medium had much less well-defined borders and did not reach confluence (Figure 4.4B, Figure 4.5B). The clones generated in the presence of FBS included a subset of more compact colonies with a broader distribution of cells of different sizes, as might be expected from a variable differentiation response to FBS (Figure 4.4D)³²¹. Hoechst 33342-stained colonies illustrating the morphological transition to a decreased nuclear to cytoplasmic area ratio for many of the clones obtained in the presence of FBS are shown in Figure 4.6A-C. Clones grown in serum-free mTESR1 yielded mainly compact colonies with more cells, while cells grown in FBS-containing medium yielded many colonies with fewer cells and a larger average cell area (Figure 4.6A-C). Individual clones also displayed pronounced heterogeneity in their growth dynamics (Figure 4.6D), with a decreasing doubling rate following their exposure to FBS (0.032 ± 0.006 cells/h in mTESR1 compared to 0.028 ± 0.004 and 0.018 ± 0.009 cells/h after 110 and 134 h in FBS, respectively). This trend did not seem to reflect altered efficiencies of clone formation, as 49% (35/72) and 30% (21/71) of the chambers with cells contained colonies after 1 week in mTESR1, whereas 47% (34/72) and 26% (19/72) of the cells exposed individually to 10% FBS in two experiments also generated clones.

4.3.3 Transcript analysis of recovered samples

To further assess the growth potential of CA1S cells generated in the microfluidic chambers, live cell recovery from a subset of chambers was performed via enzymatic dissociation followed by collection at the outlet port. Cell populations that were recovered from the device and subsequently expanded in 6-well plates displayed normal growth characteristics, as well as expected levels of expression of SSEA3 (>99%

positive) and TRA-1-60 (>99%) (Figure 4.7). RT-qPCR was next used to assess OCT4 transcript levels in extracts of individual colonies generated on the microfluidics chip. The levels of the test gene (OCT4) were compared to a housekeeping gene (GAPDH) and results are presented as relative gene expression compared to GAPDH using the $\Delta\Delta C_t$ method³²⁰. All chambers on the device were lysed simultaneously followed by the separate elution of each chamber into individual micro-centrifuge tube reactions. A total of 96 chambers were eluted (across 2 experiments) consisting of 18 NTCs (including empty, dead and re-eluted chambers), 41 chambers perfused exclusively with mTESR1, as well as 24 and 13 chambers exposed to 10% FBS for 110 and 134 h, respectively.

OCT4 and GAPDH transcript levels in the cells recovered from each chamber of each device were then measured by RT-qPCR, with GAPDH levels and Hoechst 33342 cell counts used for normalization. The magnitude of the decrease in mean OCT4 expression (1.00 ± 0.38 for mTESR1 compared to 0.73 ± 0.47 and 0.34 ± 0.56 fold expression for cells in FBS for 110 and 134 h, respectively) was similar to previous reports^{147,206}, as with the distribution of growth rates. However, the analysis revealed that individual clones exhibited considerable heterogeneity in OCT4 expression (Figure 4.8A)²⁰⁶, and the emergence of OCT4 negative clones as the cells differentiated. The distributions of clones exposed to 110 and 134 h of 10% FBS were also significantly different than those only exposed to mTESR1 ($p = 0.0249$ and 0.0242 respectively). A bimodal distribution of OCT4 expression in single hESCs differentiated under similar conditions has previously been observed²⁰⁶. Here this is extended with evidence that the bimodal distribution may also be observed at a clonal level (Figure 4.8A) however the data were not significantly bimodal according to Hartigan's dip test³²². It should be noted

that while these results raise an intriguing clonal origin of OCT4 heterogeneity in hESC populations, experiments testing single cell OCT4 expression across multiple clones, with clonal identity maintained, are needed to definitively answer this question.

Clonal OCT4 expression changes were compared to other on-chip measurements to determine the timing of observed shifts and the possibility that some responses were correlated. Colonies that proliferated more rapidly contained high OCT4 transcript levels (characteristic of undifferentiated hESCs), whereas a more slowly growing/low OCT4 expressing subpopulation emerged after 110 and 134 h of culture in FBS (Figure 4.8B). Slower growing clones were more variable in their OCT4 transcript levels as might be expected if a lengthening of the cell cycle preceded the down-regulation of OCT4 expression, consistent with previous observations that bulk cultures of CA1S cells do not normally show a decrease in OCT4 expression until after 7 – 10 days of exposure to FBS^{147,175,323}.

Similarly, clones exposed to FBS yielded mostly intermediate average cell areas ($\sim 1000 \mu\text{m}^2/\text{cell}$), with a subpopulation of clones having greater average cell areas ($\sim 2000 \mu\text{m}^2/\text{cell}$) and varied levels of OCT4 transcripts (Figure 4.8C). Clones exhibiting the least compact morphology ($\sim 2000 \mu\text{m}^2/\text{cell}$) were most likely to have lower OCT4 transcript levels, particularly after 134 h in FBS. Cell area was also negatively correlated with clonal growth rate (Figure 4.8D). Thus, by measuring and comparing several endpoints simultaneously in individual colonies produced under different conditions, the variable rates and consistency with which slower growing, lower OCT4 expressing, less morphologically compact cells emerged could be observed and the heterogeneity that

affects the onset of different features of differentiation in clonally tracked hESCs could be confirmed.

4.4 Discussion

In summary, the utility of microfluidic culture devices has been demonstrated through the multi-parameter analysis of hESC heterogeneity at a clonal level by coupling time-lapse microscopy with advantages of scalability, programmable and dynamic medium exchange, and the ability to recover either lysate or intact cells from specified clones. It is shown that by tracking cell proliferation, morphology and transcript levels, the heterogeneity of the clonal hESC responses may be resolved. The measurements revealed the emergence of an OCT4 negative subpopulation associated with a more reduced growth rate and a less compact cell morphology. The proliferative and morphological changes appeared to precede the drop in OCT4 transcript level, suggesting these could be leading indicators of a loss pluripotency. The loss of detectable OCT4 expression that is present at the clonal level was observed, suggesting that observed single cell variations in the expression of this transcript may be coordinated between cells derived from the same colony. On the other hand, clones that persist in an undifferentiated phenotype even under prolonged exposure to differentiating conditions were also observed. This again highlights the intrinsic heterogeneity of hESC populations and the need for clonal analysis.

It is expected that the main source of the observed inter-clonal variability is due to the existence of different classes of pluripotent and self-renewing clones within hESC cultures^{174,181,299}. Additional sources of heterogeneity may include differentiation towards distinct cell types during FBS exposure³²¹, or stochastic gene expression³²⁴. This study

highlights how microfluidic-based imaging may be used to evaluate clonal heterogeneity in hESC populations during the early stages of differentiation. The combination of single cell resolution and fluid-handling control should offer high potential for studying these cryptic population dynamics under a variety of directed differentiation protocols, including different combinations of cytokines and time-varying medium conditions²³⁷. Beyond hESCs, this capability might also be informative for analyses of variable subpopulation responses in other systems where they are not discerned in ensemble measurements performed on large numbers of cells.

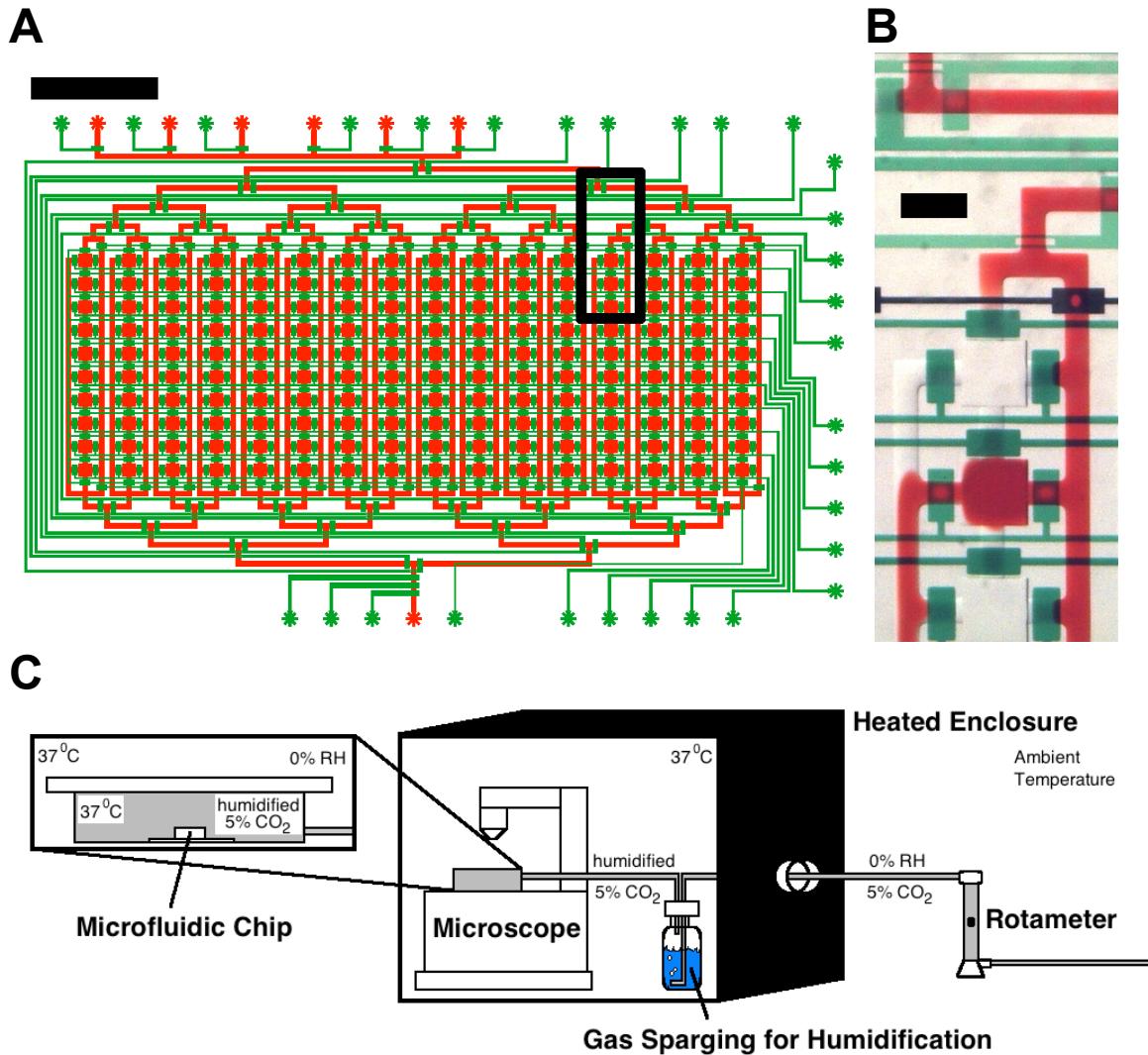


Figure 4.1 Design of the microfluidic culture device.

(A) Schematic of the device. Scale bar: 5 mm. Actuation of a column multiplexer and row valves connects an addressable array of 160 culture chambers (organized in 16 columns and 10 rows) to 6 sample inlets. The rectangular box indicates the region depicted in B. (B) Optical micrograph of array unit. To demonstrate functionality, the fluid path (of an individually addressed chamber) and control channels have been loaded with red and green dyes, respectively. Scale bar: 500 μm . (C) Schematic of the experimental setup. The device was placed inside an incubation chamber with 46 mL/min

flow of 5% CO₂/95% air, humidified using gas sparging. The entire system, including the microscope, was sealed in an enclosure heated to 37°C.

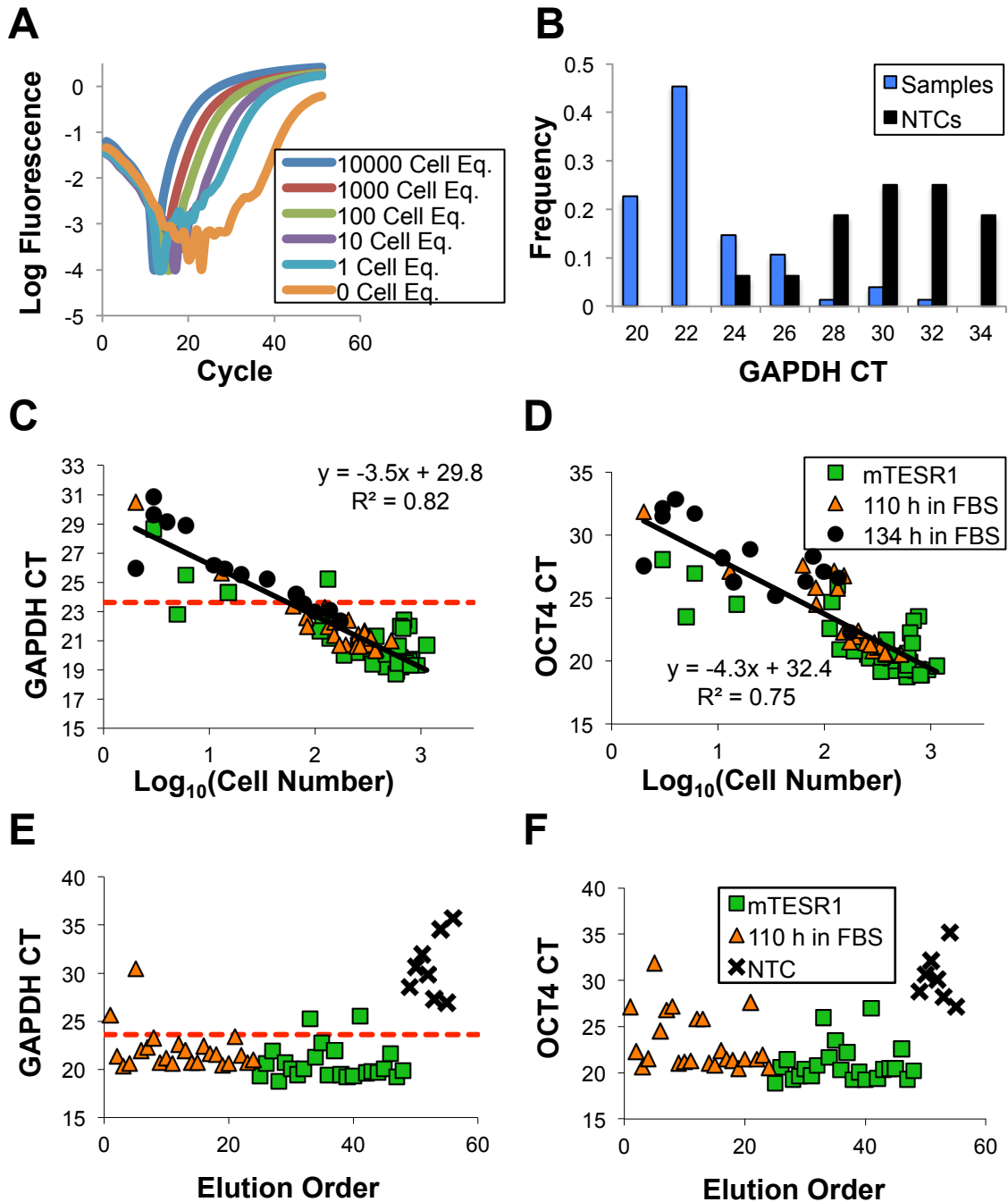


Figure 4.2 Validation of RT-qPCR analysis of clonal CA1S populations.

(A) Dilution series of GAPDH TaqMan assay performed on 10000, 1000, 100, 10, 1, and 0 cell equivalents. (B) Histogram of GAPDH CT values for all recovered samples and no template controls. (C) GAPDH CT versus number of cells counted using Hoechst 33342

for each chamber. Dashed red line is the GAPDH CT cutoff. **(D)** OCT4 CT versus number of cells counted using Hoechst 33342 for each chamber recovered. **(E)** GAPDH CT versus chamber recovery order for the 110 h differentiation experiment. Dashed red line is the GAPDH CT cutoff. **(F)** OCT4 CT versus chamber recovery order for the 110 h differentiation experiment.

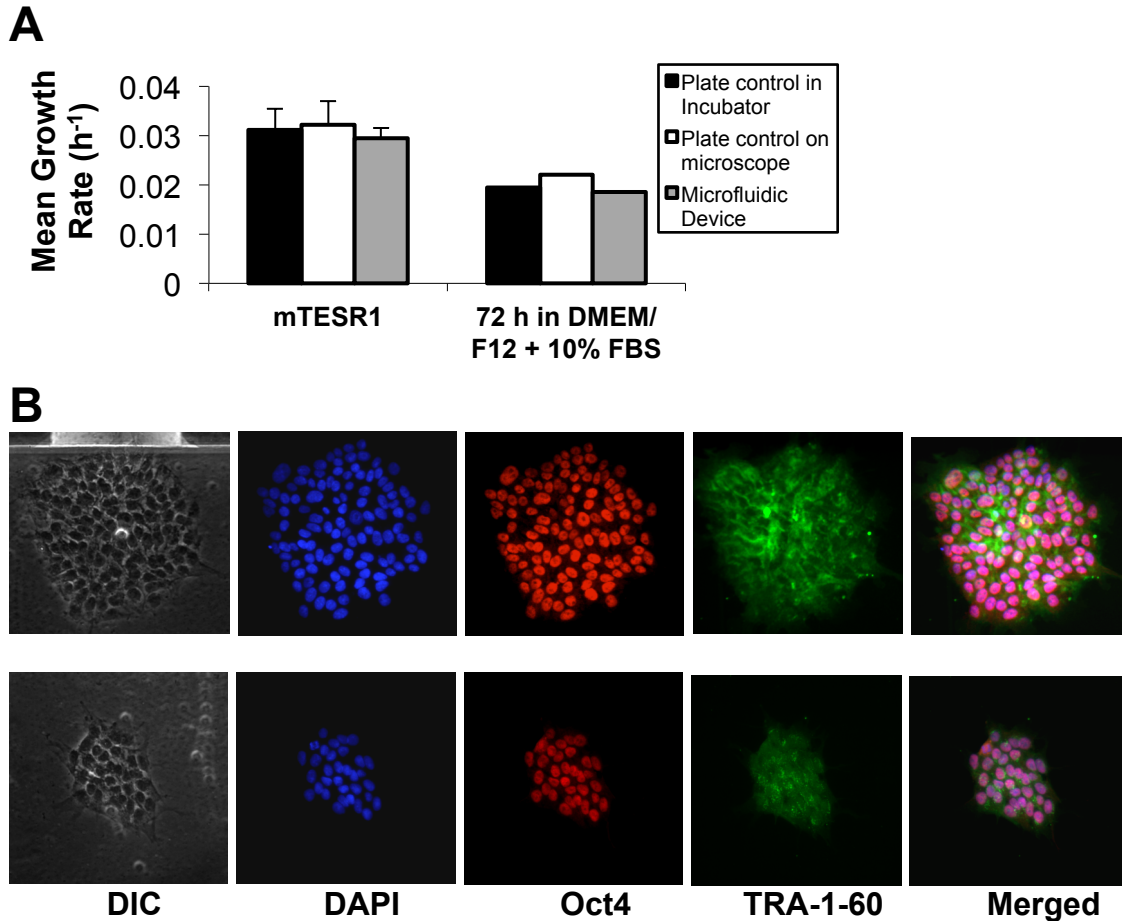


Figure 4.3 Validation of on-chip undifferentiated CA1S cell growth and immunohistochemical features.

(A) Mean cell growth rate (all chambers) compared to macroscale culture controls (grown in 22 mm tissue culture treated dishes) in mTESR1 or DMEM/F12 + 10% FBS. One 22 mm control dish was placed beside the device while the other was placed in a humidified, 37°C, 5% CO₂/95% air conventional incubator. **(B)** Fluorescent images performed on typical CA1S colonies after 96 h of culture. Scale bar: 200 μm. Merged images of DAPI, OCT4 and TRA-1-60 are shown on the right to illustrate the localization of each marker.

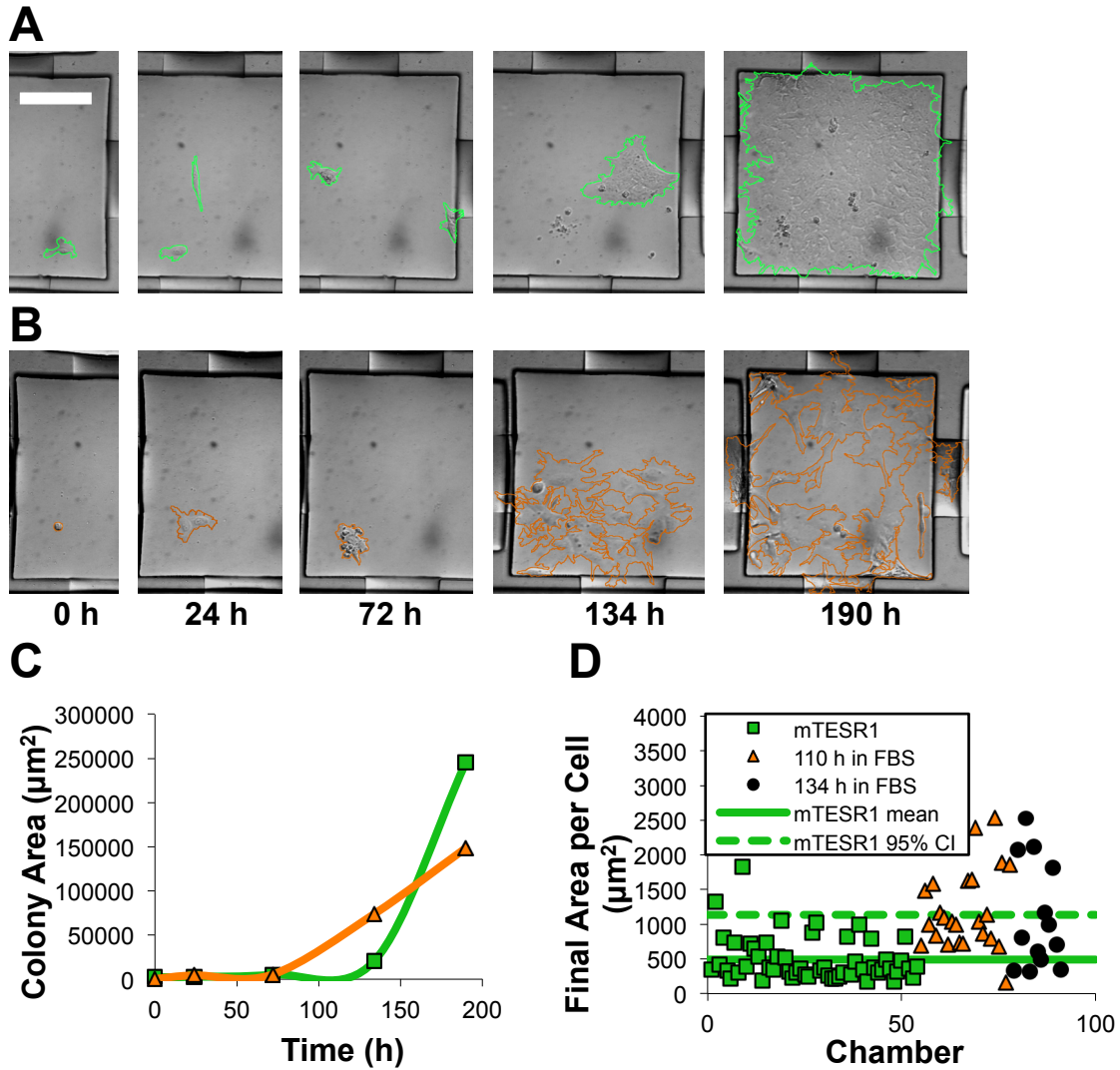


Figure 4.4 Effect of differentiation induction on CA1S colony formation.

(A) Phase contrast images illustrating typical undifferentiated colonies (scale bar: 200 μm). (B) Phase contrast images of CA1S colonies obtained under differentiating conditions. FBS was added after 72 h. (C) Evolution of the areas of the colonies shown in A (green) and B (orange) calculated by manually tracing the boundaries of the cell-covered area at each time point. (D) Area per cell for all colonies analyzed.

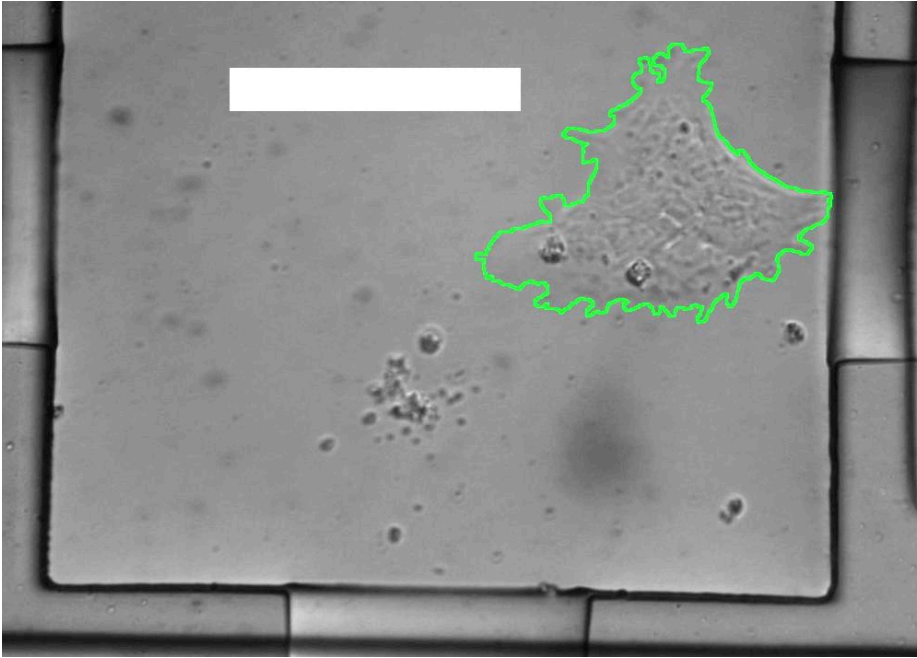
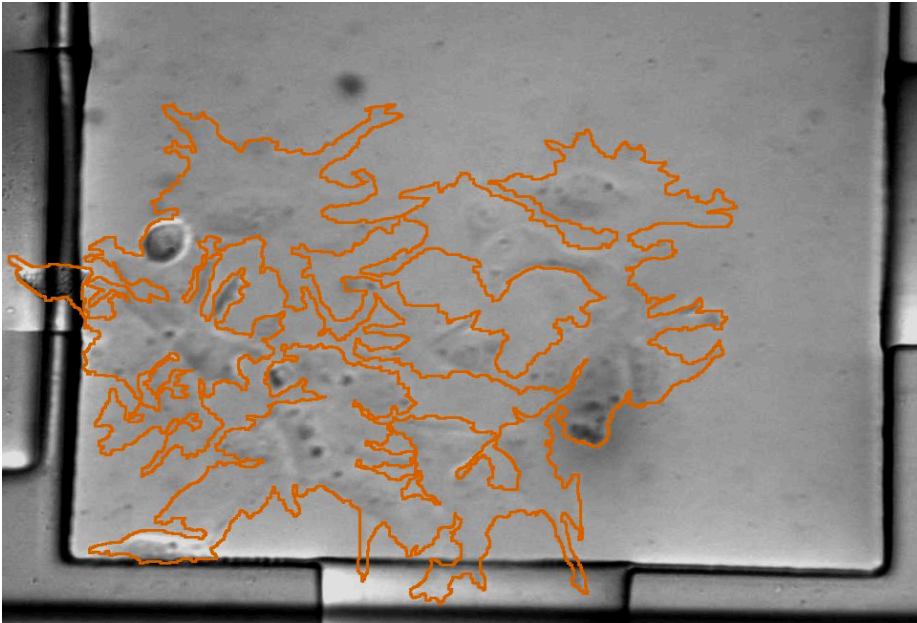
A**B**

Figure 4.5 Effect of differentiation induction on colony morphology.

(A) Enlarged phase contrast image illustrating typical undifferentiated morphology after 134 h in mTESR (scale bar: 200 μm). (B) Enlarged phase contrast image of CA1S colony under differentiating conditions at 134 h. FBS was added after 72 h.

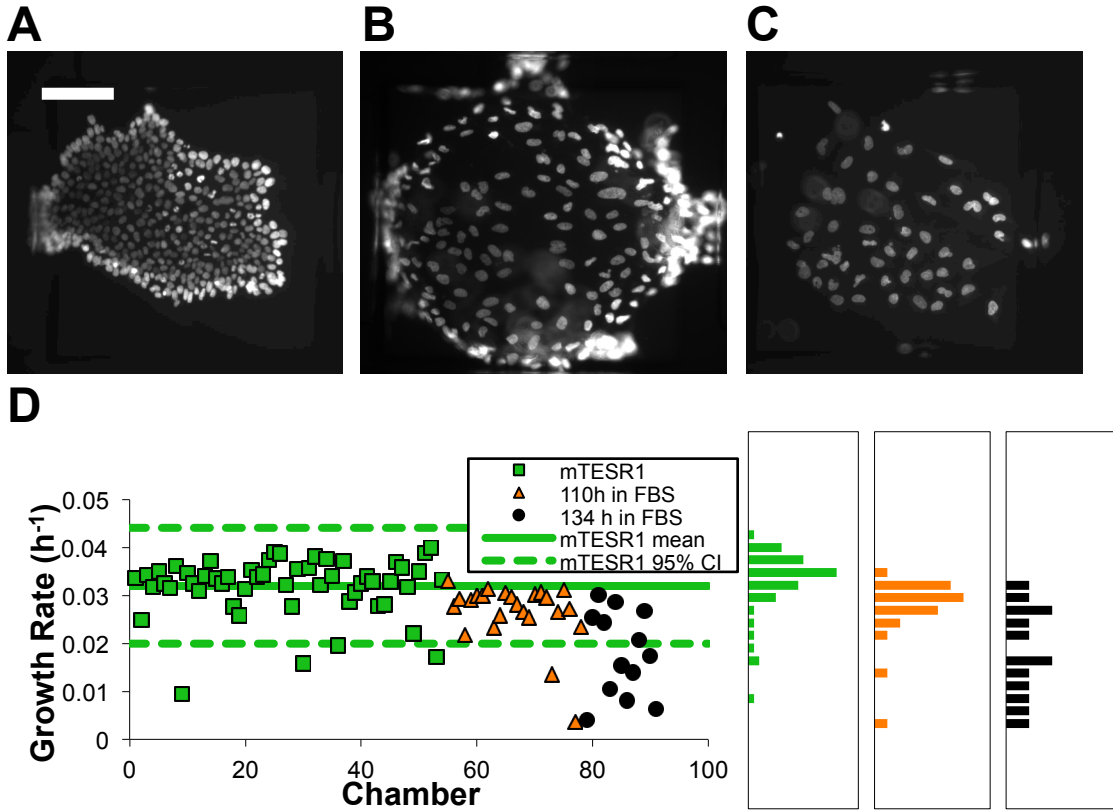


Figure 4.6 Growth rate heterogeneity of individual CA1S colonies.

(A) Colony stained with Hoechst 33342 after 190 h of growth in mTeSR1. (B) Colony stained with Hoechst 33342 after 190 h of incubation when exposed to 10% FBS for the last 110 h. (C) Colony stained with Hoechst 33342 after 165 h of incubation when exposed to 10% FBS for the last 134 h. Scale bar for A-C: 200 μm . (D) Distribution of growth rates for all colonies generated in mTESR1. Each point shows the data for a single colony and the solid and dashed green lines show the mean \pm the 95% confidence intervals. Histograms showing the distribution of growth rates for each condition projected onto the axis. Growth rates for each clone were calculated by enumerating the cells at the start (by DIC) and the nuclei (stained by Hoechst 33342) at the end of the experiment.

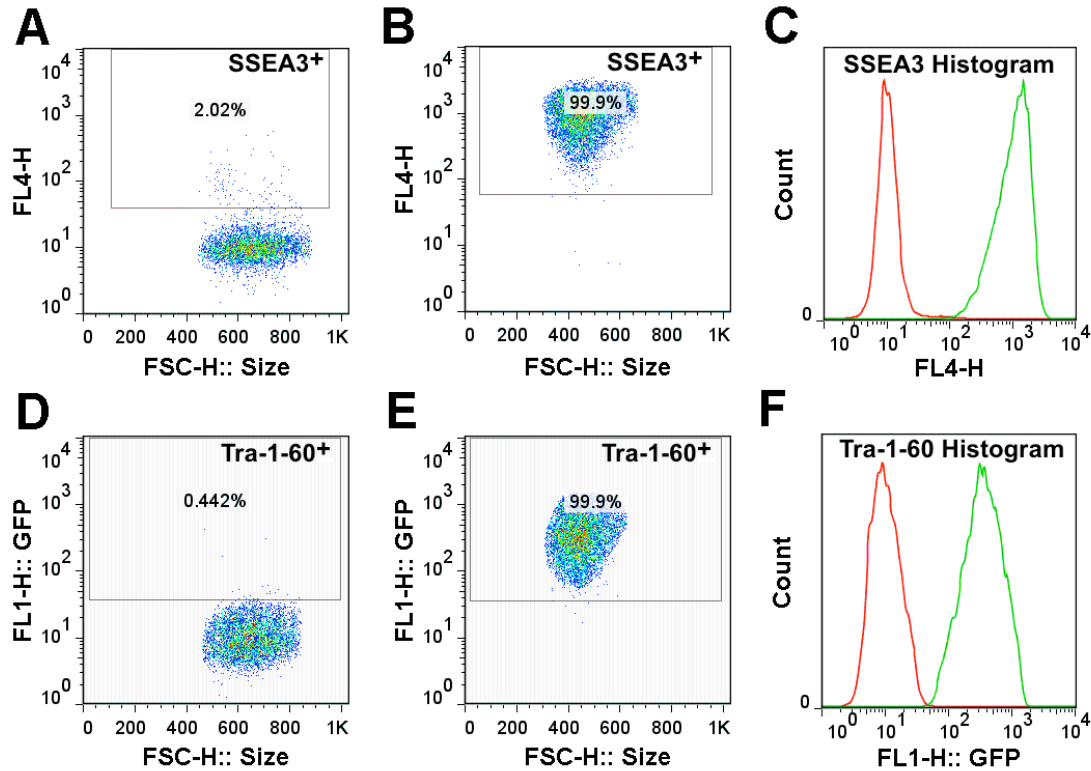


Figure 4.7 Flow cytometric analysis of CA1S cells before and after induction of their differentiation.

(A) SSEA3 expression [FL4-H channel] of CA1 cells differentiated in 22 mm tissue culture dishes for 3 weeks on gelatin in 10% FBS-supplemented medium. (B) SSEA3 expression [FL4-H channel] of undifferentiated CA1S hESCs recovered from the microfluidic device after 96 h and expanded for a subsequent 7 days in conventional cultures. (C) Histogram comparing SSEA3 expression between differentiated CA1 (red) and undifferentiated (>99% SSEA3+) CA1S (green) cells. (D) TRA-1-60 expression [FL1-H channel] of CA1 cells differentiated in 22 mm tissue culture dishes for 3 weeks on gelatin in 10% FBS-supplemented medium. (E) TRA-1-60 expression [FL1-H channel] of undifferentiated CA1S cells recovered from the microfluidic device after 96 h and expanded for a subsequent 7 days in conventional cultures. (F) Histogram comparing

TRA-1-60 expression between differentiated CA1 (red) and undifferentiated (>99% TRA-1-60+) CA1S (green) cells.

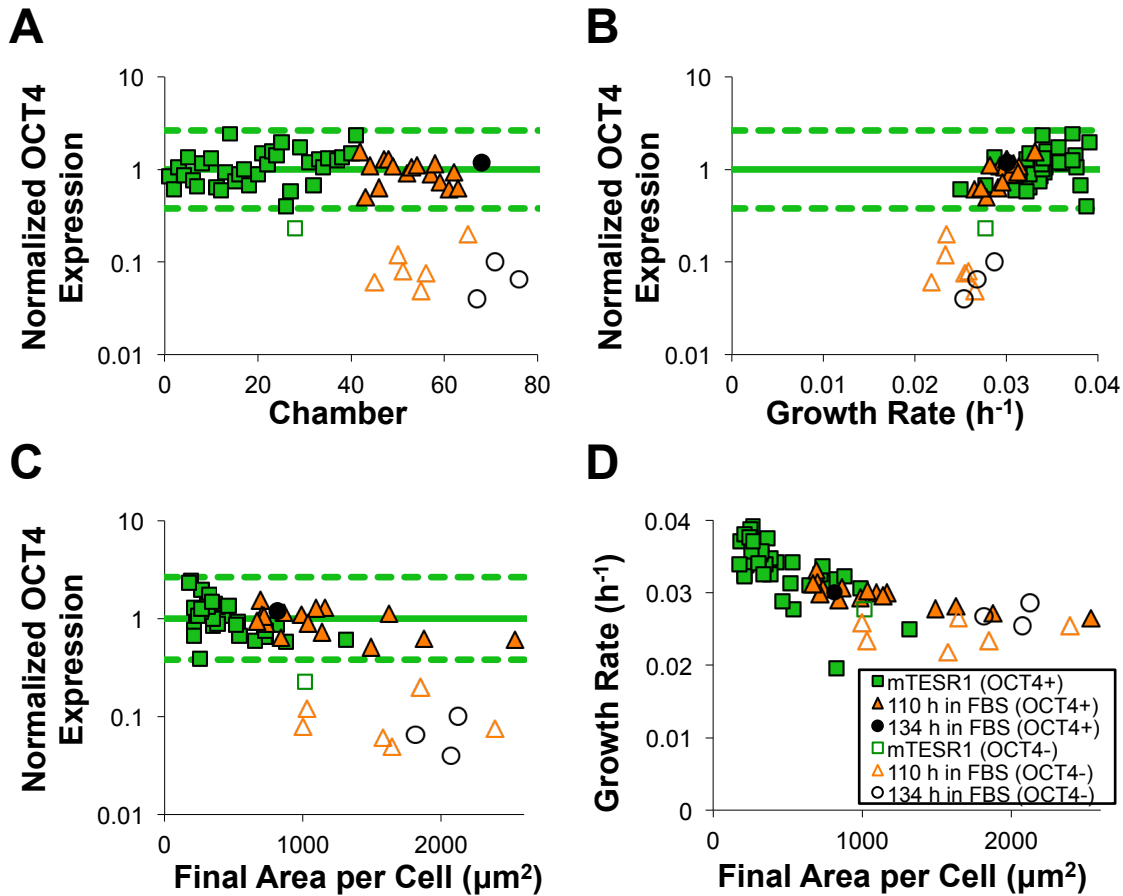


Figure 4.8 Heterogeneity in OCT4 transcript levels and relation to different culture conditions.

(A) Distribution of OCT4 transcript levels (data pooled from 2 experiments). Each point shows the result for a single colony and the green lines show the mean \pm the 95% confidence intervals. (B) Normalized OCT4 transcript level and growth rates for each colony. (C) Normalized OCT4 transcript levels and area per cell for each colony. (D) Growth rate and area per cell for each colony.

Chapter 5 Conclusions & Future Directions

This thesis set out to address the need for precise methods to assess cell populations at the clonal level through the use of small volume cell culture technology. By developing techniques such as conditioned medium perfusion and re-suspension, a dynamic single cell secretion assay and microfluidic clonal cell culture, this research has contributed to the tools available for screening and identifying important clones and subclones within heterogeneous mammalian cell populations. The efficacy of these methods was demonstrated by measuring clonal variability in two important mammalian cell systems: CHO cells and hESCs.

5.1 Significance of work

The ability to create a microenvironment capable of sustaining the robust growth of single cells is crucial when addressing fundamental questions about clonality and mammalian cell population heterogeneity. If clones are evaluated under less than ideal conditions, biological responses may be masked by variations due to environmental perturbation. This research has made a significant impact through the design and implementation of new methods to assess clonal heterogeneity and identify important sub-populations in mammalian cell systems. Moreover, these assessments were performed in conditions reflective of larger scales by taking advantage of the inherent high cell concentration in small volumes and through the perfusion and re-suspension of clones in conditioned medium. In particular, a method was devised to screen clonal productivity under simulated fed-batch conditions in both deep well plates and in a microfluidic setting, which outperformed traditional batch cultures. In the microfluidic

case, this technique was combined with a dynamic, sensitive magnetic bead assay to detect monoclonal antibodies secreted by single cells in nL volumes. This microfluidic system made multiple temporal measurements of the same clone over the course of a simulated fed-batch culture. This is superior to traditional early clonal evaluations that normally make a single measurement, and these often correlate poorly with scaled-up cultures. By combining a sensitive, dynamic microfluidic assay with precise microenvironmental control, the platform has the ability to greatly accelerate the time-consuming, expensive and laborious process of cell line selection.

Additionally, the establishment of a robust microfluidic cell culture system has allowed for the propagation of difficult to culture cell types such as hESCs. By coupling live-cell imaging with clonal recovery and transcript analysis an observation was made of the correlation of multiple cell culture variables as clones exited the pluripotent cell state. The microfluidic cell culture platform has provided new insight on stem cell fate decisions of single hESC colonies through the observed persistence of an undifferentiated clonal phenotype during prolonged exposure to differentiation. The research presented in this thesis has shown that robust microfluidic cell culture systems coupled with dynamic medium perfusion and sensitive single cell assays can evaluate clones in conditions that may not be feasible using traditional methods.

5.2 Future recommendations

5.2.1 Conditioned medium perfusion and re-suspension

The conditioned medium perfusion and re-suspension technique was demonstrated to be sufficiently robust when applied to multiple clones and cell lines.

However, additional experiments could be made in order to improve and further validate the process. For example, even though the 3 mL DWP CM re-suspension matched larger fed-batch cultures of the same clone, longitudinal studies expanding and scaling up the specific clone to 25 mL, 125 mL and 3+ L have yet to be performed. In the future subsequent experiments should scale up the clones tested in the 3 mL system and demonstrate that the performance in DWP CM re-suspended cultures is predictive of future performance when the same clone is scaled-up to larger volumes. Additionally, although 3 mL DWP CM cultures have been shown to match the performance of both 25 mL and 125 mL shake flask fed-batch cultures, correlation to larger bioreactor scales has yet to be demonstrated. Ideally the CM re-suspended cultures would need to be compared to industrial sized bioreactors (200 to 20,000 L). A more practical comparison could use 3 L bench-top bioreactors, which generate results that have been shown to correlate well with large-scale manufacturing conditions⁷¹. Additionally, larger scale comparisons could include product quality assessments into the process to ensure that clones selected using the CM technique are secreting antibody that will be of eventual therapeutic value.

CM perfusion could be validated further in static culture systems. While CM perfusion was tested in a microfluidic setting, the larger 3 mL DWP CM re-suspension experiments were performed in suspension. Thus, CM re-suspension could next be examined in a static 3 mL system to determine which parameters are required to replicate fed-batch conditions in static cultures. As static cultures normally suffer from diffusion limitations, replicating a suspension fed-batch environment in a static plate will likely prove to be non-trivial. Perhaps a G-Rex culture system should be used, providing oxygen through a silicone membrane at the bottom³²⁵. Also, microfluidic cultures, which

outperformed static batch cultures side-by-side, should be compared to suspension fed-batch cultures to determine how closely CM perfusion in a microfluidic system can mimic bioreactor perfusion.

CM culture experiments could also be extended to 14 days to more closely replicate a fed-batch system. For reasons of feasibility and to double the experimental throughput the experimental time was shortened from 14 to 7 – 8 days. However, as the majority of the product titer generation occurs between days 8 and 14 in a fed-batch bioreactor it would be prudent to evaluate and further validate the CM re-suspension and perfusion technique over the course of 14 days to ensure that the specific productivity is maintained later in the culture. Additional experiments could also modify the CM re-suspension protocol (perhaps including more medium from peak VCD days) to maximize the viable cell density and the specific productivity, extending the culture as long as possible. Re-suspending cultures in CM from later fed-batch days could reduce the culture performance due to depletion of nutrients and buildup of metabolites.

Lastly, to further improve the CM perfusion and re-suspension technique, the individual medium components of the CM could be examined. A significant effect on performance was demonstrated when the cell concentrations of the individual cultures were matched as opposed to when the day of parental CM culture was used. Therefore, there could be at least several critical medium components at play. Further experiments observing the levels of medium components such as glucose, lactate, essential metals or minerals and amino acid could provide a mechanistic understanding of the cause for increased performance of the cell concentration matching. Possible causes could include glucose or amino acid deprivation and lactate inhibition. If the CM perfusion technique is

to be widely adopted in a manufacturing setting, complete characterization of medium components may be desired.

5.2.2 Microfluidic clone selection

The microfluidic bead assay was sensitive enough to detect IgG secreted from single CHO cell clones over multiple culture days. The bulk specific productivities measured on the device matched mean productivities of the same clone in larger scale cultures (3 mL and 25 mL). While this is a significant advancement in the field of single cell analysis, further validation should ensure these measurements reflect true clonal productivity. First, subsequent experiments could recover clones from the device and scale them up to determine if microfluidic clonal measurements predict later performance. Microfluidic clonal recovery and scale up has previously been reported on hematopoietic stem cells²⁴¹. Clones should first be expanded into 3 mL DWP cultures where their performance under microfluidic CM perfusion conditions could be compared to later 3 mL DWP CM re-suspension productivity. At the DWP stage (and larger scales), product quality evaluations could also be incorporated into the selection process to add additional stringency. Following this, clones could be scaled up to 125 mL and 500 mL shake flasks or even 3 L instrumented bioreactors, to test whether microfluidic measurements predict larger scale performance. Results from these experiments could explain whether the intraclonal variability observed in the CHO-S D2 line using the microfluidic platform is due to permanent high producing subclones or are temporary states of high productivity, as reported previously¹⁰⁵. These longitudinal scale-up studies should also be performed on clones selected from transfected pools to determine if the

microfluidic device platform has the ability to generate high producing stable cell lines from a transfected population.

In addition to scale-up, the microfluidic assay could be modified to assess different antibody types or secretion rates. Currently the assay was optimized for a cell line (CHO-S D2) producing human IgG1 at ~ 2 pg/cell/day. As the dynamic range of the assay is between ~ 0.01 and 10 $\mu\text{g}/\text{mL}$ in 4 nL volumes, this would roughly correspond to clonal detection sensitivity between 0.5 and 500 pg/cell/day assuming a single cell in the chamber and a 2 h incubation time. As monoclonal antibody production cell lines can readily achieve >20 pg/cell/day²⁰, the assay thus has the dynamic range capable of detecting single high producing clones of manufacturing relevance. However, the assay may miss single cells producing below 0.5 pg/cell/day in the case of products that are not produced at high rates. For high producing clones (>20 pg/cell/day), assay saturation can be expected when there are >24 cells in the chamber (i.e. generating >10 $\mu\text{g}/\text{mL}$ in 2 h); this would occur within 6 days of microfluidic culture assuming a doubling time of ~ 30 h. Thus, to observe higher producing clones at later stages of culture, the assay would need to be modified to allow for higher titers to be measured; this could be achieved in several ways. First, the bead incubation time could be shortened at later culture times to avoid saturation. Also, microfluidic chamber volumes could be increased thereby effectively decreasing the incubated antibody concentration and increasing the saturation point. Increasing microfluidic chamber bottom area would have the added advantage of extending the monolayer culture time and allowing for more expansion in the microfluidic array prior to recovery and scale-up. Analogously, if the assay needed to be specialized to screen clones secreting below the current limit of detection, the assay times

could be lengthened and chamber volumes reduced to increase the assay sensitivity. For such lower producing clones it should be feasible to wait until the later days of culture (when there are up to 100 cells in the chamber) prior to making a measurement.

Although designed to detect human IgG1 secreted in a defined productivity range, the assay could also be modified to detect other target antibodies. Since Proteins A & G non-specifically bind to multiple antibody types (albeit with different affinities), the beads could assay a variety of targets with minimal changes to the protocol. For applications to other antibody types, the binding kinetics of the target (as well as their level of secretion in the clone of interest) would dictate the incubation time required for detection (and also possibly the chamber volume required)²¹⁶. Appropriate fluorescently labeled secondary antibodies would be needed to for each new detection system. Lastly, downstream product characterization may also have to be incorporated into the screening process for other antibodies to ensure that selected clones are also producing a high quality product. As long as a new secretion assay is designed with these parameters in mind, the technique should be applicable to a wide range of therapeutic monoclonal antibodies from many different species.

Additional areas of improvement for the microfluidic bead assay relate to increasing the throughput and improving automation. Thus far, the assay has a demonstrated throughput of 512 – 1024 chambers and up to hundreds of clonal cultures when stochastic loading is taken into account (i.e. with chambers being discarded if 0 or more than 1 cell at the start). As the current cell culture system contains 4 arrays with 2048 chambers each, the automated imaging and culture of up to 8192 chambers at a time is possible. When coupled with chamber autofocusing, this could allow for data

collection from thousands of clonal cultures essentially simultaneously²⁴¹. One current bottleneck in the system is the lack of automated bead segmentation for experiments involving cells. For thousands of clonal cultures to be analyzed practically, automated bead segmentation will be required. A bead segmentation algorithm was demonstrated which functions for fixed quantities of IgG when beads are loaded at 1 mg/mL. However, the algorithm does not segment beads properly at lower concentrations. Modification of the current bead segmentation algorithm for chambers containing less than ~50 beads (i.e. at the 0.1 mg/mL bead concentration used for cell experiments) should provide an automated and more precise way to assess titers. An improved algorithm would also ideally segment intracellular fluorescence intensities so that reporter expression in the CHO-S D2 clones could be analyzed and compared to clonal secretion in an automated fashion.

5.2.3 Microfluidic human embryonic stem cell culture

The ability to isolate and culture individual hESCs in nL volumes provides an excellent template for further study of individual stem cell fate decisions. By witnessing the loss or persistence of detectable OCT4 during early exposure to differentiating conditions (<7 days) the results have suggested that transcript expression within the same colony may be coordinated. Previous single cell measurements on OCT4 transcript levels have demonstrated the same magnitude of down-regulation during the first week of differentiation²⁰⁶. However, it is not known whether the single cells losing (or retaining) OCT4 expression are derived from the same or different colonies. Future clonal experiments could address this issue by recovering single hESC colonies after culture and subsequently performing microfluidic single cell RT-qPCR²⁰⁶ for OCT4 on a colony-by-

colony basis. Results of such experiments could provide valuable information on the mechanism of stem cell fate decisions within single hESC colonies and whether responses of neighboring cells are correlated. Other hESC transcripts or even microRNA's could be targeted in such experiments (along with current outputs such as growth rate and colony morphology), providing a more complete picture of how hESCs exit pluripotency during early differentiation.

Similarly, the microfluidic cell culture platform could be used in the future to examine cellular differentiation on timescales longer than 7 days. In such experiments clonal populations could be observed to differentiate towards more specialized lineages such as definitive endoderm¹⁴⁷ or pancreatic cell types¹²¹. Directed differentiation protocols would be more difficult to implement, however the dynamic fluidic control in the device would provide the advantage of automation and precise control of stimulus timing. For longer experiments, larger chambers may be necessary but this would depend on the growth and survival responses of the clones. As with previous experiments, it may be necessary to allow the hESC clones to establish colonies for 48 – 72 h prior to the induction of differentiation in order to increase the number of surviving progeny. The microfluidic system could also be used to screen and optimize new directed differentiation protocols varying parameters such as the exposure duration and level of each growth factor or cytokine²⁴¹. Brief pulses of stimuli (on the order of minutes to hours) are also programmable using this system; this could replace very time-consuming and laborious conventional culture methods.

Finally, the hESC microfluidic system could be applied to culture a wide range of adherent mammalian cell types including but not limited to fibroblasts¹⁴², mesenchymal

stem cells²⁴⁰ and induced pluripotent cells¹⁴⁴. For example, subsequent use of the device to culture fibroblasts could observe the transfection of such cells with the four Yamanaka factors *in situ*¹⁴⁴. If an inducible system (such as doxycycline) were to be used to transfect clones during live-cell imaging, the microfluidic platform could be used to examine the dynamics of cellular reprogramming towards induced pluripotency³²⁶. Again, the dynamic and programmable nature of the system would allow for transient stimulation of the starting population potentially uncovering new information about the stimulation threshold required to induce pluripotency or revealing a point of no return. When combined with temporal stimulation, the ability to culture single clones and subsequently analyze growth kinetics, morphology and transcript expression will undoubtedly allow us to probe the thresholds of cellular decision making on a variety of adherent cell types.

5.3 Final thoughts

The recent development of low cost, high-throughput single-cell analysis methods should lead to the widespread adoption of these technologies across the biotechnology industry. Although these tools have the ability to screen large numbers of clones very quickly they are often not performed under the proper microenvironmental conditions, potentially complicating comparisons to scaled-up cultures. The design and implementation of methods to screen clones under conditions reflective of stem cell niches and large-scale bioreactors should lead to the accelerated identification and selection of important sub-populations in heterogeneous pools of cells. The techniques reported in this thesis are a clear illustration how advances in clonal cell culture technology can provide new insight into cell line manufacturing and stem cell biology.

Bibliography

- ¹ Gest, H. The discovery of microorganisms by Robert Hooke and Antoni Van Leeuwenhoek, fellows of the Royal Society. *Notes and Records of the Royal Society of London* 58, 187-201 (2004)
- ² Gottesfeld, J. M., Neely, L., Trauger, J. W., Baird, E. E. & Dervan, P. B. Regulation of gene expression by small molecules. *Nature* 387, 202-205 (1997)
- ³ Rader, R. A. (Re)defining biopharmaceutical. *Nature Biotechnology* 26, 743-751 (2008)
- ⁴ Restifo, N. P., Dudley, M. E. & Rosenberg, S. A. Adoptive immunotherapy for cancer: harnessing the T cell response. *Nature Reviews Immunology* 12, 269-281 (2012)
- ⁵ McClellan, J. & King, M. C. Genetic Heterogeneity in Human Disease. *Cell* 141, 210-217 (2010)
- ⁶ Burrell, R. A., McGranahan, N., Bartek, J. & Swanton, C. The causes and consequences of genetic heterogeneity in cancer evolution. *Nature* 501, 338-345 (2013)
- ⁷ Graf, T. & Stadtfeld, M. Heterogeneity of embryonic and adult stem cells. *Cell Stem Cell* 3, 480-483 (2008)
- ⁸ Raj, A. & van Oudenaarden, A. Nature, nurture, or chance: stochastic gene expression and its consequences. *Cell* 135, 216-226 (2008)
- ⁹ Huh D. & Paulsson, J. Non-genetic heterogeneity from stochastic partitioning at cell division. *Nature Genetics* 43, 95-100 (2011)
- ¹⁰ Fann, C. H., Guirgis, F., Chen, G., Lao, M. S. & Piret, J. M. Limitations to the amplification and stability of human tissue-type plasminogen activator expression by Chinese hamster ovary cells. *Biotechnology and Bioengineering* 69, 204-212 (2000)
- ¹¹ Barnes, L. M., Moy, N. & Dickson, A. J. Phenotypic variation during cloning procedures: Analysis of the growth behavior of clonal cell lines. *Biotechnology and Bioengineering* 94, 530-537 (2006)
- ¹² Stockholm, D., Benchaouir, R., Picot, J., Rameau, P., Neildez, T. M. A., Landini, G., Laplace-Builhé, C. & Paldi, A. The origin of phenotypic heterogeneity in a clonal cell population in vitro. *PLOS ONE* 2, e394 (2007)
- ¹³ El-Ali, J., Sorger, P. K. & Jensen, K. F. Cells on chips. *Nature* 442, 403-411 (2006)
- ¹⁴ Lecault, V., White, A. K., Singhal, A. & Hansen, C. L. Microfluidic single cell analysis: from promise to practice. *Current Opinion in Chemical Biology* 16, 381-390 (2012)
- ¹⁵ Mehling, M. & Tay, S. Microfluidic cell culture. *Current Opinion in Biotechnology* 25, 95-102 (2014)
- ¹⁶ Paul, S. M., Mytelka, D.S., Dunwiddie, C. T., Persinger, C. C., Munos, B. H., Lindborg, S. R. & Schacht, A. L. How to improve R&D productivity: the pharmaceutical industry's grand challenge. *Nature Reviews: Drug Discovery* 9, 203-214 (2010)
- ¹⁷ Swartz, J. R. Advances in *Escherichia coli* production of therapeutic proteins. *Current opinion in Biotechnology* 12, 195-201 (2001)
- ¹⁸ Butler, M. Animal cell cultures: recent achievements and perspectives in the production of biopharmaceuticals. *Applied Microbiology and Biotechnology* 68, 283-291 (2005)

-
- ¹⁹ Gasser, B. & Mattanovich, D. Antibody production with yeasts and filamentous fungi: on the road to large scale? *Biotechnology Letters* 29, 201-212 (2007)
- ²⁰ Wurm, F. M. Production of recombinant protein therapeutics in cultivated mammalian cells. *Nature Biotechnology* 22, 1393-1398 (2004)
- ²¹ Dietmair, S., Nielsen, L. K. & Timmins, N. E. Mammalian cells as production hosts in the age of omics. *Biotechnology Journal* 7, 75-89 (2012)
- ²² Smith, M. R. Rituximab (monoclonal anti-CD20 antibody): mechanisms of action and resistance. *Oncogene* 22, 7359-7368 (2003).
- ²³ Ferrara, N., Hillan, K. J., Gerber, H. & Novotny, W. Discovery and development of bevacizumab, an anti-VEGF antibody for treating cancer. *Nature Reviews Drug Discovery* 3, 391-400 (2004)
- ²⁴ Nahta, R. & Esteva, F. J. Trastuzumab: triumphs and tribulations. *Oncogene* 26, 3637-3643 (2007)
- ²⁵ Bain, B. & Brazil, M. Adalimumab. *Nature Reviews Drug Discovery* 2, 693-694 (2003)
- ²⁶ Stohl, W. & Hilbert, D. M. The discovery and development of belimumab: the anti-BLyS–lupus connection. *Nature Biotechnology* 30, 69-77 (2012)
- ²⁷ Hirten, R., Longman, R. S., Bosworth, B. P., Steinlauf, A. & Scherl, E. Vedolizumab and Infliximab Combination Therapy in the Treatment of Crohn’s Disease. *The American Journal of Gastroenterology* 110, 1737-1738 (2015)
- ²⁸ Pavlou, A. K. & Reichert, J. M. Recombinant protein therapeutics – success rates, market trends and values to 2010. *Nature Biotechnology* 22, 1513-1519 (2004)
- ²⁹ Ecker, D. M., Jones, S. D. & Levine, H. L. The therapeutic monoclonal antibody market. *MAbs* 7, 9-14 (2015).
- ³⁰ Huggett, B., Hodgson, J. & Lahteenmaki, R. Public Biotech 2010—the numbers. *Nature Biotechnology* 29, 585-591 (2011)
- ³¹ Chirino, A. J. & Mire-Sluis, A. Characterizing biological products and assessing comparability following manufacturing changes. *Nature Biotechnology* 22, 1383-1391 (2004)
- ³² Eichler, H., Aronsson, B., Abadie, E. & Salmonson, T. New drug approval success rate in Europe in 2009. *Nature Reviews Drug Discovery* 9, 355-356 (2010)
- ³³ Tjio, J. H. & Puck, T. T. Genetics of somatic mammalian cells. *The Journal of Experimental Medicine*, 108, 259-268 (1958)
- ³⁴ Jayapal, K. P., Wlaschin, K. F., Hu, W., & Yap, M. G. S. Recombinant protein therapeutics from CHO cells - 20 years and counting. *Chemical Engineering Progress*, 103, 40-47 (2007)
- ³⁵ Puck, T. T. & Kao, F. T. Genetics of somatic mammalian cells. V. Treatment with 5-bromodeoxyuridine and visible light for isolation of nutritionally deficient mutants. *Proceedings of the National Academy of Sciences of the United States of America* 58, 1227-1234 (1967)
- ³⁶ Urlaub, G. & Chasin, L. A. Isolation of Chinese hamster cell mutants deficient in dihydrofolate-reductase activity. *Proceedings of the National Academy of Sciences of the United States of America* 77, 4216-4220 (1980)
- ³⁷ Jones, S. D., Castillo, F. J. & Levine, H. L. Advances in the development of therapeutic monoclonal antibodies. *BioPharm International* 20, 96-114 (2007)

-
- ³⁸ Bebbington, C. R., Renner, G. L., Thomson, S., King, D., Abrams, D. & Yarranton, G. T. High level expression of a recombinant antibody from myeloma cells using a glutamine synthetase gene as an amplifiable selectable marker. *Nature Biotechnology* 10, 169-175 (1992)
- ³⁹ Barnes, L. M., Bentley, C. M. & Dickson, A. J. Advances in animal cell recombinant protein production: GS-NS0 expression system. *Cytotechnology* 32, 109-123 (2000)
- ⁴⁰ Chu, L., Robinson, D. K. Industrial choices for protein production by large-scale cell culture. *Current Opinion in Biotechnology* 12, 180-187 (2001)
- ⁴¹ De Jesus, M. & Wurm, F. M. Manufacturing recombinant proteins in kg-ton quantities using animal cells in bioreactors. *European Journal of Pharmaceutics and Biopharmaceutics* 78, 184-188 (2011)
- ⁴² Scahill, S. J., Devos, R., Van der Heyden, J. & Fiers, W. Expression and characterization of the product of a human immune interferon cDNA gene in Chinese hamster ovary cells. *Proceedings of the National Academy of Sciences of the United States of America* 80, 4654-4658 (1983)
- ⁴³ McCormick, F., Trahey, M., Innis, M., Dieckmann, B. & Ringold, G. Inducible expression of amplified human beta interferon genes in CHO cells. *Molecular and Cellular Biology* 4, 166-172 (1984)
- ⁴⁴ Kaufman, R. J., Wasley, L. C., Spiliotes, A. J., Gossels, S. D., Latt, S. A., Larsen, G. R. & Kay, R. M. Coamplification and coexpression of human tissue-type plasminogen activator and murine dihydrofolate reductase sequences in Chinese hamster ovary cells. *Molecular and Cellular Biology* 5, 1750-1759 (1985)
- ⁴⁵ Sheeley, D. M., Merrill, B. M. & Taylor, L. C. E. Characterization of monoclonal antibody glycosylation: comparison of expression systems and identification of terminal N-linked galactose. *Analytical Biochemistry* 247, 102-110 (1997)
- ⁴⁶ Raju, T. S., Briggs, J. B., Borge, S. M. & Jones, A. J. S. Species-specific variation in glycosylation of IgG: evidence for the species-specific sialylation and branch-specific galactosylation and importance for engineering recombinant glycoprotein therapeutics. *Glycobiology* 10, 477-486 (2000)
- ⁴⁷ Raju, T. S. Glycosylation variations with expression systems and their impact on biological activity of therapeutic immunoglobulins. *BioProcess International* 1, 44-53 (2003)
- ⁴⁸ Eisenstein, M. Approval on a knife edge. *Nature Biotechnology* 30, 26-29 (2012)
- ⁴⁹ Harrison, C. Enbrel patent surfaces. *Nature Biotechnology* 30, 123 (2012)
- ⁵⁰ Meyer, H. P., Brass, J., Jungo, C., Klein, J., Wenger, J. & Mommers, R. An emerging start for therapeutic and catalytic protein production. *BioProcess International* 6, S10-S21 (2008)
- ⁵¹ Chan, A. C. & Carter, P. J. Therapeutic antibodies for autoimmunity and inflammation. *Nature Reviews Immunology* 10, 301-316 (2010)
- ⁵² Chartrain, M. & Chu, L. Development and Production of Commercial Therapeutic Monoclonal Antibodies in Mammalian Cell Expression Systems: An Overview of the Current Upstream Technologies. *Current Pharmaceutical Biotechnology* 9, 447-467 (2008)
- ⁵³ Browne, S. M. & Al Rubeai, M. Selection methods for high producing mammalian cell lines. *Trends in Biotechnology* 25, 425-432 (2007)

-
- ⁵⁴ Birch, J. R. & Racher, A. J. Antibody production. *Advanced Drug Delivery Reviews* 58, 671-685 (2006)
- ⁵⁵ Lai, T., Yang, Y. & Ng, S. K. Advances in Mammalian Cell Line Development Technologies for Recombinant Protein Production. *Pharmaceuticals* 6, 579-603 (2013)
- ⁵⁶ Underwood, P. A. & Bean, P. A. Hazards of the limiting-dilution method of cloning hybridomas. *Journal of Immunological Methods* 107, 119-128 (1988).
- ⁵⁷ Kennard, M. L., Goosney, D. L., Monteith, D., Zhang, L., Moffat, M., Fischer, D. & Mott, J. The generation of stable, high mAb expressing CHO cell lines based on artificial chromosome expression (ACE) technology. *Biotechnology and Bioengineering* 104, 540-553 (2009)
- ⁵⁸ Borth, N., Zeyda, M. & Katinger, H. Efficient selection of high-producing subclones during gene amplification of recombinant Chinese hamster ovary cells by flow cytometry and cell sorting. *Biotechnology and Bioengineering* 71, 266-273 (2000)
- ⁵⁹ Dharshanan, S., Chong, H., Hung, C. S., Zamrod, Z. & Kamal, N. Rapid automated selection of mammalian cell line secreting high level of humanized monoclonal antibody using Clone Pix FL system and the correlation between exterior median intensity and antibody productivity. *Electronic Journal of Biotechnology* 14 (2011)
- ⁶⁰ Jain, E. & Kumar, A. Upstream processes in antibody production: evaluation of critical parameters. *Biotechnology Advancement* 26, 46-71 (2008).
- ⁶¹ Rodrigues, M. E., Costa, A. R., Henriques, M., Azeredo, J. & Oliveira, R. Technological progresses in monoclonal antibody production systems. *Biotechnology Progress* 26, 332-351 (2010)
- ⁶² Porter, A. J., Dickson, A. J., & Racher, A. J. Strategies for Selecting Recombinant CHO Cell Lines for cGMP Manufacturing: Realizing the Potential in Bioreactors. *Biotechnology Progress* 26, 1446-1454 (2010)
- ⁶³ Grammatikos, S. I., Bergemann, K., Werz, W., Brax, I., Bux, R., Eberhardt, P., Fieder, J. & Noe, W. The real meaning of high expression. In: Bernard, A., Griffiths, B., Noe, W. & Wurm, F. Editors. *Animal Cell Technology: Products from Cells, Cells as Products*. Netherlands: Springer; 11-17 (1999)
- ⁶⁴ Strutzenberger, K., Borth, N., Kunert, R., Steinfeldner, W. & Katinger, H. Changes during subclone development and ageing of human antibody producing recombinant CHO cells. *Biotechnology Journal* 69, 215-226 (1999)
- ⁶⁵ Chusainow, J., Yang, Y. S., Yeo, J. H., Toh, P. C., Asvadi, P., Wong, N. S. & Yap, M. G. A study of monoclonal antibody-producing CHO cell lines: what makes a stable high producer? *Biotechnology and Bioengineering* 102, 1182-1196 (2009)
- ⁶⁶ Yang, Y., Mariati, Chusainow, J. & Yap, M. G. DNA methylation contributes to loss in productivity of monoclonal antibody-producing CHO cell lines. *Biotechnology Journal* 147, 180-185 (2010)
- ⁶⁷ Kim, M., O'Callaghan, P. M., Droms, K. A. & James, D. C. A mechanistic understanding of production instability in CHO cell lines expressing recombinant monoclonal antibodies. *Biotechnology and Bioengineering* 108, 2434-2446 (2011)
- ⁶⁸ Page, M. J. & Sydenham, M. A. High level expression of humanized monoclonal antibody CAMPATH-1H in Chinese Hamster Ovary cells. *Nature Biotechnology* 9, 64-68 (1991)

-
- ⁶⁹ Sinacore, M. S., Charlebois, T. S., Harrison, S., Brennan, S., Richards, T., Hamilton, M., Scott, S., Brodeur, S., Oakes, P., Leonard, M., Switzer, M., Anagnostopoulos, A., Foster, B., Harris, A., Jankowski, M., Bond, M., Martin, S. & Adamson, S. R. CHO DUKX cell lineages preadapted to growth in serum-free suspension culture enable rapid development of cell culture processes for the manufacture of recombinant proteins. *Biotechnology and Bioengineering* 52, 518-528 (1996)
- ⁷⁰ Sinacore, M. S., Drapeau, D & Adamson, S. R. Adaptation of mammalian cells to growth in serum-free media. *Molecular Biotechnology* 15, 249-257 (2000)
- ⁷¹ Porter, A. J., Racher, A. J., Preziosi, R. & Dickson, A. J. Strategies for selecting recombinant CHO cell lines for cGMP manufacturing: improving the efficiency of cell line generation. *Biotechnology Progress* 26, 1455-1464 (2010)
- ⁷² Legmann, R., Benoit, B., Fedechko, R. W., Deppeler, C. L., Srinivasan, S., Robins, R. H., McCormick, E. L., Ferrick, D. A., Rodgers, S. T. & Russo, A. P. A strategy for clone selection under different production conditions. *Biotechnology Progress* 27, 757-765 (2011)
- ⁷³ Kondragunta, B., Drew, J. L., Brorson, K. A., Moreira A. R. & Rao, G. Advances in clone selection using high-throughput bioreactors. *Biotechnology Progress* 26, 1095-1103 (2010)
- ⁷⁴ Engvall, E. & Perlmann, P. Enzyme-linked immunosorbent assay, ELISA III. Quantitation of specific antibodies by enzyme-labeled anti-immunoglobulin in antigen-coated tubes. *The Journal of Immunology* 10, 129-135 (1972)
- ⁷⁵ Berg, M., Undisz, K., Thiericke, R., Zimmermann, P., Moore, T. & Posten, C. Evaluation of liquid handling conditions in microplates. *Journal of Biomolecular Screening* 6, 47-56 (2001)
- ⁷⁶ Eagle, H. & Piez, K. The population-dependent requirement by cultured mammalian cells for metabolites which they can synthesize. *Journal of Experimental Medicine* 116, 29-43 (1962)
- ⁷⁷ Ham, R. G. & McKeehan, W. L. Media and growth requirements. *Methods in Enzymology* 58, 44-93 (1979)
- ⁷⁸ Lim, H. C. & Shin, H. S. *Fed-batch Cultures: Principles and Applications of Semi-batch Bioreactors*. Cambridge University Press (2013)
- ⁷⁹ Bibila, T. A. & Robinson, D. K. In pursuit of the optimal fed-batch process for monoclonal antibody production. *Biotechnology Progress* 11, 1-13 (1995)
- ⁸⁰ Zhou, W., Rehm, J., Europa, A. & Hu, W. S. Alteration of mammalian cell metabolism by dynamic nutrient feeding. *Cytotechnology* 24, 99-108 (1997)
- ⁸¹ Minihane, B. J. & Brown, D. E. Fed-batch culture technology. *Biotechnology Advances* 4, 207-218 (1986)
- ⁸² Li, F., Vijayasankaran, N., Shen, A., Kiss, R. & Amanullah, A. Cell culture processes for monoclonal antibody production. *MAbs* 2, 466-477 (2010)
- ⁸³ Collier R. Drug development cost estimates hard to swallow. *Canadian Medical Association Journal* 180, 279-280 (2009)
- ⁸⁴ Bareither, R. & Pollard, D. A review of advanced small-scale parallel bioreactor technology for accelerated process development: Current state and future need. *Biotechnology Progress* 27, 2-14 (2011)

-
- ⁸⁵ Chen, A., Chitta, R., Chang, D. & Amanullah, A. Twenty-four well plate miniature bioreactor system as a scale-down model for cell culture process development. *Biotechnology and Bioengineering* 102, 148-160 (2009)
- ⁸⁶ Legmann, R., Schreyer, B., Combs, R., McCormick, E., Russo, P. & Rodgers, S. A predictive high-throughput scale-down model of monoclonal antibody production in CHO cells. *Biotechnology and Bioengineering* 104, 1107-1120 (2009)
- ⁸⁷ Bower, D. M., Lee, K. S., Ram, R. J. & Prather, K. L. J. Fed-batch microbioreactor platform for scale down and analysis of a plasmid DNA production process. *Biotechnology and Bioengineering* 109, 1976-1986 (2012)
- ⁸⁸ Kumar, S., Wittmann, C. & Heinzle, E. Review: Minibioreactors. *Biotechnology Letters* 26, 1-10 (2004)
- ⁸⁹ Duetz, W. A. Microtiter plates as mini-bioreactors: miniaturization of fermentation methods. *Trends in Microbiology* 15, 469-475 (2007)
- ⁹⁰ Duetz, W. A., Rüedi, L., Hermann, R., Connor, K. O., Büchs, J. & Witholt, B. Methods for intense aeration, growth, storage and replication of bacterial strains in microtitre plates. *Applied Environmental Microbiology* 66, 2641-2646 (2000)
- ⁹¹ Duetz, W. A. & Witholt, B. Effectiveness of orbital shaking for the aeration of suspended bacteria in square-deep well microtiter plates. *Biochemical Engineering Journal* 7, 113-115 (2001)
- ⁹² Weiss, S., John, G. T., Klimant, I. & Heinzle, E. Modelling of mixing in 96-well microplates observed with fluorescence indicators. *Biotechnology Progress* 18, 821-830 (2002)
- ⁹³ Wittmann, C., Kim, H. M., John, G. & Heinzle, E. Characterization and application of an optical sensor for quantification of dissolved O₂ in shake-flasks. *Biotechnology Letters* 25, 377-380 (2003)
- ⁹⁴ Zimmermann, H. F., John, G. T., Trauthwein, H., Dingerdissen, U. & Huthmacher, K. Rapid evaluation of oxygen and water permeation through microplate sealing tapes. *Biotechnology Progress* 9, 1061-1063 (2003)
- ⁹⁵ Wang, G., Zhang, W. & Mirro, R. New benchtop bioreactor uses presterilized, prevalidated, single use vessels to simplify cell culture. *Nature Methods* 6, (2009)
- ⁹⁶ Huang, Y. M., Hu, W. W., Rustandi, E., Chang, K., Yusuf-Makagiansar, H. & Ryll, T. Maximizing productivity of CHO cell-based fed-batch culture using chemically defined media conditions and typical manufacturing equipment. *Biotechnology Progress* 26, 1400-1410 (2010)
- ⁹⁷ Gu, M. B., Todd, P. & Kompala, D. S. Metabolic burden in recombinant CHO cells: Effect of dhfr gene amplification and laxZ expression. *Cytotechnology* 18, 159-166 (1996)
- ⁹⁸ Banik, G. G., Todd, P. W. & Kompala, D. S. Foreign protein expression from S phase specific promoters in continuous cultures of recombinant CHO cells. *Cytotechnology* 22, 179-184 (1996)
- ⁹⁹ Chai, H., Al-Rubeai, M., Chua, K. L., Oh, S. K. W. & Yap, M. G. S. Insect cell line dependent gene expression of recombinant human tumor necrosis factor- β . *Enzyme Microbial Technology* 18, 126-132 (1996)

-
- ¹⁰⁰ He, L., Winterrowd, C., Kadura, I. & Frye, C. Transgene copy number distribution profiles in recombinant CHO cell lines revealed by single cell analyses. *Biotechnology and Bioengineering* 109, 1713-1722 (2012)
- ¹⁰¹ Kromenaker, S. J. and Srienc, F. Cell-cycle-dependent protein accumulation by producer and nonproducer murine hybridoma cell lines: A population analysis. *Biotechnology and Bioengineering* 28, 665-677 (1991)
- ¹⁰² Kubbies, M. & Stockinger, H. Cell cycle-dependent DHFR and t-PA production in cotransfected, MTX-amplified CHO cells revealed by dual-laser flow cytometry. *Experimental Cell Research* 188, 267-271 (1990)
- ¹⁰³ Aggeler, J., Kapp, L. N., Tseng, S. C. G. & Werb, Z. Regulation of protein secretion in Chinese hamster ovary cells by cell cycle position and cell density. *Experimental Cell Research* 139, 275-283 (1982)
- ¹⁰⁴ Lloyd, D. R., Holmes, P., Jackson, L.P., Emery, A. N., Al-Rubeai, M. Relationship between cell size, cell cycle and specific recombinant protein productivity. *Cytotechnology* 34, 59-70 (2000)
- ¹⁰⁵ Pilbrough, W., Munro, T. P. & Gray, P. Intracloal protein expression heterogeneity in recombinant CHO cells. *PLOS ONE* 4, e8432 (2009)
- ¹⁰⁶ Yoon, S. K., Hwang, S. O. & Lee, G. M. Enhancing effect of low culture temperature on specific antibody productivity of recombinant Chinese hamster ovary cells: Clonal variation. *Biotechnology Progress* 20, 1683-1688 (2004)
- ¹⁰⁷ Pichler, J., Galosy, S., Mott, J. & Borth, N. Selection of CHO host cell subclones with increased specific antibody production rates by repeated cycles of transient transfection and cell sorting. *Biotechnology and Bioengineering* 108, 386-394 (2010)
- ¹⁰⁸ Wurm, F. N. & Hacker, D. First CHO genome. *Nature Biotechnology* 29, 718-720 (2011)
- ¹⁰⁹ Davies, S. L., Lovelady, C. S., Grainger, R. K., Racher, A. J., Young, R. J. & James, D. C. Functional heterogeneity and heritability in CHO cell populations. *Biotechnology and Bioengineering* 110, 260-274 (2013)
- ¹¹⁰ Sigal, A., Milo, R., Cohen, A., Geva-Zatorsky, N., Klein, Y., Liron, Y., Rosenfeld, N., Danon, T., Perzov, N. & Alon, U. Variability and memory of protein levels in human cells. *Nature* 444, 643-646 (2006)
- ¹¹¹ Raj, A., Peskin, C. S., Tranchina, D., Vargas, D. Y. & Tyagi, S. Stochastic mRNA synthesis in mammalian cells. *PLOS Biology* 4, e309 (2006)
- ¹¹² Chang, H. H., Hemberg, M., Barahona, M., Ingber, D. E. & Huang, S. Transcriptome-wide noise controls lineage choice in mammalian progenitor cells. *Nature* 453, 544-547 (2008)
- ¹¹³ Raj, A. & van Oudenaarden, A. Nature, Nurture, or Chance: Stochastic Gene Expression and Its Consequences. *Cell* 135, 216-226 (2008)
- ¹¹⁴ Sleiman, R. J., Gray, P. P., McCall, M. N., Codamo, J. & Sunstrom, N.A. Accelerated cell line development using two-color fluorescence activated cell sorting to select highly expressing antibody-producing clones. *Biotechnology and Bioengineering* 99, 578-587 (2008)
- ¹¹⁵ Czerkinsky, C., Nilsson, L., Nygren, H., Ouchterlony, O. & Tarkowski, A. A solid-phase enzyme-linked immunospot (ELISPOT) assay for enumeration of specific antibody-secreting cells. *Journal of Immunological Methods* 65, 109-121 (1983)

-
- ¹¹⁶ Meilhoc, E., Wittrup, K. D., & Bailey, J. E. Application of flow cytometric measurement of surface IgG in kinetic-analysis of monoclonal antibody synthesis and secretion by murine hybridoma cells. *Journal of Immunological Methods* 121, 167-174 (1989)
- ¹¹⁷ Brezinsky, S. C., Chiang, G. G., Szilvasi, A., Mohan, S., Shapiro, R. I., MacLean, A., Sisk, W. & Thill, G. A simple method for enriching populations of transfected CHO cells for cells of higher specific productivity. *Journal of Immunological Methods* 277, 141-155 (2003)
- ¹¹⁸ Carroll, S. & Al-Rubeai, M. The selection of high-producing cell lines using flow cytometry and cell sorting. *Expert Opinion on Biological Therapy* 4, 1821-1829 (2004)
- ¹¹⁹ Kumar, N. & Borth, N. Flow-cytometry and cell sorting: An efficient approach to investigate productivity and cell physiology in mammalian cell factories. *Methods* 56, 366-374 (2012)
- ¹²⁰ Powell, K. T. & Weaver, J. C. Gel microdroplets and flow-cytometry - Rapid determination of antibody secretion by individual cells within a cell population. *Nature Biotechnology* 8, 333-337 (1990)
- ¹²¹ Caron, A. W., Nicolas, C., Gaillet, B., Ba, I., Pinard, M., Garnier, A., Massie, B. & Gilbert, R. Fluorescent labeling in semi-solid medium for selection of mammalian cells secreting high levels of recombinant proteins. *BMC Biotechnology* 9, 42 (2009)
- ¹²² Manz, R., Assenmacher, M., Pfluger, E., Miltenyi, S. & Radbruch, A. Analysis and sorting of live cells according to secreted molecules, relocated to a cell-surface affinity matrix. *Proceedings of the National Academy of Sciences of the United States of America* 92, 1921-1925 (1995)
- ¹²³ Serpieri, F., Inocencio, A., de Oliveira, J. M., Pimenta Jr., A. A., Garbuio, A., Kalil, J., Brigido, M. M. & Moro, A. M. Comparison of humanized IgG and FvFc anti-CD3 monoclonal antibodies expressed in CHO cells. *Molecular Biotechnology* 45, 218-225 (2010)
- ¹²⁴ Hou, J. J., Hughes, B. S., Smede, M., Leung, K. M., Levine, K., Rigby, S., Gray, P. P. & Munro, T. P. High-throughput ClonePix FL analysis of mAb-expressing clones using the UCOE expression system. *New Biotechnology* 31, 214-220 (2014)
- ¹²⁵ Jostock, T. & Knopf, H. P. Mammalian stable expression of biotherapeutics. *Methods in Molecular Biology* 899, 227-238 (2012)
- ¹²⁶ Estes, S. & Melville, M. Mammalian cell line developments in speed and efficiency. In: *Mammalian cell cultures for biologics manufacturing. Advances in biochemical engineering/biotechnology* 139, 11-33 (2014)
- ¹²⁷ Kelly, S. J. Studies of the developmental potential of 4- and 8-cell stage blastomeres. *Journal of Experimental Zoology* 200, 365-376 (1977)
- ¹²⁸ De Los Angeles, A., Ferrari, F., Xi, R., Fujiwara, Y., Benvenisty, N., Deng, H., Hochedlinger, K., Jaenisch, R., Lee, S., Leitch, H. G. & Lensch, M. W. Hallmarks of pluripotency. *Nature* 525, 469-478 (2015)
- ¹²⁹ Thomson, J. A., Itskovitz-Eldor, J., Shapiro, S. S., Waknitz, M. A., Swiergiel, J. J., Marshall, V. S. & Jones, J. M. Embryonic stem cell lines derived from human blastocysts. *Science* 282, 1145-1147 (1998)
- ¹³⁰ Amit, M., Carpenter, M. K., Inokuma, M. S., Chiu, C. P., Harris, C. P., Waknitz, M. A., Itskovitz-Eldor, J. & Thomson, J. A. Clonally derived human embryonic stem cell

lines maintain pluripotency and proliferative potential for prolonged periods of culture. *Developmental Biology* 227, 271-278 (2000)

¹³¹ Hoffman, L. M. & Carpenter, M. K. Characterization and culture of human embryonic stem cells. *Nature Biotechnology* 23, 699-708 (2005)

¹³² Moon, S. Y., Park, Y. B., Kim, D. S., Oh, S. K. & Kim, D. W. Generation, culture, and differentiation of human embryonic stem cells for therapeutic applications. *Molecular Therapy* 13, 5-14 (2006)

¹³³ O'Connor, M. D., Kardel, M. D., Iosfina, I., Youssef, D., Lu, M., Li, M. M., Vercauteren, S., Nagy, A. & Eaves, C. J. Alkaline phosphatase-positive colony formation is a sensitive, specific, and quantitative indicator of undifferentiated human embryonic stem cells. *Stem Cells* 26, 1109-1116 (2008)

¹³⁴ O'Connor, M. D., Kardel, M. D. & Eaves, C. J. Functional assays for human embryonic stem cell pluripotency. *Embryonic Stem Cell Therapy for Osteo-Degenerative Diseases: Methods and Protocols*, 67-80 (2011)

¹³⁵ Cowan, C. A., Klimanskaya, I., McMahon, J., Atienza, J., Witmyer, J., Zucker, J. P., Wang, S., Morton, C. C., McMahon, A. P., Powers, D. & Melton, D. A. Derivation of embryonic stem-cell lines from human blastocysts. *New England Journal of Medicine* 350, 1353-1356 (2004)

¹³⁶ Shevinsky, L., Knowles, B. B., Damjanov, I. & Solter, D. Monoclonal antibody to murine embryos defines a stage-specific embryonic antigen expressed on mouse embryos and human teratocarcinoma cells. *Cell* 30, 697-705 (1982)

¹³⁷ Nichols, J., Zevnik, B., Anastassiadis, K., Niwa, H., Klewe-Nebenius, D., Chambers, I., Schöler, H. & Smith, A. Formation of pluripotent stem cells in the mammalian embryo depends on the POU transcription factor Oct4. *Cell* 95, 379-391 (1998)

¹³⁸ Brivanlou, A. H., Gage, F. H., Jaenisch, R., Jessell, T., Melton, D. & Rossant, J. Stem cells: setting standards for human embryonic stem cells. *Science* 300, 913-916 (2003)

¹³⁹ Masui, S., Nakatake, Y., Toyooka, Y., Shimosato, D., Yagi, R., Takahashi, K., Okochi, H., Okuda, A., Matoba, R., Sharov, A. A. & Ko, M. S. Pluripotency governed by Sox2 via regulation of Oct3/4 expression in mouse embryonic stem cells. *Nature Cell Biology* 9, 625-635 (2007)

¹⁴⁰ Wang, Z., Oron, E., Nelson, B., Razis, S. & Ivanova, N. Distinct lineage specification roles for NANOG, OCT4, and SOX2 in human embryonic stem cells. *Cell Stem Cell* 10, 440-454 (2012)

¹⁴¹ Avilion, A. A., Nicolis, S. K., Pevny, L. H., Perez, L., Vivian, N. & Lovell-Badge, R. Multipotent cell lineages in early mouse development depend on SOX2 function. *Genes & Development* 17, 126-140 (2003)

¹⁴² Takahashi, K. & Yamanaka, S. Induction of pluripotent stem cells from mouse embryonic and adult fibroblast cultures by defined factors. *Cell* 126, 663-676 (2006)

¹⁴³ Okita, K., Ichisaka, T. & Yamanaka, S. Generation of germline-competent induced pluripotent stem cells. *Nature* 448, 313-317 (2007)

¹⁴⁴ Takahashi, K., Tanabe, K., Ohnuki, M., Narita, M., Ichisaka, T., Tomoda, K. & Yamanaka, S. Induction of pluripotent stem cells from adult human fibroblasts by defined factors. *Cell* 131, 861-872 (2007)

-
- ¹⁴⁵ Yu, J., Vodyanik, M. A., Smuga-Otto, K., Antosiewicz-Bourget, J., Frane, J. L., Tian, S., Nie, J., Jonsdottir, G. A., Ruotti, V., Stewart, R. & Slukvin, I. I. Induced pluripotent stem cell lines derived from human somatic cells. *Science* 318, 1917-1920 (2007)
- ¹⁴⁶ Zhang, S. C., Wernig, M., Duncan, I. D., Brüstle, O. & Thomson, J. A. In vitro differentiation of transplantable neural precursors from human embryonic stem cells. *Nature Biotechnology* 19, 1129-1133 (2001)
- ¹⁴⁷ D'Amour, K. A., Agulnick, A. D., Eliazer, S., Kelly, O. G., Kroon, E. & Baetge, E. E. Efficient differentiation of human embryonic stem cells to definitive endoderm. *Nature Biotechnology* 23, 1534-1541 (2005)
- ¹⁴⁸ Enver, T., Pera, M., Peterson, C. & Andrews, P. W. Stem cell states, fates, and the rules of attraction. *Cell Stem Cell* 4, 387-397 (2009)
- ¹⁴⁹ Narsinh, K. H., Sun, N., Sanchez-Freire, V., Lee, A. S., Almeida, P., Hu, S., Jan, T., Wilson, K. D., Leong, D., Rosenberg, J. & Yao, M. Single cell transcriptional profiling reveals heterogeneity of human induced pluripotent stem cells. *Journal of Clinical Investigation* 121, 1217-1221 (2011)
- ¹⁵⁰ Toyooka, Y., Shimosato, D., Murakami, K., Takahashi, K. & Niwa, H. Identification and characterization of subpopulations in undifferentiated ES cell culture. *Development* 135, 909-918 (2008)
- ¹⁵¹ Kalmar, T., Lim, C., Hayward, P., Muñoz-Descalzo, S., Nichols, J., Garcia-Ojalvo, J. & Arias, A. M. Regulated fluctuations in nanog expression mediate cell fate decisions in embryonic stem cells. *PLOS Biology* 7, e1000149 (2009)
- ¹⁵² Guo, G., Huss, M., Tong, G. Q., Wang, C., Sun, L. L., Clarke, N. D. & Robson, P. Resolution of cell fate decisions revealed by single-cell gene expression analysis from zygote to blastocyst. *Developmental Cell* 18, 675-685 (2010)
- ¹⁵³ Canham, M. A., Sharov, A. A., Ko, M. S. & Brickman, J. M. Functional heterogeneity of embryonic stem cells revealed through translational amplification of an early endodermal transcript. *PLOS Biology* 8, e1000379 (2010)
- ¹⁵⁴ Singh, A. M., Hamazaki, T., Hankowski, K. E. & Terada, N. A heterogeneous expression pattern for Nanog in embryonic stem cells. *Stem cells* 25, 2534-2542 (2007)
- ¹⁵⁵ Graf, T. & Stadtfeld, M. Heterogeneity of embryonic and adult stem cells. *Cell Stem Cell* 3, 480-483 (2008)
- ¹⁵⁶ Chambers, I., Silva, J., Colby, D., Nichols, J., Nijmeijer, B., Robertson, M., Vrana, J., Jones, K., Grotewold, L. & Smith, A. Nanog safeguards pluripotency and mediates germline development. *Nature* 450, 1230-1234 (2007)
- ¹⁵⁷ MacArthur, B. D. & Lemischka, I. R. Statistical mechanics of pluripotency. *Cell* 154, 484-489 (2013)
- ¹⁵⁸ Eldar, A. & Elowitz, M. B. Functional roles for noise in genetic circuits. *Nature* 467, 167-173 (2010)
- ¹⁵⁹ Altschuler, S. J. & Wu, L. F. Cellular heterogeneity: do differences make a difference? *Cell* 141, 559-563 (2010)
- ¹⁶⁰ Singer, Z. S., Yong, J., Tischler, J., Hackett, J. A., Altinok, A., Surani, M. A., Cai, L. & Elowitz, M. B. Dynamic heterogeneity and DNA methylation in embryonic stem cells. *Molecular Cell* 55, 319-331 (2014)

-
- ¹⁶¹ Gupta, P. B., Fillmore, C. M., Jiang, G., Shapira, S. D., Tao, K., Kuperwasser, C. & Lander, E. S. Stochastic state transitions give rise to phenotypic equilibrium in populations of cancer cells. *Cell* 146, 633-644 (2011)
- ¹⁶² Shalek, A. K., Satija, R., Adiconis, X., Gertner, R. S., Gaublomme, J. T., Raychowdhury, R., Schwartz, S., Yosef, N., Malboeuf, C., Lu, D. & Trombetta, J. J. Single-cell transcriptomics reveals bimodality in expression and splicing in immune cells. *Nature* 498, 236-240 (2013)
- ¹⁶³ Arias, A. M. & Brickman, J. M. Gene expression heterogeneities in embryonic stem cell populations: origin and function. *Current Opinion in Cell Biology* 23, 650-656 (2011)
- ¹⁶⁴ Hu, M., Krause, D., Greaves, M., Sharkis, S., Dexter, M., Heyworth, C. & Enver, T. Multilineage gene expression precedes commitment in the hemopoietic system. *Genes & Development* 11, 774-785 (1997)
- ¹⁶⁵ Hope, K. & Bhatia, M. Clonal interrogation of stem cells. *Nature Methods* 8, S36-S40 (2011)
- ¹⁶⁶ Evans, M. J. & Kaufman, M. H. Establishment in culture of pluripotential cells from mouse embryos. *Nature* 292, 154-156 (1981)
- ¹⁶⁷ Mazurier, F., Gan, O. I., McKenzie, J. L., Doedens, M. & Dick, J. E. Lentivector-mediated clonal tracking reveals intrinsic heterogeneity in the human hematopoietic stem cell compartment and culture-induced stem cell impairment. *Blood* 103, 545-552 (2004)
- ¹⁶⁸ Scadden, D. T. The stem-cell niche as an entity of action. *Nature* 441, 1075-1079 (2006)
- ¹⁶⁹ Bendall, S. C., Stewart, M. H. & Bhatia, M. Human embryonic stem cells: lessons from stem cell niches in vivo. *Regenerative Medicine* 3, 365-376 (2008)
- ¹⁷⁰ Heins, N., Lindahl, A., Karlsson, U., Rehnström, M., Caisander, G., Emanuelsson, K., Hanson, C., Semb, H., Björquist, P., Sartipy, P. & Hyllner, J. Clonal derivation and characterization of human embryonic stem cell lines. *Journal of Biotechnology* 122, 511-520 (2006)
- ¹⁷¹ Hasegawa, K., Fujioka, T., Nakamura, Y., Nakatsuji, N. & Suemori, H. A method for the selection of human embryonic stem cell sublines with high replating efficiency after single-cell dissociation. *Stem Cells* 12, 2649-2660 (2006)
- ¹⁷² Watanabe, K., Ueno, M., Kamiya, D., Nishiyama, A., Matsumura, M., Wataya, T., Takahashi, J. B., Nishikawa, S., Nishikawa, S. I., Muguruma, K. & Sasai, Y. A ROCK inhibitor permits survival of dissociated human embryonic stem cells. *Nature Biotechnology* 25, 681-686 (2007)
- ¹⁷³ Bendall, S. C., Stewart, M. H., Menendez, P., George, D., Vijayaragavan, K., Werbowetski-Ogilvie, T., Ramos-Mejia, V., Rouleau, A., Yang, J., Bossé, M. & Lajoie, G. IGF and FGF cooperatively establish the regulatory stem cell niche of pluripotent human cells in vitro. *Nature* 448, 1015-1021 (2007)
- ¹⁷⁴ Stewart, M. H., Bosse, M., Chadwick, K., Menendez, P., Bendall, S. C. & Bhatia, M. Clonal isolation of hESCs reveals heterogeneity within the pluripotent stem cell compartment. *Nature Methods* 3, 807-815 (2006)
- ¹⁷⁵ Caron, N. J., Gage, B. K., O'Connor, M. D., Eaves, C. J., Kieffer, T. J. & Piret, J. M. A human embryonic stem cell line adapted for high throughput screening. *Biotechnology and Bioengineering* 110, 2706-2716 (2013)

-
- ¹⁷⁶ Lefort, N., Feyeux, M., Bas, C., Féraud, O., Bennaceur-Griscelli, A., Tachdjian, G., Peschanski, M. & Perrier, A. L. Human embryonic stem cells reveal recurrent genomic instability at 20q11.21. *Nature Biotechnology* 26, 1364-1366 (2008).
- ¹⁷⁷ Werbowetski-Ogilvie, T. E., Bossé, M., Stewart, M., Schnerch, A., Ramos-Mejia, V., Rouleau, A., Wynder, T., Smith, M. J., Dingwall, S., Carter, T. & Williams, C. Characterization of human embryonic stem cells with features of neoplastic progression. *Nature Biotechnology* 27, 91-97 (2009)
- ¹⁷⁸ Lund, R. J., Narva, E. & Lahesmaa, R. Genetic and epigenetic stability of human pluripotent stem cells. *Nature Reviews Genetics* 13, 732-744 (2012)
- ¹⁷⁹ Stewart, M. H., Bendall, S. C. & Bhatia, M. Deconstructing human embryonic stem cell cultures: niche regulation of self-renewal and pluripotency. *Journal of Molecular Medicine* 86, 875-886 (2008).
- ¹⁸⁰ Pera, M. F. Defining Pluripotency. *Nature Methods* 7, 885-887 (2010)
- ¹⁸¹ Stewart, M. H., Bendall, S. C., Levadoux-Martin, M., Bhatia, M. Clonal tracking of hESCs reveals differential contribution to functional assays. *Nature Methods* 7, 917-922 (2010)
- ¹⁸² Bhatia, M. Microenvironment mimicry. *Science* 329, 1024-1025 (2010).
- ¹⁸³ Pimpin A, Srituravanich W. Review on micro-and nanolithography techniques and their applications. *Engineering Journal* 16, 37-56 (2011)
- ¹⁸⁴ Brambley, D., Martin, B. & Prewett, P. D. Microlithography: an overview. *Advanced Materials for Optics and Electronics* 4, 55-74 (1994)
- ¹⁸⁵ Xia, Y. N. & Whitesides, G. M. Soft lithography. *Annual Review of Material Science* 28, 153-184 (1998)
- ¹⁸⁶ Weibel, D. B., DiLuzio, W. R. & Whitesides, G. M. Microfabrication meets microbiology. *Nature Reviews Microbiology* 5, 209-218 (2007)
- ¹⁸⁷ Duffy, D. C., McDonald, J. C., Schueller, O. J. A. & Whitesides, G. M. Rapid prototyping of microfluidic systems in poly(dimethylsiloxane). *Analytical Chemistry* 70, 4974-4984 (1998)
- ¹⁸⁸ Linder, V., Wu, H. K., Jiang, X. Y. & Whitesides, G. M. Rapid prototyping of 2D structures with feature sizes larger than 8 μm . *Analytical Chemistry* 75, 2522-2527 (2003)
- ¹⁸⁹ del Campo, A. & Greiner, C. SU-8: a photoresist for high-aspect-ratio and 3D submicron lithography. *Journal of Micromechanics and Microengineering* 7, R81 (2007)
- ¹⁹⁰ Yao, P., Schneider, G. J., Miao, B., Murakowski, J., Prather, D. W., Wetzel, E. D. & O'Brien, D. J. Multilayer three-dimensional photolithography with traditional planar method. *Applied Physics Letters* 85, 3920-3922 (2004)
- ¹⁹¹ Unger, M. A., Chou, H. P., Thorsen, T., Scherer, A. & Quake, S. R. Monolithic microfabricated valves and pumps by multilayer soft lithography. *Science* 288, 113-116 (2000)
- ¹⁹² Squires, T. M. & Quake, S. R. Microfluidics: Fluid physics at the nanoliter scale. *Reviews of Modern Physics* 77, 977 (2005)
- ¹⁹³ Oh, K. W. & Ahn, C. H. A review of microvalves. *Journal of Micromechanics and Microengineering* 16, R13 (2006)
- ¹⁹⁴ Thorsen, T., Maerkl, S. J. & Quake, S. R. Microfluidic large-scale integration. *Science* 298, 580-584 (2002)

-
- ¹⁹⁵ Melin, J. & Quake, S. R. Microfluidic large-scale integration: the evolution of design rules for biological automation. *Annual Review of Biophysics and Biomolecular Structure* 36, 213-231 (2007)
- ¹⁹⁶ Zare, R. N. & Kim, S. Microfluidic platforms for single-cell analysis. *Annual Review of Biomedical Engineering* 12, 187-201 (2010)
- ¹⁹⁷ Yin, H. & Marshall, D. Microfluidics for single cell analysis. *Current Opinion in Biotechnology* 23, 110-119 (2012)
- ¹⁹⁸ Wheeler, A. R., Thronset, W. R., Whelan, R. J., Leach, A. M., Zare, R. N., Liao, Y. H., Farrell, K., Manger, I. D. & Daridon, A. Microfluidic device for single-cell analysis. *Analytical Chemistry* 75, 3581-3586 (2003)
- ¹⁹⁹ Li, P. C., de Camprieu, L., Cai, J. & Sangar, M. Transport, retention and fluorescent measurement of single biological cells studied in microfluidic chips. *Lab on a Chip* 4, 174-180 (2004)
- ²⁰⁰ Rettig, J. R. & Folch, A. Large-scale single-cell trapping and imaging using microwell arrays. *Analytical Chemistry* 77, 5628-5634 (2005)
- ²⁰¹ Di Carlo, D., Aghdam, N. & Lee, L. P. Single-cell enzyme concentrations, kinetics, and inhibition analysis using high-density hydrodynamic cell isolation arrays. *Analytical Chemistry* 78, 4925-4930 (2006)
- ²⁰² Kobel, S., Valero, A., Latt, J., Renaud, P. & Lutolf, M. Optimization of microfluidic single cell trapping for long-term on-chip culture. *Lab on a Chip* 10, 857-863 (2010)
- ²⁰³ Warren, L., Bryder, D., Weissman, I. L. & Quake, S. R. Transcription factor profiling in individual hematopoietic progenitors by digital RT-PCR. *Proceedings of the National Academy of Sciences of the United States of America* 103, 17807-17812 (2006)
- ²⁰⁴ Zhong, J. F., Chen, Y., Marcus, J. S., Scherer, A., Quake, S. R., Taylor, C. R. & Weiner, L. P. A microfluidic processor for gene expression profiling of single human embryonic stem cells. *Lab on a Chip* 8, 68-74 (2007)
- ²⁰⁵ Bontoux, N., Dauphinot, L., Vitalis, T., Studer, V., Chen, Y., Rossier, J. & Potier, M. C. Integrating whole transcriptome assays on a lab-on-a-chip for single cell gene profiling. *Lab on a Chip* 8, 443-450 (2008)
- ²⁰⁶ White, A. K., VanInsberghe, M., Petriv, O. I., Hamidi, M., Sikorski, D., Marra, M. A., Piret, J., Aparicio, S. & Hansen, C. L. High-throughput microfluidic single-cell RT-qPCR. *Proceedings of the National Academy of Sciences of the United States of America* 108, 13999-14004 (2011)
- ²⁰⁷ Ottesen, E. A., Hong, J. W., Quake, S. R. & Leadbetter, J. R. Microfluidic digital PCR enables multigene analysis of individual environmental bacteria. *Science* 314, 1464-1467 (2006)
- ²⁰⁸ Heyries, K. A., Tropini, C., VanInsberghe, M., Doolin, C., Petriv, O. I., Singhal, A., Leung, K., Hughesman, C.B. & Hansen, C. L. Megapixel digital PCR. *Nature Methods* 8, 649-651 (2011)
- ²⁰⁹ White, A. K., Heyries, K. A., Doolin, C., Vaninsberghe, M. & Hansen, C. L. High-throughput microfluidic single-cell digital polymerase chain reaction. *Analytical Chemistry* 85, 7182-7190 (2013)
- ²¹⁰ Marcy, Y., Ishoey, T., Lasken, R. S., Stockwell, T. B., Walenz, B. P., Halpern, A. L., Beeson, K. Y., Goldberg, S. M. D. & Quake, S. R. Nanoliter reactors improve multiple

displacement amplification of genomes from single cells. *PLOS Genetics* 3, 1702-1708 (2007)

²¹¹ Taniguchi, Y., Choi, P., Li, G., Chen, H., Babu, M., Hearn, J., Emili, A. & Xie X. Quantifying E-coli proteome and transcriptome with singlemolecule sensitivity in single cells. *Science* 329, 533-538 (2010)

²¹² Fan, H. C., Wang, J., Potanina, A. & Quake, S. R. Whole-genome molecular haplotyping of single cells. *Nature Biotechnology* 29, 51-57 (2011)

²¹³ Leung, K., Zahn, H., Leaver, T., Konwar, K. M., Hanson, N. W., Pagé, A. P., Lo, C. C., Chain, P. S., Hallam, S. J. & Hansen, C. L. A programmable droplet-based microfluidic device applied to multiparameter analysis of single microbes and microbial communities. *Proceedings of the National Academy of Sciences of the United States of America* 109, 7665-7670 (2012)

²¹⁴ Streets, A. M., Zhang, X., Cao, C., Pang, Y., Wu, X., Xiong, L., Yang, L., Fu, Y., Zhao, L., Tang, F. & Huang, Y. Microfluidic single-cell whole-transcriptome sequencing. *Proceedings of the National Academy of Sciences of the United States of America* 111, 7048-7053 (2014)

²¹⁵ Cheong, R., Wang, C. J. & Levchenko, A. High content cell screening in a microfluidic device. *Molecular Cell Proteomics* 8, 433-442 (2009)

²¹⁶ Singhal, A., Haynes, C. A. & Hansen, C. L. Microfluidic measurement of antibody-antigen binding kinetics from low-abundance samples and single cells. *Analytical Chemistry* 82, 8671-8679 (2010)

²¹⁷ Shi, Q., Qin, L., Wei, W., Geng, F., Fan, R., Shin, Y. S., Guo, D., Hood, L., Mischel, P. S. & Heath, J. R. Single-cell proteomic chip for profiling intracellular signaling pathways in single tumor cells. *Proceedings of the National Academy of Sciences of the United States of America* 109, 419-424 (2011)

²¹⁸ Ma, C., Fan, R., Ahmad, H., Shi, Q., Comin-Anduix, B., Chodon, T., Koya, R. C., Liu, C. C., Kwong, G. A., Radu, C. G., Ribas, A. & Heath, J. R. A clinical microchip for evaluation of single immune cells reveals high functional heterogeneity in phenotypically similar T cells. *Nature Medicine* 17, 738-743 (2011)

²¹⁹ Shi, Q., Qin, L., Wei, W., Geng, F., Fan, R., Shin, Y. S., Guo, D., Hood, L., Mischel, P. S. & Heath, J. R. Single-cell proteomic chip for profiling intracellular signaling pathways in single tumor cells. *Proceedings of the National Academy of Sciences of the United States of America* 109, 419-424 (2011)

²²⁰ Tumarkin, E., Tzadu, L., Csaszar, E., Seo, M., Zhang, H., Lee, A., Peerani, R., Purpura, K., Zandstra, P. W. & Kumacheva, E. Highthroughput combinatorial cell co-culture using microfluidics. *Integrative Biology* 3, 653-662 (2011)

²²¹ Tekin, H. C. & Gijs, M. A. Ultrasensitive protein detection: a case for microfluidic magnetic bead-based assays. *Lab on a Chip* 13, 4711-4739 (2013)

²²² Whitesides, G. M., Ostuni, E., Takayama, S., Jiang, X. Y. & Ingber, D. E. Soft lithography in biology and biochemistry. *Annual Review of Biomedical Engineering* 3, 335-373 (2001)

²²³ Hansen, C. L., Skordalakes, E., Berger, J. M. & Quake, S. R. A robust and scalable microfluidic metering method that allows protein crystal growth by free interface diffusion. *Proceedings of the National Academy of Sciences of the United States of America* 99, 16531-16536 (2002)

-
- ²²⁴ Balagadde, F.K., You, L.C., Hansen, C.L., Arnold, F.H. & Quake, S.R. Long-term monitoring of bacteria undergoing programmed population control in a microchemostat. *Science* 309, 137-140 (2005)
- ²²⁵ Taylor, R. J., Falconnet, D., Niemisto, A., Ramsey, S. A., Prinz, S., Shmulevich, I., Galitski, T. & Hansen, C. L. Dynamic analysis of MAPK signaling using a high-throughput microfluidic single-cell imaging platform. *Proceedings of the National Academy of Sciences of the United States of America* 106, 3758-3763 (2009)
- ²²⁶ Falconnet, D., Niemisto, A., Taylor, R. J., Ricicova, M., Galitski, T., Shmulevich, I. & Hansen, C. L. High-throughput tracking of single yeast cells in a microfluidic matrix. *Lab on a Chip* 11, 466-473 (2011)
- ²²⁷ Paliwal, S., Iglesias, P. A., Campbell, K., Hilioti, Z., Groisman, A. & Levchenko, A. MAPK-mediated bimodal gene expression and adaptive gradient sensing in yeast. *Nature* 446, 46-51 (2007)
- ²²⁸ Bennett, M. R., Pang, W. L., Ostroff, N. A., Baumgartner, B. L., Nayak, S., Tsimring, L. S. & Hasty, J. Metabolic gene regulation in a dynamically changing environment. *Nature* 454, 1119-1122 (2008)
- ²²⁹ Hersen, P., McClean, M. N., Mahadevan, L. & Ramanathan, S. Signal processing by the HOG MAP kinase pathway. *Proceedings of the National Academy of Sciences of the United States of America* 105, 7165-7170 (2008)
- ²³⁰ Frith, J. E., Titmarsh, D. M., Padmanabhan, H. & Cooper-White, J. J. Microbioreactor array screening of Wnt modulators and microenvironmental factors in osteogenic differentiation of mesenchymal progenitor cells. *PLOS ONE* 8, e82931 (2013)
- ²³¹ Taylor, A. M., Rhee, S. W., Tu, C. H., Cribbs, D. H., Cotman, C. W. & Jeon, N. L. Microfluidic multicompartiment device for neuroscience research. *Langmuir* 19, 1551-1556 (2003)
- ²³² Chung, B. G., Flanagan, L. A., Rhee, S. W., Schwartz, P. H., Lee, A. P., Monuki, E. S. & Jeon, N. L. Human neural stem cell growth and differentiation in a gradient-generating microfluidic device. *Lab on a Chip* 5, 401-406 (2005)
- ²³³ Kim, L., Vahey, M. D., Lee, H. Y. & Voldman, J. Microfluidic arrays for logarithmically perfused embryonic stem cell culture. *Lab on a Chip* 6, 394-406 (2006)
- ²³⁴ Villa-Diaz, L. G., Torisawa, Y. S., Uchida, T., Ding, J., Nogueira-de-Souza, N. C., O'Shea, K. S., Takayama, S. & Smith, G. D. Microfluidic culture of single human embryonic stem cell colonies. *Lab on a Chip* 9, 1749-1755 (2009)
- ²³⁵ Korin, N., Bransky, A., Dinnar, U. & Levenberg, S. Periodic "flow-stop" perfusion microchannel bioreactors for mammalian and human embryonic stem cell long-term culture. *Biomedical Microdevices* 11, 87-94 (2009)
- ²³⁶ Titmarsh, D., Hidalgo, A., Turner, J., Wolvetang, E. & Cooper-White, J. Optimization of flowrate for expansion of human embryonic stem cells in perfusion microbioreactors. *Biotechnology and Bioengineering* 108, 2894-2904 (2011)
- ²³⁷ Titmarsh, D. M., Ovchinnikov, D. A., Wolvetang, E. J. & Cooper-White, J. J. Full factorial screening of human embryonic stem cell maintenance with multiplexed microbioreactor arrays. *Biotechnology Journal* 8, 822-834 (2013)
- ²³⁸ Lee, P. J., Hung, P. J., Rao, V. M. & Lee, L. P. Nanoliter scale microbioreactor array for quantitative cell biology. *Biotechnology and Bioengineering* 94, 5-14 (2006)

-
- ²³⁹ Kane, B. J., Zinner, M. J., Yarmush, M. L. & Toner, M. Liver-specific functional studies in a microfluidic array of primary mammalian hepatocytes. *Analytical Chemistry* 78, 4291-4298 (2006)
- ²⁴⁰ Gomez-Sjoberg, R., Leyrat, A. A., Pirone, D. M., Chen, C. S. & Quake, S. R. Versatile, fully automated, microfluidic cell culture system. *Analytical Chemistry* 79, 8557-8563 (2007)
- ²⁴¹ Lecault, V., VanInsberghe, M., Sekulovic, S., Knapp, D. J. H. F., Wohrer, S., et al. High-throughput analysis of single hematopoietic stem cell proliferation in microfluidic cell culture arrays. *Nature Methods* 8, 581-586 (2011)
- ²⁴² Tay, S., Hughey, J. J., Lee, T. K., Lipniacki, T., Quake, S. R. & Covert, M. W. Single-cell NF-kappa B dynamics reveal digital activation and analogue information processing. *Nature* 466, 267-271 (2010)
- ²⁴³ Albrecht, D. R., Underhill, G. H., Resnikoff, J., Mendelson, A., Bhatia, S. N. & Shah, J. V. Microfluidics-integrated time-lapse imaging for analysis of cellular dynamics. *Integrative Biology* 2, 278-287 (2010)
- ²⁴⁴ Moledina, F., Clarke, G., Oskooei, A., Onishi, K., Gunther, A. & Zandstra, P. W. Predictive microfluidic control of regulatory ligand trajectories in individual pluripotent cells. *Proceedings of the National Academy of Sciences of the United States of America* 109, 3264-3269 (2012)
- ²⁴⁵ Wang, Z. H., Kim, M. C., Marquez, M. & Thorsen, T. High-density microfluidic arrays for cell cytotoxicity analysis. *Lab on a Chip* 7, 740-745 (2007)
- ²⁴⁶ Cheong, R., Wang, C. J. & Levchenko, A. High Content Cell Screening in a Microfluidic Device. *Molecular & Cellular Proteomics* 8, 433-442 (2009)
- ²⁴⁷ ForáYu, Z. T. An integrated microfluidic culture device for quantitative analysis of human embryonic stem cells. *Lab on a Chip* 9, 555-563 (2009)
- ²⁴⁸ Kamei, K. I., Ohashi, M., Gschwend, E., Ho, Q., Suh, J., Tang, J., Clark, A. T., Pyle, A. D., Teitell, M. A., Lee, K. B. & Witte, O. N. Microfluidic image cytometry for quantitative single-cell profiling of human pluripotent stem cells in chemically defined conditions. *Lab on a Chip* 10, 1113-1119 (2010)
- ²⁴⁹ Chen, H., Sun, J., Wolvetang, E. & Cooper-White, J. High-throughput, deterministic single cell trapping and long-term clonal cell culture in microfluidic devices. *Lab on a Chip* 15, 1072-1083 (2015)
- ²⁵⁰ Hansen, C. L., Classen, S., Berger, J. M. & Quake, S. R. A microfluidic device for kinetic optimization of protein crystallization and in situ structure determination. *Journal of the American Chemical Society* 128, 3142-3143 (2006)
- ²⁵¹ Heo, Y. S., Cabrera L. M., Song J. W., Futai N., Tung Y., Smith G. D. & Takayama S. Characterization and Resolution of Evaporation-Mediated Osmolality Shifts that Constrain Microfluidic Cell Culture in Poly(dimethylsiloxane) Devices. *Analytical Chemistry* 79, 1126-1134 (2007)
- ²⁵² Toepke, M. W. & Beebe, D. J. PDMS absorption of small molecules and consequences in microfluidic applications. *Lab on a Chip* 6, 1484-1486 (2006)
- ²⁵³ Regehr, K. J., Domenech, M., Koepsel, J. T., Carver, K. C., Ellison-Zelski, S. J., Murphy, W. L., Schuler, L. A., Alarid, E. T. & Beebe, D. J. Biological implications of polydimethylsiloxane-based microfluidic cell culture. *Lab on a Chip* 9, 2132-2139 (2009)

-
- ²⁵⁴ Song, J. W., Gu, W., Futai, N., Warner, K. A., Nor, J. E. & Takayama, S. Computer-controlled microcirculatory support system for endothelial cell culture and shearing. *Analytical Chemistry* 77, 3993-3999 (2005)
- ²⁵⁵ Gu, W., Zhu, X., Futai, N., Cho, B. S. & Takayama, S. Computerized microfluidic cell culture using elastomeric channels and Braille displays. *Proceedings of the National Academy of Sciences of the United States of America* 101, 15861-15866 (2004)
- ²⁵⁶ Funke, M., Buchenauer, A., Mokwa, W., Kluge, S., Hein, L., Muller, C., Kensy, F. & Buchs, J. Bioprocess Control in Microscale: Scalable Fermentations in Disposable and User-Friendly Microfluidic Systems. *Microbial Cell Factories* 9, 86 (2010)
- ²⁵⁷ Lin, C. F., Lee, G. B., Wang, C. H., Lee, H. H., Liao, W. Y. & Chou, T. C. Microfluidic pH-sensing chips integrated with pneumatic fluid-control devices. *Biosensors and Bioelectronics* 21, 1468-1475 (2006)
- ²⁵⁸ Velve-Casquillas, G., Fu, C., Le Berre, M., Cramer, J., Meance, S., Plecis, A., Baigl, D., Greffet, J. J., Chen, Y., Piel, M. & Tran, P. T. Fast microfluidic temperature control for high resolution live cell imaging. *Lab on a Chip* 11, 484-489 (2011)
- ²⁵⁹ Wang, B., Ho, J., Fei, J., Gonzalez, R. L. & Lin, Q. A microfluidic approach for investigating the temperature dependence of biomolecular activity with single-molecule resolution. *Lab on a Chip* 11, 274-281 (2011)
- ²⁶⁰ Ai, X., Liang, Q., Luo, M., Zhang, K., Pan, J. & Luo, G. Controlling gas/liquid exchange using microfluidics for real-time monitoring of flagellar length in living *Chlamydomonas* at the single-cell level. *Lab on a Chip* 12, 4516-4522 (2012)
- ²⁶¹ Mehta, G., Mehta, K., Sud, D., Song, J. W., Bersano-Begey, T., Futai, N., Heo, Y. S., Mycek, M. A., Linderman, J. J. & Takayama, S. Quantitative measurement and control of oxygen levels in microfluidic poly(dimethylsiloxane) bioreactors during cell culture. *Biomedical Microdevices* 9, 123-134 (2007)
- ²⁶² Lam, R. H. W., Kim, M. C. & Thorsen, T. Culturing Aerobic and Anaerobic Bacteria and Mammalian Cells with a Microfluidic Differential Oxygenator. *Analytical Chemistry* 81, 5918-5924 (2009)
- ²⁶³ Klein, T., Schneider, K. & Heinzle, E. A system of miniaturized stirred bioreactors for parallel continuous cultivation of yeast with online measurement of dissolved oxygen and off-gas. *Biotechnology and Bioengineering* 110, 535-542 (2013)
- ²⁶⁴ Grunberger, A., van Ooyen, J., Paczia, N., Rohe, P., Schiendzielorz, G., Eggeling, L., Wiechert, W., Kohlheyer, D. & Noack, S. Beyond growth rate 0.6: *Corynebacterium glutamicum* cultivated in highly diluted environments. *Biotechnology and Bioengineering* 110, 220-228 (2013)
- ²⁶⁵ Takagi, M., Hayashi, H. & Yoshida, T. The effect of osmolarity on metabolism and morphology in adhesion and suspension chinese hamster ovary cells producing tissue plasminogen activator. *Cytotechnology* 32, 171-179 (2000)
- ²⁶⁶ DeMaria, C. T., Cairns, V., Schwarz, C., Zhang, J., Guerin, M., Zuena, E., Estes, S. & Karey, K. P. Accelerated clone selection for recombinant CHO CELLS using a FACS-based high-throughput screen. *Biotechnology Progress* 23, 465-472 (2007)
- ²⁶⁷ Wilson, C., Bellen, H. J. & Gehring, W. J. Position effects on eukaryotic gene expression. *Annual Review of Cell Biology* 6, 679-714 (1990)
- ²⁶⁸ Derouazi, M., Martinet, D., Besuchet Schmutz, N., Flaction, R., Wicht, M., Bertschinger, M., Hacker, D. L., Beckmann, J. S. & Wurm, F. M. Genetic

-
- characterization of CHO production host DG44 and derivative recombinant cell lines. *Biochemical and Biophysical Research Communications* 340,1069-1077 (2006)
- ²⁶⁹ Xu, X., Nagarajan, H., Lewis, N. E., Pan, S., Cai, Z., Liu, X., Chen, W., Xie, M., Wang, W., Hammond, S., Andersen, M. R., Neff, N., Passarelli, B., Koh, W., Fan, H. C., Wang, J., Gui, Y., Lee, K. H., Betenbaugh, M. J., Quake, S. R., Famili, I., Palsson, B. O. & Wang, J. The genomic sequence of the Chinese hamster ovary (CHO)-K1 cell line. *Nature Biotechnology* 29, 735-741 (2011)
- ²⁷⁰ Sander, J. D. & Joung, J. K. CRISPR-Cas systems for editing, regulating and targeting genomes. *Nature Biotechnology* 32, 347-355 (2014)
- ²⁷¹ Huang, Y., Li, Y., Wang, Y. G., Gu, X., Wang, Y. & Shen, B. F. An efficient and targeted gene integration system for high-level antibody expression. *Journal of Immunological Methods* 322, 28-39 (2007)
- ²⁷² Santiago, Y., Chan, E., Liu, P.-Q., Orlando, S., Zhang, L., Urnov, F.D., Holmes, M.C., Guschin, D., Waite, A., Miller, J. C., Rebar, E. J., Gregory, P. D., Klug, A. & Collingwood, T. N. Targeted gene knockout in mammalian cells by using engineered zinc-finger nucleases. *Proceedings of the National Academy of Sciences of the United States of America* 105, 5809-5814 (2008)
- ²⁷³ Agrawal, V. & Bal, M. Strategies for rapid production of therapeutic proteins in mammalian cells. *BioProcess International* 10, 32-48 (2012)
- ²⁷⁴ Guarna, M., Fann, C. H., Busby, S. J., Walker, K. M., Kilburn, D. G. & Piret, J. M. Effect of cDNA Copy Number on the Secretion Rate of Activated Protein C. *Biotechnology and Bioengineering* 46, 22-27 (1995)
- ²⁷⁵ Kwaks, T. H. & Otte, A. P. Employing epigenetics to augment the expression of therapeutic proteins in mammalian cells. *Trends in Biotechnology* 24, 137-142 (2006)
- ²⁷⁶ Paredes, V., Park, J. S., Jeong, Y., Yoon, J. & Baek, K. Unstable expression of recombinant antibody during long-term culture of CHO cells is accompanied by histone H3 hypoacetylation. *Biotechnology Letters* 35, 987-993 (2013)
- ²⁷⁷ Veith, N., Ziehr, H., MacLeod, R. A. & Reamon-Buettner, S. M. Mechanisms underlying epigenetic and transcriptional heterogeneity in Chinese hamster ovary (CHO) cell lines. *BMC Biotechnology* 16 (2016)
- ²⁷⁸ Li, F., Hashimura, Y., Pendleton, R., Harms, J., Collins, E. & Lee, B. A systematic approach for scale-down model development and characterization of commercial cell culture processes. *Biotechnology Progress* 22, 696-703 (2006)
- ²⁷⁹ Chaturvedi, K., Sun, S. Y., O'Brien, T., Liu, Y. J. & Brooks, J. W. Comparison of the behavior of CHO cells during cultivation in 24-square deep well microplates and conventional shake flask systems. *Biotechnology Reports* 1, 22-26 (2014)
- ²⁸⁰ Delouvroy, F., Le Reverend, G., Fessler, B., Mathy, G., Harmsen, M., Kochanowski, N. & Malphettes, L. Evaluation of the advanced micro-scale bioreactor (ambr™) as a highthroughput tool for cell culture process development. *Biomed Central Proceedings* 7, P73 (2013)
- ²⁸¹ Dowling, P. & Clynes, M. Conditioned media from cell lines: a complementary model to clinical specimens for the discovery of disease-specific biomarkers. *Proteomics* 11, 794-804 (2011)
- ²⁸² Pawitan, J. A. Prospect of Stem Cell Conditioned Medium in Regenerative Medicine. *BioMed Research International* 965849 (2014)

-
- ²⁸³ Barcelos, L. S., Duplaa, C., Krainkel, N., Graiani, G., Invernici, G., Katare, R., Siragusa, M., Meloni, M., Campesi, I., Monica, M., Simm, A., Campagnolo, P., Mangialardi, G., Stevanato, L., Alessandri, G., Emanuelli, C. & Madeddu, P. Human CD133 progenitor cells promote the healing of diabetic ischemic ulcers by paracrine stimulation of angiogenesis and activation of Wnt signaling. *Circulation Research* 104, 1095-1102 (2009)
- ²⁸⁴ Cai, L., Johnstone, B. H., Cook, T. G., Tan, J., Fishbein, M. C., Chen, P. S. & March, K. L. IFATS collection: human adipose tissue-derived stem cells induce angiogenesis and nerve sprouting following myocardial infarction, in conjunction with potent preservation of cardiac function. *Stem Cells* 27, 230-237 (2009)
- ²⁸⁵ Perin, E. C. & Silva, G. V. Autologous cell-based therapy for ischemic heart disease: clinical evidence, proposed mechanisms of action, and current limitations. *Catheterization and Cardiovascular Interventions* 73, 281-288 (2009)
- ²⁸⁶ Cho, Y. J., Song, H. S., Bhang, S., Lee, S., Kang, B. G., Lee, J. C., An, J., Cha, C. I., Nam, D. H., Kim, B. S. & Joo, K. M. Therapeutic effects of human adipose stem cell-conditioned medium on stroke. *Journal of Neuroscience Research* 90, 1794-1802 (2012)
- ²⁸⁷ Lim, U. M., Yap, M. G., Lim, Y. P., Goh, L. T. & Ng, S. K. Identification of autocrine growth factors secreted by CHO cells for applications in single-cell cloning media. *Journal of Proteome Research* 12, 3496-3510 (2013)
- ²⁸⁸ Dhulipala, P., Liu, M., Beatty, S., Sabourin, M., Piras, G., Barrett, S., Hassett, R. & Gorfien, S. Differential cell culture media for single-cell cloning. *BioProcess International* 44-51 (2011)
- ²⁸⁹ Valamehr, B. S. & Seewoester, T. Method and Media for Single Cell Serum-Free Culture of CHO Cells. U.S. Patent 20060115901 A1 (2006)
- ²⁹⁰ Warr, W. R. C., White, S. L., Chim, Y., Patel, J. & Bosteels, H. Cell line selection using the Duetz Microflask system. *BMC Proceedings* 5, 15 (2011)
- ²⁹¹ Rice, J. A. *Mathematical Statistics and Data Analysis*, 2nd edition. Duxbury Press: Belmont, CA, (1995)
- ²⁹² Wilson, C., Bellen, H. J. & Gehring, W. J. Position effects on eukaryotic gene expression. *Annual Review of Cell Biology* 6, 679-714 (1990)
- ²⁹³ Derouazi, M., Martinet, D., Besuchet Schmutz, N., Flaction, R., Wicht, M., Bertschinger, M., Hacker, D. L., Beckmann, J. S. & Wurm, F. M. Genetic characterization of CHO production host DG44 and derivative recombinant cell lines. *Biochemical and Biophysical Research Communications* 340, 1069-1077 (2006)
- ²⁹⁴ Xu, X., Nagarajan, H., Lewis, N. E., Pan, S., Cai, Z., Liu, X., Chen, W., Xie, M., Wang, W., Hammond, S., Andersen, M. R., Neff, N., Passarelli, B., Koh, W., Fan, H. C., Wang, J., Gui, Y., Lee, K. H., Betenbaugh, M. J., Quake, S. R., Famili, I., Palsson, B. O. & Wang, J. The genomic sequence of the Chinese hamster ovary (CHO)-K1 cell line. *Nature Biotechnology* 29, 735-741 (2011)
- ²⁹⁵ Kwaks, T. H. & Otte, A. P. Employing epigenetics to augment the expression of therapeutic proteins in mammalian cells. *Trends in Biotechnology* 24, 137-142 (2006)
- ²⁹⁶ Paredes, V., Park, J. S., Jeong, Y., Yoon, J. & Baek, K. Unstable expression of recombinant antibody during long-term culture of CHO cells is accompanied by histone H3 hypoacetylation. *Biotechnology Letters* 35, 987-993 (2013)

-
- ²⁹⁷ Veith, N., Ziehr, H., MacLeod, R. A. & Reamon-Buettner, S. M. Mechanisms underlying epigenetic and transcriptional heterogeneity in Chinese hamster ovary (CHO) cell lines. *BMC Biotechnology* 16 (2016)
- ²⁹⁸ Metallo, C. M., Mohr, J. C., Detzel, C. J., de Pablo, J. J., Van Wie, B. J. & Palecek, S. P. Engineering the stem cell microenvironment. *Biotechnology Progress* 23, 18-23 (2007)
- ²⁹⁹ Bhatia, S., Pilquil, C., Roth-Albin, I. & Draper, J. S. Demarcation of stable subpopulations within the pluripotent hESC compartment. *PLOS ONE* 8, e57276 (2013)
- ³⁰⁰ Carpenter, M. K., Frey-Vasconcells, J. & Rao, M. S. Developing safe therapies from human pluripotent stem cells. *Nature Biotechnology* 27, 606-613 (2009)
- ³⁰¹ Roy, N. S., Cleren, C., Singh, S. K., Yang, L., Beal, M. F. & Goldman, S. A. Functional engraftment of human ES cell-derived dopaminergic neurons enriched by coculture with telomerase-immortalized midbrain astrocytes. *Nature Medicine* 12, 1259-1268 (2007)
- ³⁰² Azarin, S. M. & Palecek, S. P. Matrix Revolutions: A trinity of defined substrates for long-term expansion of human ESCs. *Cell Stem Cell* 7, 7-8 (2010)
- ³⁰³ Chaddah, R., Arntfield, M., Runciman, S., Clarke, L. & van der Kooy, D. Clonal neural stem cells from human embryonic stem cell colonies. *The Journal of Neuroscience* 32, 7771-7781 (2012)
- ³⁰⁴ Braam, S. R., Denning, C., Matsa, E., Young, L. E., Passier, R. & Mummery, C. L. Feeder-free culture of human embryonic stem cells in conditioned medium for efficient genetic modification. *Nature Protocols* 3, 1435-1443 (2008)
- ³⁰⁵ Mitalipova, M. M., Rao, R. R., Hoyer, D. M., Johnson, J. A., Meisner, L. F., Jones, K. L., Dalton, S. & Stice S. L. Preserving the genetic integrity of human embryonic stem cells. *Nature Biotechnology* 23, 19-20 (2005)
- ³⁰⁶ Chan, E. M., Yates, F., Boyer, L. F., Schlaeger, T. M. & Daley, G. Q. Enhanced plating efficiency of trypsin-adapted human embryonic stem cells is reversible and independent of trisomy 12/17. *Cloning and Stem Cells* 10, 107-118 (2008)
- ³⁰⁷ Baker, D. E., Harrison, N. J., Maltby, E., Smith, K., Moore, H. D., Shaw, P. J., Heath, P. R., Holden, H. & Andrews, P. W. Adaptation to culture of human embryonic stem cells and oncogenesis *in vivo*. *Nature Biotechnology* 25, 207-215 (2007)
- ³⁰⁸ Ishizaki, T., Uehata, M., Tamechika, I., Keel, J., Nonomura, K., Maekawa, M. & Narumiya, S. Pharmacological properties of Y-27632, a specific inhibitor of rho-associated kinases. *Molecular Pharmacology* 57, 976-983 (2000)
- ³⁰⁹ Riento, K. & Ridley, A. J. Rocks: multifunctional kinases in cell behavior. *Nature Reviews Molecular Cell Biology* 4, 446-456 (2003)
- ³¹⁰ Desbordes, S. C. & Studer, L. Adapting human pluripotent stem cells to high-throughput and high-content screening. *Nature Protocols* 8, 111-130 (2013)
- ³¹¹ Sanchez-Freire, V., Ebert, A. D., Kalisky, T., Quake, S. R. & Wu, J. C. Microfluidic single-cell real-time PCR for comparative analysis of gene expression patterns. *Nature Protocols* 7, 829-838 (2012)
- ³¹² Halldorsson, S., Lucumi, E., Gomez-Sjoberg, R. & Fleming, R. M. T. Advantages and challenges of microfluidic cell culture in polydimethylsiloxane devices. *Biosensors and Bioelectronics* 63, 218-231 (2015)

-
- ³¹³ Kellogg, R. A., Gomez-Sjoberg, R., Leyrat, A. A. & Tay, S. High-throughput microfluidic single-cell analysis pipeline for studies of signaling dynamics. *Nature Protocols* 9, 1713-1726 (2014)
- ³¹⁴ Figallo, E., Cannizzaro, C., Gerecht, S., Burdick, J. A., Langer, R., Elvassore, N. & Vunjak-Novakovic, G. Micro-bioreactor array for controlling cellular microenvironments. *Lab on a Chip* 7, 710-719 (2007)
- ³¹⁵ Kamei, K. I., Guo, S., Yu, Z. T., Takahashi, H., Gschweng, E., Suh, C., Wang, X., Tang, J., McLaughlin, J., Witte, O. N., Lee, K. B. & Tseng, H. R. An integrated microfluidic culture device for quantitative analysis of human embryonic stem cells. *Lab on a Chip* 9, 555-563 (2009)
- ³¹⁶ Chen, Q., Wu, J., Zhuang, Q., Lin, X., Zhang, J. & Lin, J. Microfluidic isolation of highly pure embryonic stem cells using feeder-separated co-culture system. *Scientific Reports* 3, 2433 (2013)
- ³¹⁷ Singh, A., Suri, S., Lee, T., Chilton, J. M., Cooke, M. T., Chen, W., Fu, J., Stice, S. L., Lu, H., McDevitt, T. C. & Garcia, A. J. Adhesion strength-based, label-free isolation of human pluripotent stem cells. *Nature Methods* 10, 438-444 (2013)
- ³¹⁸ Titmarsh, D. M., Hudson, J. E., Hidalgo, A., Elefanty, A. G., Stanley, E. G., Wolvetang, E. J. & Cooper-White, J. J. Microbioreactor arrays for full factorial screening of exogenous and paracrine factors in human embryonic stem cell differentiation. *PLOS ONE* 7, e52405 (2013)
- ³¹⁹ Schulze, H. G., Konorov, S. O., Caron, N. J., Piret, J. M., Blades, M. W. & Turner, R. F. Assessing Differentiation Status of Human Embryonic Stem Cells Noninvasively Using Raman Microspectroscopy. *Analytical Chemistry* 82, 5020-5027 (2010)
- ³²⁰ Livak, K. J. & Schmittgen, T. D. Analysis of relative gene expression data using real-time quantitative PCR and the $2^{-\Delta\Delta C(T)}$ method. *Methods* 25, 402-408 (2001)
- ³²¹ Bettiol, E., Sartiani, L., Chicha, L., Krause, K. H., Cerbai, E. & Jaconi, M. E. Fetal bovine serum enables cardiac differentiation of human embryonic stem cells. *Differentiation* 75, 660-681 (2007)
- ³²² Hartigan, J. A. & Hartigan, P. M. The dip test of unimodality. *Annals of Statistics* 13, 70-84 (1985)
- ³²³ Adewumi, O., Aflatoonian, B., Ahrlund-Richter, L., Amit, M., Andrews, P. W., Beighton, G., Bello, P. A., Benvenisty, N., Berry, L. S., Bevan, S., Blum, B., Brooking, J., Chen, K. G., Choo, A. B., Churchill, G. A., Corbel, M., Damjanov, I., Draper, J. S., Dvorak, P., Emanuelsson, K., Fleck, R. A., Ford, A., Gertow, K., Gertsenstein, M., Gokhale, P. J., Hamilton, R. S., Hampl, A., Healy, L. E., Hovatta, O., Hyllner, J., Imreh, M. P., Itskovitz-Eldor, J., Jackson, J., Johnson, J. L., Jones, M., Kee, K., King, B. L., Knowles, B. B., Lako, M., Lebrin, F., Mallon, B. S., Manning, D., Mayshar, Y., McKay, R. D., Michalska, A. E., Mikkola, M., Mileikovsky, M., Minger, S. L., Moore, H. D., Mummery, C. L., Nagy, A., Nakatsuji, N., O'Brien, C. M., Oh, S. K., Olsson, C., Otonkoski, T., Park, K. Y., Passier, R., Patel, H., Patel, M., Pedersen, R., Pera, M. F., Piekarczyk, M. S., Pera, R. A., Reubinoff, B. E., Robins, A. J., Rossant, J., Rugg-Gunn, P., Schulz, T. C., Semb, H., Sherrer, E. S., Siemen, H., Stacey, G. N., Stojkovic, M., Suemori, H., Szatkiewicz, J., Turetsky, T., Tuuri, T., van den Brink, S., Vintersten, K., Vuoristo, S., Ward, D., Weaver, T. A., Young, L. A. & Zhang, W. Characterization of

human embryonic stem cell lines by the International Stem Cell Initiative. *Nature Biotechnology* 25, 803-816 (2007)

³²⁴ Wu, J. & Tzanakakis, E. S. Contribution of Stochastic Partitioning at Human Embryonic Stem Cell Division to NANOG Heterogeneity. *PLOS ONE* 7, e50715 (2012)




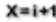










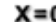







³²⁵ Bajgain, P., Mucharla, R., Wilson, J., Welch, D., Anurathapan, U., Liang, B., Lu, X., Ripple, K., Centanni, J. M., Hall, C., Hsu, D., Couture, L. A., Gupta, S., Gee, A. P., Heslop, H. E., Leen, A. M., Rooney, C. M. & Vera1, J. F. Optimizing the production of suspension cells using the G-Rex 'M' series. *Molecular Therapy Methods and Clinical Development* 1, 14015 (2014)

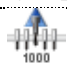



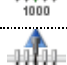

³²⁶ Woltjen, K., Michael, I. P., Mohseni, P., Desai, R., Mileikovsky, M., Hämäläinen, R., Cowling, R., Wang, W., Liu, P., Gertsenstein, M., Kaji, K., Sung, H. & Nagy, A. piggyBac transposition reprograms fibroblasts to induced pluripotent stem cells. *Nature* 458, 766-770 (2009)










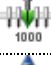



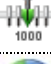




Appendices

Appendix A: Hamilton Methods




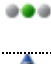












Trypsin and Sample Dispense into Cedex Fed-Batch and Batch 16.12.2015 (6 samples)



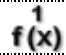

	Method
1	 Initialize on NimbusChannel Sequence: NimbusChannel"Waste" 0 return value(s)
2	 User Input Dialog Title: ", Return Value: ", Buttons: 'Only 'OK' button', Default: 'OK', Sound: ", Timeout: 'infinite' Input: Volume ("How much volume (ul) is in each well?", Integer, 3000, 0, 3000) PBS_Vol ("What volume of PBS to add to Cedex cups?", Integer, 600, 0, 1000) TrypIE_Vol ("What volume of Trypsin to add to Cedex cups?", Integer, 200, 0, 1000) Cedex_vol ("What volume of sample to add to Cedex cups?", Integer, 200, 0, 1000) mct_vol ("What volume of sample to add to microcentrifuge tubes?", Integer, 100, 0, 1000) startingposfb ("In which column are your fed-batch cultures?", Integer, 2, 1, 6) startingposbatch ("In which well does your batch samples start (1, 3, 5, 7, 9, 11, 13, 15, 17, 19, 21, 23)?", Integer, 17, 1, 23)
3	 Assignment with Calculation 'Sample_vol' = 'mct_vol' + 'Cedex_vol'
4	 Assignment with Calculation 'mixingnum' = 'Volume' * '0.9'
5	 If, Else (mixingnum is greater than 1000)
6	 Assignment 'mixingnum' = '1000'
7	 End If
8	 If, Else (startingposbatch is equal to 1)
9	 Assignment 'side' = '0'
10	 Else
11	 If, Else (startingposbatch is equal to 5)
12	 Assignment 'side' = '0'
13	 Else
14	 If, Else (startingposbatch is equal to 9)
15	 Assignment 'side' = '0'
16	 Else
17	 If, Else (startingposbatch is equal to 13)
18	 Assignment 'side' = '0'
19	 Else
20	 If, Else (startingposbatch is equal to 17)
21	 Assignment 'side' = '0'
22	 Else

		Method
23		If, Else (startingposbatch is equal to 21)
24		X=0 Assignment 'side' = '0'
25		Else
26		X=0 Assignment 'side' = '1'
27		End If
28		End If
29		End If
30		End If
31		End If
32		End If
33	X=0	Assignment 'Tip_Cnt1000FTR' = ""Tip_Cnt1000FTR""
34	1 f(x)	Edit2 of HSLTipCountingNimbusLib TipCount1::Edit2(NimbusChannel.Ham_FTR_1000_0001, Tip_Cnt1000FTR, NimbusChannel, 999)
35	ABC	Comment <Loop for PBS>
36		If, Else (PBS_Vol is NOT equal to 0)
37		Tip Pickup on NimbusChannel Sequence: "NimbusChannel.Ham_FTR_1000_0001" Tip Type: 1000ul High Volume Tip (Ham org. name) 0 return value(s).
38		Aspirate on NimbusChannel Sequence: "NimbusChannel.UBC_RGT_CONT_50mL_0002" Volume: PBS_Vol 4 return value(s).
39		Dispense on NimbusChannel Sequence: "NimbusChannel.UBC_Cedex_32POS_spaced" HxCommandDetailLevel: allDetails Volume: PBS_Vol 4 return value(s).
40		Tip Eject on NimbusChannel Sequence: "Waste" 0 return value(s).
41		Tip Pickup on NimbusChannel Sequence: "NimbusChannel.Ham_FTR_1000_0001" Tip Type: 1000ul High Volume Tip (Ham org. name) 0 return value(s).
42		Aspirate on NimbusChannel Sequence: "NimbusChannel.UBC_RGT_CONT_50mL_0002" Individual Volumes: (PBS_Vol,PBS_Vol,Disabled,Disabled) 4 return value(s).


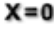

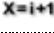




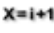



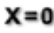
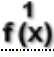





		Method
43		Dispense on NimbusChannel Sequence: "NimbusChannel.UBC_Cedex_32POS_spaced" HxCommandDetailLevel: allDetails Individual Volumes: (PBS_Vol,PBS_Vol,Disabled,Disabled) 4 return value(s) .
44		Tip Eject on NimbusChannel Sequence: "Waste" 0 return value(s) .
45		SeqResetSequenceIndexes of HSLSeqLib SeqResetSequenceIndexes(NimbusChannel.UBC_Cedex_32POS_spaced)
46		End If
47		Comment <Loop for trypsin>
48		If, Else (TrypIE_Vol is NOT equal to 0)
49		Tip Pickup on NimbusChannel Sequence: "NimbusChannel.Ham_FTR_1000_0001" Tip Type: 1000ul High Volume Tip (Ham org. name) 0 return value(s) .
50		Aspirate on NimbusChannel Sequence: "NimbusChannel.UBC_RGT_CONT_50mL_0001" Volume: TrypIE_Vol 4 return value(s) .
51		Dispense on NimbusChannel Sequence: "NimbusChannel.UBC_Cedex_32POS_spaced" HxCommandDetailLevel: allDetails Volume: TrypIE_Vol 4 return value(s) .
52		Tip Eject on NimbusChannel Sequence: "Waste" 0 return value(s) .
53		Tip Pickup on NimbusChannel Sequence: "NimbusChannel.Ham_FTR_1000_0001" Tip Type: 1000ul High Volume Tip (Ham org. name) 0 return value(s) .
54		Aspirate on NimbusChannel Sequence: "NimbusChannel.UBC_RGT_CONT_50mL_0001" Individual Volumes: (TrypIE_Vol,TrypIE_Vol,Disabled,Disabled) 4 return value(s) .
55		Dispense on NimbusChannel Sequence: "NimbusChannel.UBC_Cedex_32POS_spaced" HxCommandDetailLevel: allDetails Individual Volumes: (TrypIE_Vol,TrypIE_Vol,Disabled,Disabled) 4 return value(s) .
56		Tip Eject on NimbusChannel Sequence: "Waste" 0 return value(s) .
57		SeqResetSequenceIndexes of HSLSeqLib SeqResetSequenceIndexes(NimbusChannel.UBC_Cedex_32POS_spaced)
58		End If
59		Comment <Sample from DWP>
60		If, Else (startingposfb is equal to 1)











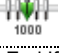






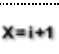


		Method
61		Sequence: Set Current Position current position of sequence 'NimbusChannel.UBC_RoundBottom_DeepWell_Sq_24POS_0001' = '1'
62		End If
63		If, Else (startingposfb is equal to 2)
64		Sequence: Set Current Position current position of sequence 'NimbusChannel.UBC_RoundBottom_DeepWell_Sq_24POS_0001' = '5'
65		End If
66		If, Else (startingposfb is equal to 3)
67		Sequence: Set Current Position current position of sequence 'NimbusChannel.UBC_RoundBottom_DeepWell_Sq_24POS_0001' = '9'
68		End If
69		If, Else (startingposfb is equal to 4)
70		Sequence: Set Current Position current position of sequence 'NimbusChannel.UBC_RoundBottom_DeepWell_Sq_24POS_0001' = '13'
71		End If
72		If, Else (startingposfb is equal to 5)
73		Sequence: Set Current Position current position of sequence 'NimbusChannel.UBC_RoundBottom_DeepWell_Sq_24POS_0001' = '17'
74		End If
75		If, Else (startingposfb is equal to 6)
76		Sequence: Set Current Position current position of sequence 'NimbusChannel.UBC_RoundBottom_DeepWell_Sq_24POS_0001' = '21'
77		End If
78		Tip Pickup on NimbusChannel Sequence: "NimbusChannel.Ham_FTR_1000_0001" Tip Type: 1000ul High Volume Tip (Ham org. name) 0 return value(s).
79		Aspirate on NimbusChannel Sequence: "NimbusChannel.UBC_RoundBottom_DeepWell_Sq_24POS_0001" Volume: Sample_vol 4 return value(s).
80		Dispense on NimbusChannel Sequence: "NimbusChannel.UBC_32POS_Microtube_0001" HxCommandDetailLevel: allDetails Volume: mct_vol 4 return value(s).


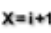



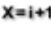



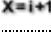



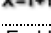







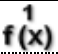

Method	
81	 Dispense on NimbusChannel Sequence: "NimbusChannel.UBC_Cedex_32POS_spaced" HxCommandDetailLevel: allDetails Volume: Cedex_vol 4 return value(s) .
82	 Tip Eject on NimbusChannel Sequence: "Waste" 0 return value(s) .
83	 If, Else (side is equal to 0)
84	 Sequence: Set Current Position current position of sequence 'NimbusChannel.UBC_RoundBottom_DeepWell_Sq_24POS_0001' = 'startingposbatch'
85	 Tip Pickup on NimbusChannel Sequence: "NimbusChannel.Ham_FTR_1000_0001" Tip Type: 1000ul High Volume Tip (Ham org. name) 0 return value(s) .
86	 Aspirate on NimbusChannel Sequence: "NimbusChannel.UBC_RoundBottom_DeepWell_Sq_24POS_0001" Individual Volumes: (Sample_vol,Sample_vol,Disabled,Disabled) 4 return value(s) .
87	 Dispense on NimbusChannel Sequence: "NimbusChannel.UBC_32POS_Microtube_0001" HxCommandDetailLevel: allDetails Individual Volumes: (mct_vol,mct_vol,Disabled,Disabled) 4 return value(s) .
88	 Dispense on NimbusChannel Sequence: "NimbusChannel.UBC_Cedex_32POS_spaced" HxCommandDetailLevel: allDetails Individual Volumes: (Cedex_vol,Cedex_vol,Disabled,Disabled) 4 return value(s) .
89	 Tip Eject on NimbusChannel Sequence: "Waste" 0 return value(s) .
90	 End If
91	 If, Else (side is equal to 1)
92	 Sequence: Set Current Position current position of sequence 'NimbusChannel.UBC_RoundBottom_DeepWell_Sq_24POS_0001' = 'startingposbatch'
93	 Tip Pickup on NimbusChannel Sequence: "NimbusChannel.Ham_FTR_1000_0001" Tip Type: 1000ul High Volume Tip (Ham org. name) 0 return value(s) .
94	 Aspirate on NimbusChannel Sequence: "NimbusChannel.UBC_RoundBottom_DeepWell_Sq_24POS_0001" Individual Volumes: (Disabled,Disabled,Sample_vol,Sample_vol) 4 return value(s) .
95	 Dispense on NimbusChannel Sequence: "NimbusChannel.UBC_32POS_Microtube_0001" HxCommandDetailLevel: allDetails Individual Volumes: (Disabled,Disabled,mct_vol,mct_vol) 4 return value(s) .
96	 Dispense on NimbusChannel Sequence: "NimbusChannel.UBC_Cedex_32POS_spaced" HxCommandDetailLevel: allDetails Individual Volumes: (Disabled,Disabled,Cedex_vol,Cedex_vol) 4 return value(s) .

	Method
97	 Tip Eject on NimbusChannel Sequence: "Waste" 0 return value(s) .
98	 End If
99	 Write2 of HSLTipCountingNimbusLib TipCount1::Write2(NimbusChannel.Ham_FTR_1000_0001, Tip_Cnt1000FTR, NimbusChannel)
100	 User Output Dialog Title: ", Return Value: ", Buttons: 'Only 'OK' button', Default: 'OK', Icons: 'Display information message icon', Sound: ", Timeout: 'infinite' Output: "Method Complete!"
101	



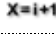




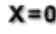
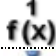






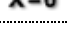



Trypsin and Sample Dispense into Cedex CM Fed-Batch (16.12.2015)


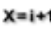
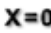
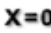
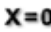
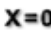
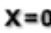












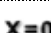
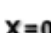
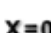


	Method
1	 Initialize on NimbusChannel Sequence: NimbusChannel"Waste" 0 return value(s)
2	 Assignment 'PLT_NUM' = '0'
3	 User Input Dialog Title: ", Return Value: ", Buttons: 'Only 'OK' button', Default: 'OK', Sound: ", Timeout: 'infinite' Input: SAMPLE_NUM ("How many samples do you have?", Integer, 4, 0, 24) Volume ("How much volume (ul) is in each well?", Integer, 3000, 0, 3000) PBS_Vol ("What volume of PBS to add?", Integer, 500, 0, 1000) TrypIE_Vol ("What volume of trypsin to add?", Integer, 250, 0, 1000) Sample_vol ("What volume of sample to add?", Integer, 250, 0, 1000) startingpos ("Which column do your samples start in?", Integer, 2, 1, 6)
4	 Assignment with Calculation 'SAMPLE_CHK' = 'SAMPLE_NUM' % '4'
5	 If, Else (SAMPLE_CHK is NOT equal to 0)
6	 User Output Dialog Title: ", Return Value: ", Buttons: 'Only 'OK' button', Default: 'OK', Icons: 'Display information message icon', Sound: ", Timeout: 'infinite' Output: "Please check your sample number"
7	 Abort
8	 End If
9	 Assignment with Calculation 'mixingnum' = 'Volume' * '0.9'
10	 If, Else (mixingnum is greater than 1000)
11	 Assignment 'mixingnum' = '1000'
12	 End If
13	 Assignment 'Tip_Cnt1000FTR' = ""Tip_Cnt1000FTR""
14	 Edit2 of HSLTipCountingNimbusLib TipCount1::Edit2(NimbusChannel.Ham_FTR_1000_0001, Tip_Cnt1000FTR, NimbusChannel, 999)
15	 Sequence: Set End Position end position of sequence 'NimbusChannel.UBC_Cedex_32POS_spaced' = 'SAMPLE_NUM'
16	 If, Else (PBS_Vol is NOT equal to 0)
17	 Tip Pickup on NimbusChannel Sequence: "NimbusChannel.Ham_FTR_1000_0001" Tip Type: 1000ul High Volume Tip (Ham org. name) 0 return value(s)
18	 Loop over following sequences: - NimbusChannel.UBC_Cedex_32POS_spaced (Controlling), Adjust for '1' times consumption 'loopCounter2' used as loop counter variable
19	 Aspirate on NimbusChannel Sequence: "NimbusChannel.UBC_RGT_CONT_50mL_0002" Volume: PBS_Vol 4 return value(s)


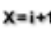
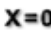
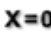



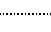
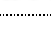








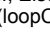

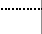
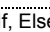
		Method
20		Dispense on NimbusChannel Sequence: "NimbusChannel.UBC_Cedex_32POS_spaced" HxCommandDetailLevel: allDetails Volume: PBS_Vol 4 return value(s).
21		End Loop - Reset sequence after loop: NimbusChannel.UBC_Cedex_32POS_spaced
22		Tip Eject on NimbusChannel Sequence: "Waste" 0 return value(s).
23		End If
24		If, Else (TryplE_Vol is NOT equal to 0)
25		Tip Pickup on NimbusChannel Sequence: "NimbusChannel.Ham_FTR_1000_0001" Tip Type: 1000ul High Volume Tip (Ham org. name) 0 return value(s).
26		Loop over following sequences: - NimbusChannel.UBC_Cedex_32POS_spaced (Controlling), Adjust for '1' times consumption 'loopCounter2' used as loop counter variable
27		Aspirate on NimbusChannel Sequence: "NimbusChannel.UBC_RGT_CONT_50mL_0001" Volume: TryplE_Vol 4 return value(s).
28		Dispense on NimbusChannel Sequence: "NimbusChannel.UBC_Cedex_32POS_spaced" HxCommandDetailLevel: allDetails Volume: TryplE_Vol 4 return value(s).
29		End Loop - Reset sequence after loop: NimbusChannel.UBC_Cedex_32POS_spaced
30		Tip Eject on NimbusChannel Sequence: "Waste" 0 return value(s).
31		End If
32		If, Else (startingpos is equal to 1)
33		Sequence: Set Current Position current position of sequence 'NimbusChannel.UBC RoundBottom DeepWell Sq 24POS 0001' = '1'
34		End If
35		If, Else (startingpos is equal to 2)
36		Sequence: Set Current Position current position of sequence 'NimbusChannel.UBC RoundBottom DeepWell Sq 24POS 0001' = '5'
37		Assignment with Calculation $X=i+1$ 'SAMPLE_NUM' = 'SAMPLE_NUM' + '4'
38		End If
39		If, Else (startingpos is equal to 3)















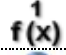
		Method
40		Sequence: Set Current Position current position of sequence 'NimbusChannel.UBC_RoundBottom_DeepWell_Sq_24POS_0001' = '9'
41		Assignment with Calculation 'SAMPLE_NUM' = 'SAMPLE_NUM' + '8'
42		End If
43		If, Else (startingpos is equal to 4)
44		Sequence: Set Current Position current position of sequence 'NimbusChannel.UBC_RoundBottom_DeepWell_Sq_24POS_0001' = '13'
45		Assignment with Calculation 'SAMPLE_NUM' = 'SAMPLE_NUM' + '12'
46		End If
47		If, Else (startingpos is equal to 5)
48		Sequence: Set Current Position current position of sequence 'NimbusChannel.UBC_RoundBottom_DeepWell_Sq_24POS_0001' = '17'
49		Assignment with Calculation 'SAMPLE_NUM' = 'SAMPLE_NUM' + '16'
50		End If
51		If, Else (startingpos is equal to 6)
52		Sequence: Set Current Position current position of sequence 'NimbusChannel.UBC_RoundBottom_DeepWell_Sq_24POS_0001' = '21'
53		Assignment with Calculation 'SAMPLE_NUM' = 'SAMPLE_NUM' + '20'
54		End If
55		Loop over following sequences: - NimbusChannel.UBC_Cedex_32POS_spaced (Controlling), Adjust for '1' times consumption 'loopCounter2' used as loop counter variable
56		Tip Pickup on NimbusChannel Sequence: "NimbusChannel.Ham_FTR_1000_0001" Tip Type: 1000ul High Volume Tip (Ham org. name) 0 return value(s).
57		Aspirate on NimbusChannel Sequence: "NimbusChannel.UBC_RoundBottom_DeepWell_Sq_24POS_0001" Volume: Sample_vol 4 return value(s).
58		Dispense on NimbusChannel Sequence: "NimbusChannel.UBC_Cedex_32POS_spaced" HxCommandDetailLevel: allDetails Volume: Sample_vol 4 return value(s).
59		Tip Eject on NimbusChannel Sequence: "Waste" 0 return value(s).
60		End Loop - Reset sequence after loop: NimbusChannel.UBC_Cedex_32POS_spaced
		Method
61		Write2 of HSLTipCountingNimbusLib TipCount1::Write2(NimbusChannel.Ham_FTR_1000_0001, Tip_Cnt1000FTR, NimbusChannel)
62		User Output Dialog Title: ", Return Value: ", Buttons: 'Only 'OK' button', Default: 'OK', Icons: 'Display information message icon', Sound: ", Timeout: 'infinite' Output: "Method Complete!"
63		

Feed DWP (all wells) (15.12.2015)






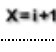
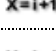
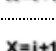
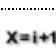
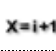
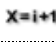
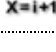
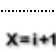
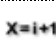
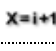
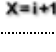
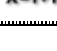
	Method
1	 Initialize on NimbusChannel Sequence: NimbusChannel"Waste" 0 return value(s)
2	 User Input Dialog Title: ", Return Value: ", Buttons: 'Only 'OK' button', Default: 'OK', Sound: ", Timeout: 'infinite' Input: sample_num ("How many samples do you have?", Integer, 4, 0, 16) column ("Which column do you want to start dispensing feed in?", Integer, 2, 1, 6) feed_vol1 ("What volume of feed (ul) do you want dispensed into wells in column 1?", Integer, 0, 0, 1000) feed_vol2 ("What volume of feed (ul) do you want dispensed into wells in column 2?", Integer, 204, 0, 1000) feed_vol3 ("What volume of feed (ul) do you want dispensed into wells in column 3?", Integer, 0, 0, 1000) feed_vol4 ("What volume of feed (ul) do you want dispensed into wells in column 4?", Integer, 0, 0, 1000)
3	 X=i+1 Assignment with Calculation 'sample_numcheck' = 'sample_num' % '4'
4	 If, Else (sample_numcheck is NOT equal to 0)
5	 User Output Dialog Title: ", Return Value: ", Buttons: 'Only 'OK' button', Default: 'OK', Icons: 'Display information message icon', Sound: ", Timeout: 'infinite' Output: "Sample number must be divisible by 4."
6	 User Input Dialog Title: ", Return Value: ", Buttons: 'Only 'OK' button', Default: 'OK', Sound: ", Timeout: 'infinite' Input: sample_num ("Please enter the number of samples you have.", Integer, 12, 0, 24)
7	 End If
8	 X=0 Assignment 'Tip_Cnt1000FTR' = ""Tip_Cnt1000FTR""
9	 1 f(x) Edit2 of HSLTipCountingNimbusLib TipCount1::Edit2(NimbusChannel.Ham_FTR_1000_0001, Tip_Cnt1000FTR, NimbusChannel, 999)
10	 If, Else (column is equal to 1)
11	 Sequence: Set Current Position current position of sequence 'NimbusChannel.UBC_RoundBottom_DeepWell_Sq_24POS_0001' = '1'
12	 X=0 Assignment 'feed1' = 'feed_vol1'
13	 X=0 Assignment 'feed2' = 'feed_vol2'
14	 X=0 Assignment 'feed3' = 'feed_vol3'
15	 X=0 Assignment 'feed4' = 'feed_vol4'
16	 X=0 Assignment 'feed5' = 'feed_vol5'
17	 X=0 Assignment 'feed6' = 'feed_vol6'
18	 End If
19	 If, Else (column is equal to 2)







		Method
20		Sequence: Set Current Position current position of sequence 'NimbusChannel.UBC_RoundBottom_DeepWell_Sq_24POS_0001' = '5'
21		Assignment with Calculation 'sample_num' = 'sample_num' + '4'
22		Assignment 'feed1' = 'feed_vol2'
23		Assignment 'feed2' = 'feed_vol3'
24		Assignment 'feed3' = 'feed_vol4'
25		Assignment 'feed4' = 'feed_vol5'
26		Assignment 'feed5' = 'feed_vol6'
27		End If
28		If, Else (column is equal to 3)
29		Sequence: Set Current Position current position of sequence 'NimbusChannel.UBC_RoundBottom_DeepWell_Sq_24POS_0001' = '9'
30		Assignment with Calculation 'sample_num' = 'sample_num' + '8'
31		Assignment 'feed1' = 'feed_vol3'
32		Assignment 'feed2' = 'feed_vol4'
33		Assignment 'feed3' = 'feed_vol5'
34		Assignment 'feed4' = 'feed_vol6'
35		End If
36		If, Else (column is equal to 4)
37		Sequence: Set Current Position current position of sequence 'NimbusChannel.UBC_RoundBottom_DeepWell_Sq_24POS_0001' = '13'
38		Assignment with Calculation 'sample_num' = 'sample_num' + '12'
39		Assignment 'feed1' = 'feed_vol4'
40		Assignment 'feed2' = 'feed_vol5'
41		Assignment 'feed3' = 'feed_vol6'
42		End If
43		If, Else (column is equal to 5)

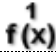




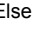



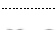
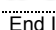
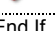
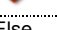



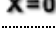

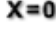

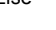
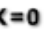



	Method	
44		Sequence: Set Current Position current position of sequence 'NimbusChannel.UBC_RoundBottom_DeepWell_Sq_24POS_0001' = '17'
45		Assignment with Calculation 'sample_num' = 'sample_num' + '16'
46		Assignment 'feed1' = 'feed_vol5'
47		Assignment 'feed2' = 'feed_vol6'
48		End If
49		If, Else (column is equal to 6)
50		Sequence: Set Current Position current position of sequence 'NimbusChannel.UBC_RoundBottom_DeepWell_Sq_24POS_0001' = '21'
51		Assignment with Calculation 'sample_num' = 'sample_num' + '20'
52		Assignment 'feed1' = 'feed_vol6'
53		End If
54		Sequence: Set End Position end position of sequence 'NimbusChannel.UBC_RoundBottom_DeepWell_Sq_24POS_0001' = 'sample_num'
55		Loop over following sequences: - NimbusChannel.UBC_RoundBottom_DeepWell_Sq_24POS_0001 (Controlling), Adjust for '1' times consumption 'loopCounter2' used as loop counter variable
56		Tip Pickup on NimbusChannel Sequence: "NimbusChannel.Ham_FTR_1000_0001" Tip Type: 1000ul High Volume Tip (Ham org. name) 0 return value(s)
57		If, Else (loopCounter2 is equal to 1)
58		Aspirate on NimbusChannel Sequence: "NimbusChannel.UBC_RGT_CONT_50mL_0003" Volume: feed1 4 return value(s)
59		End If
60		If, Else (loopCounter2 is equal to 2)
61		Aspirate on NimbusChannel Sequence: "NimbusChannel.UBC_RGT_CONT_50mL_0003" Volume: feed2 4 return value(s)
62		End If
63		If, Else (loopCounter2 is equal to 3)
64		Aspirate on NimbusChannel Sequence: "NimbusChannel.UBC_RGT_CONT_50mL_0003" Volume: feed3 4 return value(s)

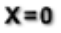
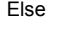






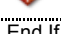


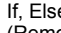








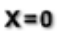
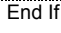
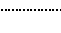
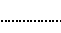
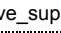
	Method
65	 End If
66	 If, Else (loopCounter2 is equal to 4)
67	 Aspirate on NimbusChannel Sequence: "NimbusChannel.UBC_RGT_CONT_50mL_0003" Volume: feed4 4 return value(s)
68	 End If
69	 If, Else (loopCounter2 is equal to 5)
70	 Aspirate on NimbusChannel Sequence: "NimbusChannel.UBC_RGT_CONT_50mL_0003" Volume: feed5 4 return value(s)
71	 End If
72	 If, Else (loopCounter2 is equal to 6)
73	 Aspirate on NimbusChannel Sequence: "NimbusChannel.UBC_RGT_CONT_50mL_0003" Volume: feed6 4 return value(s)
74	 End If
75	 Dispense on NimbusChannel Sequence: "NimbusChannel.UBC_RoundBottom_DeepWell_Sq_24POS_0001" HxCommandDetailLevel: allDetails Volume: 0 4 return value(s)
76	 Tip Eject on NimbusChannel Sequence: "Waste" 0 return value(s)
77	 End Loop - Reset sequence after loop: NimbusChannel.UBC_RoundBottom_DeepWell_Sq_24POS_0001
78	 Write2 of HSLTipCountingNimbusLib TipCount1::Write2(NimbusChannel.Ham_FTR_1000_0001, Tip_Cnt1000FTR, NimbusChannel)
79	 User Output Dialog Title: "", Return Value: "", Buttons: 'Only 'OK' button', Default: 'OK', Icons: 'Display information message icon', Sound: "", Timeout: 'infinite' Output: "Method Complete!"
80	

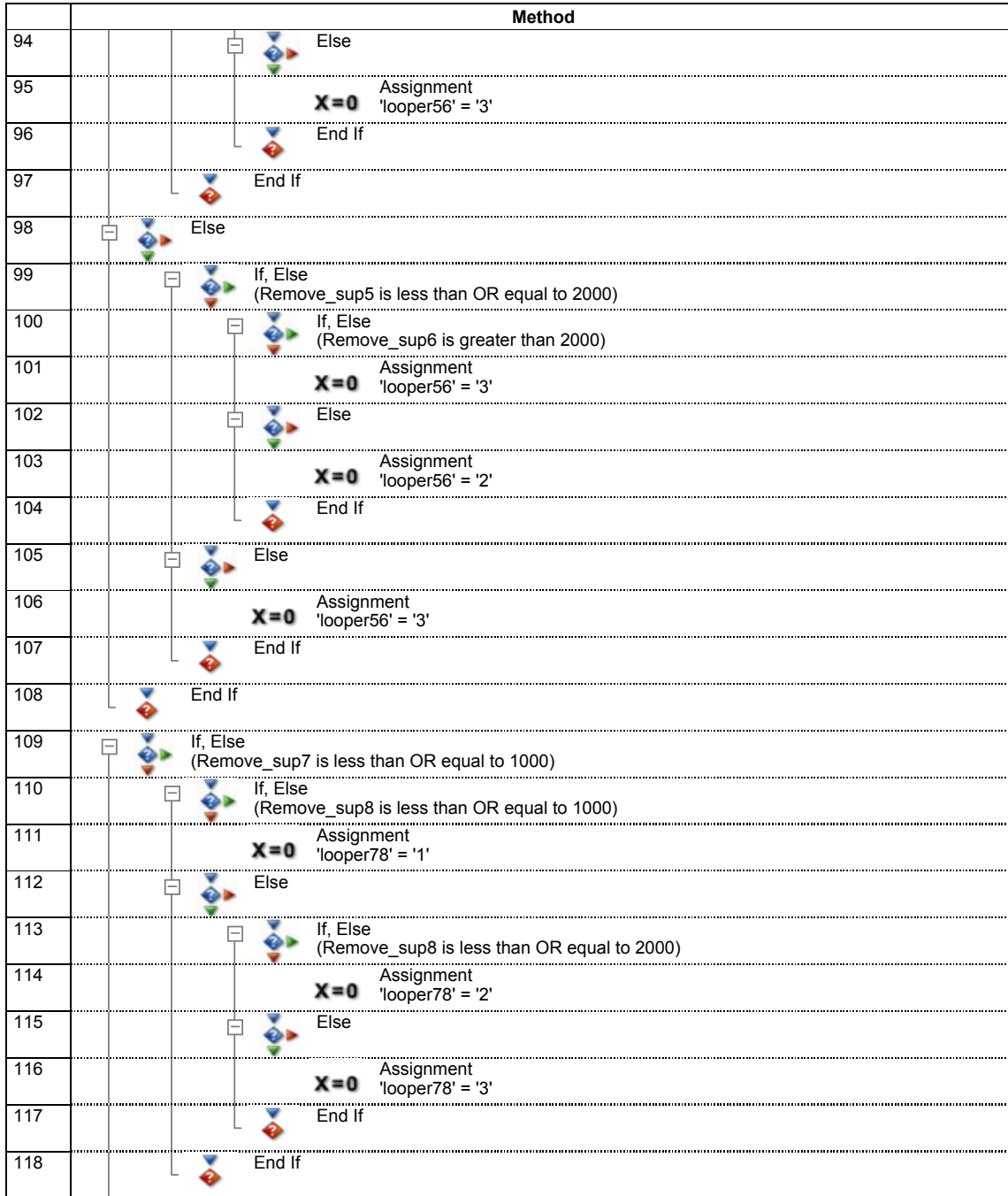
Supernatant Removal and Re-suspension CM Fed-Batch (18.12.2015)

	Method
1	 Initialize on NimbusChannel Sequence: NimbusChannel"Waste" 0 return value(s)
2	 Comment <Ask for values>
3	 User Input Dialog Title: ", Return Value: ", Buttons: 'Only 'OK' button', Default: 'OK', Sound: ", Timeout: 'infinite' Input: Sample_num ("How many samples do you have?", Integer, 4, 0, 16) Volume ("How much volume (ul) is in each sample?", Integer, 3000, 0, 3000) Trituration_num ("How many triturations would you like during cell resuspension?", Integer, 20, 0, 100)
4	 User Input Dialog Title: ", Return Value: ", Buttons: 'Only 'OK' button', Default: 'OK', Sound: ", Timeout: 'infinite' Input: Percent_sup1 ("Percentage of supernatant to be removed in wells A2 and B2?", Integer, 70, 0, 100) Percent_sup2 ("Percentage of supernatant to be removed in wells C2 and D2?", Integer, 70, 0, 100) Percent_sup3 ("Percentage of supernatant to be removed in wells A3 and B3?", Integer, 70, 0, 100) Percent_sup4 ("Percentage of supernatant to be removed in wells C3 and D3?", Integer, 70, 0, 100) Percent_sup5 ("Percentage of supernatant to be removed in wells A4 and B4?", Integer, 70, 0, 100) Percent_sup6 ("Percentage of supernatant to be removed in wells C4 and D4?", Integer, 70, 0, 100) Percent_sup7 ("Percentage of supernatant to be removed in wells A5 and B5?", Integer, 70, 0, 100) Percent_sup8 ("Percentage of supernatant to be removed in wells C5 and D5?", Integer, 70, 0, 100)
5	 Comment <Calculate fraction of volume to be removed>
6	 Assignment with Calculation 'Percent_sup1' = 'Percent_sup1' / '100' result as floating point number
7	 Assignment with Calculation 'Remove_sup1' = 'Percent_sup1' * 'Volume'
8	 Assignment with Calculation 'Percent_sup2' = 'Percent_sup2' / '100' result as floating point number
9	 Assignment with Calculation 'Remove_sup2' = 'Percent_sup2' * 'Volume'
10	 Assignment with Calculation 'Percent_sup3' = 'Percent_sup3' / '100' result as floating point number
11	 Assignment with Calculation 'Remove_sup3' = 'Percent_sup3' * 'Volume'
12	 Assignment with Calculation 'Percent_sup4' = 'Percent_sup4' / '100' result as floating point number
13	 Assignment with Calculation 'Remove_sup4' = 'Percent_sup4' * 'Volume'
14	 Assignment with Calculation 'Percent_sup5' = 'Percent_sup5' / '100' result as floating point number
15	 Assignment with Calculation 'Remove_sup5' = 'Percent_sup5' * 'Volume'
16	 Assignment with Calculation 'Percent_sup6' = 'Percent_sup6' / '100' result as floating point number
17	 Assignment with Calculation 'Remove_sup6' = 'Percent_sup6' * 'Volume'
18	 Assignment with Calculation 'Percent_sup7' = 'Percent_sup7' / '100' result as floating point number
19	 Assignment with Calculation 'Remove_sup7' = 'Percent_sup7' * 'Volume'
20	 Assignment with Calculation 'Percent_sup8' = 'Percent_sup8' / '100' result as floating point number

	Method
21	X=i+1 Assignment with Calculation 'Remove_sup8' = 'Percent_sup8' * 'Volume'
22	 Comment <Factor in rotation day (Cedex sampled wells)>
23	X=i+1 Assignment with Calculation 'Remove_sup1' = 'Remove_sup1' - '250'
24	X=i+1 Assignment with Calculation 'Remove_sup2' = 'Remove_sup2' - '250'
25	X=i+1 Assignment with Calculation 'Remove_sup3' = 'Remove_sup3' - '250'
26	X=i+1 Assignment with Calculation 'Remove_sup4' = 'Remove_sup4' - '250'
27	X=i+1 Assignment with Calculation 'Remove_sup5' = 'Remove_sup5' - '250'
28	X=i+1 Assignment with Calculation 'Remove_sup6' = 'Remove_sup6' - '250'
29	X=i+1 Assignment with Calculation 'Remove_sup7' = 'Remove_sup7' - '250'
30	X=i+1 Assignment with Calculation 'Remove_sup8' = 'Remove_sup8' - '250'
31	 Comment <Calculate volume to be used for mixing>
32	X=i+1 Assignment with Calculation 'mixingnum' = 'Volume' * '0.9'
33	 If, Else (mixingnum is greater than 1000)
34	X=0 Assignment 'mixingnum' = '1000'
35	End If
36	 Comment <Checking for appropriate sample number.>
37	X=i+1 Assignment with Calculation 'Trituration_num' = 'Trituration_num' / '2'
38	X=i+1 Assignment with Calculation 'Sample_check' = 'Sample_num' % '4'
39	 If, Else (Sample_check is NOT equal to 0)
40	 User Output Dialog Title: ", Return Value: ", Buttons: 'Only 'OK' button', Default: 'OK', Icons: 'Display information message icon', Sound: ", Timeout: 'infinite' Output: "Sample number must be in fours."
41	 User Input Dialog Title: ", Return Value: ", Buttons: 'Only 'OK' button', Default: 'OK', Sound: ", Timeout: 'infinite' Input: Sample_num ("How many samples do you have?"; Integer, 0, 0, 16)
42	End If
43	X=0 Assignment 'Tip_Cnt1000FTR' = ""Tip_Cnt1000FTR""







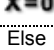




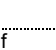
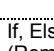
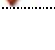




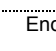
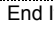
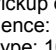
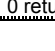


	Method
44	 Edit2 of HSLTipCountingNimbusLib TipCount1::Edit2(NimbusChannel.Ham_FTR_1000_0001, Tip_Cnt1000FTR, NimbusChannel, 999)
45	 Comment <Calculate loops>
46	 If, Else (Remove_sup1 is less than OR equal to 1000)
47	 If, Else (Remove_sup2 is less than OR equal to 1000)
48	 X=0 Assignment 'looper12' = '1'
49	 Else
50	 If, Else (Remove_sup2 is less than OR equal to 2000)
51	 X=0 Assignment 'looper12' = '2'
52	 Else
53	 X=0 Assignment 'looper12' = '3'
54	 End If
55	 End If
56	 Else
57	 If, Else (Remove_sup1 is less than OR equal to 2000)
58	 If, Else (Remove_sup2 is greater than 2000)
59	 X=0 Assignment 'looper12' = '3'
60	 Else
61	 X=0 Assignment 'looper12' = '2'
62	 End If
63	 Else
64	 X=0 Assignment 'looper12' = '3'
65	 End If
66	 End If
67	 If, Else (Remove_sup3 is less than OR equal to 1000)
68	 If, Else (Remove_sup4 is less than OR equal to 1000)










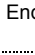

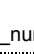




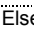

	Method	
69		Assignment 'looper34' = '1'
70		Else
71		If, Else (Remove_sup4 is less than OR equal to 2000)
72		Assignment 'looper34' = '2'
73		Else
74		Assignment 'looper34' = '3'
75		End If
76		End If
77		Else
78		If, Else (Remove_sup3 is less than OR equal to 2000)
79		If, Else (Remove_sup4 is greater than 2000)
80		Assignment 'looper34' = '3'
81		Else
82		Assignment 'looper34' = '2'
83		End If
84		Else
85		Assignment 'looper34' = '3'
86		End If
87		End If
88		If, Else (Remove_sup5 is less than OR equal to 1000)
89		If, Else (Remove_sup6 is less than OR equal to 1000)
90		Assignment 'looper56' = '1'
91		Else
92		If, Else (Remove_sup6 is less than OR equal to 2000)
93		Assignment 'looper56' = '2'

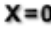



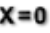


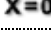

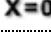


















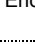












	Method
119	Else
120	If, Else (Remove_sup7 is less than OR equal to 2000)
121	If, Else (Remove_sup8 is greater than 2000)
122	Assignment X=0 'looper78' = '3'
123	Else
124	Assignment X=0 'looper78' = '2'
125	End If
126	Else
127	Assignment X=0 'looper78' = '3'
128	End If
129	End If
130	Comment <Start taking up supernatant>
131	Sequence: Set Current Position current position of sequence 'NimbusChannel.UBC_RoundBottom_DeepWell_Sq_24POS_0001' = '5'
132	If, Else (Sample_num is greater than OR equal to 4)
133	Loop 'looper12' times 'loopCounter3' used as loop counter variable
134	Comment <Counting>
135	If, Else (Remove_sup1 is greater than 1000)
136	Assignment X=0 'sup1' = '1000'
137	Else
138	If, Else (Remove_sup1 is greater than 0)
139	Assignment X=0 'sup1' = 'Remove_sup1'
140	Else
141	Assignment X=0 'sup1' = '0'
142	End If
143	End If




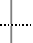
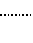








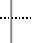


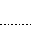

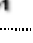

		Method	
144		If, Else (Remove_sup2 is greater than 1000)	
145		Assignment 'sup2' = '1000'	X=0
146		Else	
147		If, Else (Remove_sup2 is greater than 0)	
148		Assignment 'sup2' = 'Remove_sup2'	X=0
149		Else	
150		Assignment 'sup2' = '0'	X=0
151		End If	
152		End If	
153		Tip Pickup on NimbusChannel Sequence: "NimbusChannel.Ham_FTR_1000_0001" Tip Type: 1000ul High Volume Tip (Ham org. name) 0 return value(s)	
154		Aspirate on NimbusChannel Sequence: "NimbusChannel.UBC_RoundBottom_DeepWell_Sq_24POS_0001" Individual Volumes: (sup1,sup1,sup2,sup2) 4 return value(s)	
155		If, Else (loopCounter3 is equal to 1)	
156		Dispense on NimbusChannel Sequence: "NimbusChannel.UBC_32POS_Microtube_0001" HxCommandDetailLevel: allDetails Volume: 0.00 4 return value(s)	
157		Else	
158		Dispense on NimbusChannel Sequence: "NimbusChannel.UBC_RGT_CONT_50mL_0001" HxCommandDetailLevel: allDetails Volume: 0 4 return value(s)	
159		End If	
160		Tip Eject on NimbusChannel Sequence: "Waste" 0 return value(s)	
161		Assignment with Calculation 'Remove_sup1' = 'Remove_sup1' - '1000'	X=i+1
162		Assignment with Calculation 'Remove_sup2' = 'Remove_sup2' - '1000'	X=i+1
163		End Loop	
164		SeqIncrement of HSLSeqLib SeqIncrement(NimbusChannel.UBC_RoundBottom_DeepWell_Sq_24POS_0001, 4)	
165		End If	


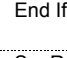



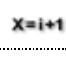
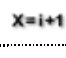
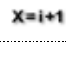
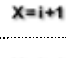
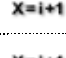
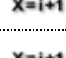
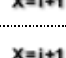













	Method	
166		Comment <2nd column>
167		Sequence: Set Current Position current position of sequence 'NimbusChannel.UBC_RoundBottom_DeepWell_Sq_24POS_0001' = '9'
168		If, Else (Sample_num is greater than OR equal to 8)
169		Loop 'looper34' times 'loopCounter3' used as loop counter variable
170		Comment <Counting>
171		If, Else (Remove_sup3 is greater than 1000)
172		Assignment X=0 'sup3' = '1000'
173		Else
174		If, Else (Remove_sup3 is greater than 0)
175		Assignment X=0 'sup3' = 'Remove_sup3'
176		Else
177		Assignment X=0 'sup3' = '0'
178		End If
179		End If
180		If, Else (Remove_sup4 is greater than 1000)
181		Assignment X=0 'sup4' = '1000'
182		Else
183		If, Else (Remove_sup4 is greater than 0)
184		Assignment X=0 'sup4' = 'Remove_sup4'
185		Else
186		Assignment X=0 'sup4' = '0'
187		End If
188		End If
189		Tip Pickup on NimbusChannel Sequence: "NimbusChannel.Ham_FTR_1000_0001" Tip Type: 1000ul High Volume Tip (Ham org. name) 0 return value(s)

		Method	
190			Aspirate on NimbusChannel Sequence: "NimbusChannel.UBC_RoundBottom_DeepWell_Sq_24POS_0001" Individual Volumes: (sup3,sup3,sup4,sup4) 4 return value(s) .
191			If, Else (loopCounter3 is equal to 1)
192			Dispense on NimbusChannel Sequence: "NimbusChannel.UBC_32POS_Microtube_0001" HxCommandDetailLevel: allDetails Volume: 0.00 4 return value(s) .
193			Else
194			Dispense on NimbusChannel Sequence: "NimbusChannel.UBC_RGT_CONT_50mL_0001" HxCommandDetailLevel: allDetails Volume: 0 4 return value(s) .
195			End If
196			Tip Eject on NimbusChannel Sequence: "Waste" 0 return value(s) .
197		$X=i+1$	Assignment with Calculation 'Remove_sup3' = 'Remove_sup3' - '1000'
198		$X=i+1$	Assignment with Calculation 'Remove_sup4' = 'Remove_sup4' - '1000'
199			End Loop
200			SeqIncrement of HSLSeqLib SeqIncrement(NimbusChannel.UBC_RoundBottom_DeepWell_Sq_24POS_0001, 4)
201			End If
202			Comment <3rd column>
203			If, Else (Sample_num is greater than OR equal to 12)
204			Loop 'looper56' times 'loopCounter3' used as loop counter variable
205			Comment <Counting>
206			If, Else (Remove_sup5 is greater than 1000)
207		$X=0$	Assignment 'sup5' = '1000'
208			Else
209			If, Else (Remove_sup5 is greater than 0)
210		$X=0$	Assignment 'sup5' = 'Remove_sup5'
211			Else

				Method
212				Assignment 'sup5' = '0'
213				End If
214				End If
215				If, Else (Remove_sup6 is greater than 1000)
216				Assignment 'sup6' = '1000'
217				Else
218				If, Else (Remove_sup6 is greater than 0)
219				Assignment 'sup6' = 'Remove_sup6'
220				Else
221				Assignment 'sup6' = '0'
222				End If
223				End If
224				Tip Pickup on NimbusChannel Sequence: "NimbusChannel.Ham_FTR_1000_0001" Tip Type: 1000ul High Volume Tip (Ham org. name) 0 return value(s) .
225				Aspirate on NimbusChannel Sequence: "NimbusChannel.UBC_RoundBottom_DeepWell_Sq_24POS_0001" Individual Volumes: (sup5,sup5,sup6,sup6) 4 return value(s) .
226				If, Else (Day is equal to 3)
227				If, Else (loopCounter3 is equal to 1)
228				Dispense on NimbusChannel Sequence: "NimbusChannel.UBC_32POS_Microtube_0001" HxCommandDetailLevel: allDetails Volume: 0.00 4 return value(s) .
229				Else
230				Dispense on NimbusChannel Sequence: "NimbusChannel.UBC_RGT_CONT_50mL_0001" HxCommandDetailLevel: allDetails Volume: 0 4 return value(s) .
231				End If
232				Else

			Method
233			Dispense on NimbusChannel Sequence: "NimbusChannel.UBC_RGT_CONT_50mL_0001" HxCommandDetailLevel: allDetails Volume: 0 4 return value(s) .
234			End If
235			Tip Eject on NimbusChannel Sequence: "Waste" 0 return value(s) .
236		X=i+1	Assignment with Calculation 'Remove_sup5' = 'Remove_sup5' - '1000'
237		X=i+1	Assignment with Calculation 'Remove_sup6' = 'Remove_sup6' - '1000'
238			End Loop
239			SeqIncrement of HSLSeqLib SeqIncrement(NimbusChannel.UBC_RoundBottom_DeepWell_Sq_24POS_0001, 4)
240			End If
241			Comment <4th column>
242			If, Else (Sample_num is equal to 16)
243			Loop 'looper78' times 'loopCounter3' used as loop counter variable
244			Comment <Counting>
245			If, Else (Remove_sup7 is greater than 1000)
246		X=0	Assignment 'sup7' = '1000'
247			Else
248			If, Else (Remove_sup7 is greater than 0)
249		X=0	Assignment 'sup7' = 'Remove_sup7'
250			Else
251		X=0	Assignment 'sup7' = '0'
252			End If
253			End If
254			If, Else (Remove_sup8 is greater than 1000)
255		X=0	Assignment 'sup8' = '1000'
256			Else

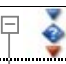



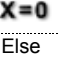




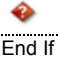
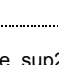




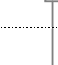



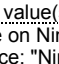




		Method	
257			If, Else (Remove_sup8 is greater than 0)
258			Assignment 'sup8' = 'Remove_sup8'
259			Else
260			Assignment 'sup8' = '0'
261			End If
262			End If
263			Tip Pickup on NimbusChannel Sequence: "NimbusChannel.Ham_FTR_1000_0001" Tip Type: 1000ul High Volume Tip (Ham org. name) 0 return value(s)
264			Aspirate on NimbusChannel Sequence: "NimbusChannel.UBC_RoundBottom_DeepWell_Sq_24POS_0001" Individual Volumes: (sup7,sup7,sup8,sup8) 4 return value(s)
265			If, Else (Day is equal to 4)
266			If, Else (loopCounter3 is equal to 1)
267			Dispense on NimbusChannel Sequence: "NimbusChannel.UBC_32POS_Microtube_0001" HxCommandDetailLevel: allDetails Volume: 0.00 4 return value(s)
268			Else
269			Dispense on NimbusChannel Sequence: "NimbusChannel.UBC_RGT_CONT_50mL_0001" HxCommandDetailLevel: allDetails Volume: 0 4 return value(s)
270			End If
271			Else
272			Dispense on NimbusChannel Sequence: "NimbusChannel.UBC_RGT_CONT_50mL_0001" HxCommandDetailLevel: allDetails Volume: 0 4 return value(s)
273			End If
274			Tip Eject on NimbusChannel Sequence: "Waste" 0 return value(s)
275			Assignment with Calculation 'Remove_sup7' = 'Remove_sup7' - '1000'
276			Assignment with Calculation 'Remove_sup8' = 'Remove_sup8' - '1000'

















	Method
277	 End Loop
278	 End If
279	 SeqResetSequenceIndexes of HSLSeqLib SeqResetSequenceIndexes(NimbusChannel.UBC_RoundBottom_DeepWell_Sq_24POS_0001)
280	 Comment <END SUPERNATANT REMOVAL START RESUSPENSION>
281	 Comment <Reset Remove_sup#s>
282	 X=i+1 Assignment with Calculation 'Remove_sup1' = 'Percent_sup1' * 'Volume'
283	 X=i+1 Assignment with Calculation 'Remove_sup2' = 'Percent_sup2' * 'Volume'
284	 X=i+1 Assignment with Calculation 'Remove_sup3' = 'Percent_sup3' * 'Volume'
285	 X=i+1 Assignment with Calculation 'Remove_sup4' = 'Percent_sup4' * 'Volume'
286	 X=i+1 Assignment with Calculation 'Remove_sup5' = 'Percent_sup5' * 'Volume'
287	 X=i+1 Assignment with Calculation 'Remove_sup6' = 'Percent_sup6' * 'Volume'
288	 X=i+1 Assignment with Calculation 'Remove_sup7' = 'Percent_sup7' * 'Volume'
289	 X=i+1 Assignment with Calculation 'Remove_sup8' = 'Percent_sup8' * 'Volume'
290	 Comment <Recalculate loops>
291	 If, Else (Remove_sup1 is less than OR equal to 1000)
292	 If, Else (Remove_sup2 is less than OR equal to 1000)
293	 X=0 Assignment 'looper12' = '1'
294	 Else
295	 If, Else (Remove_sup2 is less than OR equal to 2000)
296	 X=0 Assignment 'looper12' = '2'
297	 Else
298	 X=0 Assignment 'looper12' = '3'
299	 End If
300	 End If
301	 Else



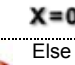

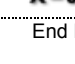
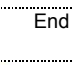



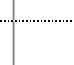

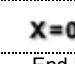

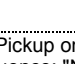
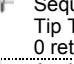







Method	
302	If, Else (Remove_sup1 is less than OR equal to 2000)
303	If, Else (Remove_sup2 is greater than 2000)
304	Assignment X=0 'looper12' = '3'
305	Else
306	Assignment X=0 'looper12' = '2'
307	End If
308	Else
309	Assignment X=0 'looper12' = '3'
310	End If
311	End If
312	If, Else (Remove_sup3 is less than OR equal to 1000)
313	If, Else (Remove_sup4 is less than OR equal to 1000)
314	Assignment X=0 'looper34' = '1'
315	Else
316	If, Else (Remove_sup4 is less than OR equal to 2000)
317	Assignment X=0 'looper34' = '2'
318	Else
319	Assignment X=0 'looper34' = '3'
320	End If
321	End If
322	Else
323	If, Else (Remove_sup3 is less than OR equal to 2000)
324	If, Else (Remove_sup4 is greater than 2000)
325	Assignment X=0 'looper34' = '3'
326	Else

















		Method
327		X=0 Assignment 'looper34' = '2'
328		End If
329		Else
330		X=0 Assignment 'looper34' = '3'
331		End If
332		End If
333		If, Else (Remove_sup5 is less than OR equal to 1000)
334		If, Else (Remove_sup6 is less than OR equal to 1000)
335		X=0 Assignment 'looper56' = '1'
336		Else
337		If, Else (Remove_sup6 is less than OR equal to 2000)
338		X=0 Assignment 'looper56' = '2'
339		Else
340		X=0 Assignment 'looper56' = '3'
341		End If
342		End If
343		Else
344		If, Else (Remove_sup5 is less than OR equal to 2000)
345		If, Else (Remove_sup6 is greater than 2000)
346		X=0 Assignment 'looper56' = '3'
347		Else
348		X=0 Assignment 'looper56' = '2'
349		End If
350		Else
351		X=0 Assignment 'looper56' = '3'




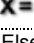

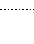













	Method
352	End If
353	End If
354	If, Else (Remove_sup7 is less than OR equal to 1000)
355	If, Else (Remove_sup8 is less than OR equal to 1000)
356	X=0 Assignment 'looper78' = '1'
357	Else
358	If, Else (Remove_sup8 is less than OR equal to 2000)
359	X=0 Assignment 'looper78' = '2'
360	Else
361	X=0 Assignment 'looper78' = '3'
362	End If
363	End If
364	Else
365	If, Else (Remove_sup7 is less than OR equal to 2000)
366	If, Else (Remove_sup8 is greater than 2000)
367	X=0 Assignment 'looper78' = '3'
368	Else
369	X=0 Assignment 'looper78' = '2'
370	End If
371	Else
372	X=0 Assignment 'looper78' = '3'
373	End If
374	End If
375	Comment <Start resuspension>
376	Sequence: Set Current Position current position of sequence 'NimbusChannel.UBC_RoundBottom_DeepWell_Sq_24POS_0001' = '5'


















	Method	
377		If, Else (Sample_num is greater than OR equal to 4)
378		Loop 'looper12' times 'loopCounter3' used as loop counter variable
379		Comment <Counting>
380		If, Else (Remove_sup1 is greater than 1000)
381		Assignment X=0 'sup1' = '1000'
382		Else
383		If, Else (Remove_sup1 is greater than 0)
384		Assignment X=0 'sup1' = 'Remove_sup1'
385		Else
386		Assignment X=0 'sup1' = '0'
387		End If
388		End If
389		If, Else (Remove_sup2 is greater than 1000)
390		Assignment X=0 'sup2' = '1000'
391		Else
392		If, Else (Remove_sup2 is greater than 0)
393		Assignment X=0 'sup2' = 'Remove_sup2'
394		Else
395		Assignment X=0 'sup2' = '0'
396		End If
397		End If
398		Tip Pickup on NimbusChannel Sequence: "NimbusChannel.Ham_FTR_1000_0001" Tip Type: 1000ul High Volume Tip (Ham org. name) 0 return value(s).
399		Aspirate on NimbusChannel Sequence: "NimbusChannel.UBC_RGT_CONT_50mL_0004" Individual Volumes: (sup1,sup1,sup2,sup2) 4 return value(s).
400		If, Else (loopCounter3 is less than looper12)

		Method	
401			Dispense on NimbusChannel Sequence: "NimbusChannel.UBC_RoundBottom_DeepWell_Sq_24POS_0001" HxCommandDetailLevel: allDetails Individual Volumes: (sup1,sup1,sup2,sup2) 4 return value(s) .
402			Else
403			Dispense on NimbusChannel Sequence: "NimbusChannel.UBC_RoundBottom_DeepWell_Sq_24POS_0001" HxCommandDetailLevel: allDetails Individual Volumes: (sup1,sup1,sup2,sup2) 4 return value(s) .
404			Aspirate on NimbusChannel Sequence: "NimbusChannel.UBC_RoundBottom_DeepWell_Sq_24POS_0001" Volume: 1000 4 return value(s) .
405			Dispense on NimbusChannel Sequence: "NimbusChannel.UBC_RoundBottom_DeepWell_Sq_24POS_0001" HxCommandDetailLevel: allDetails Volume: 0 4 return value(s) .
406			Aspirate on NimbusChannel Sequence: "NimbusChannel.UBC_RoundBottom_DeepWell_Sq_24POS_0001" Volume: 250 4 return value(s) .
407			Dispense on NimbusChannel Sequence: "NimbusChannel.UBC_RoundBottom_DeepWell_Sq_24POS_0001" HxCommandDetailLevel: allDetails Volume: 0 4 return value(s) .
408			End If
409			Tip Eject on NimbusChannel Sequence: "Waste" 0 return value(s) .
410	$X=i+1$		Assignment with Calculation 'Remove_sup1' = 'Remove_sup1' - '1000'
411	$X=i+1$		Assignment with Calculation 'Remove_sup2' = 'Remove_sup2' - '1000'
412			End Loop
413			End If
414			Comment <2nd column>
415			If, Else (Sample_num is greater than OR equal to 8)
416			Loop 'looper34' times 'loopCounter3' used as loop counter variable
417			Comment <Counting>
418			If, Else (Remove_sup3 is greater than 1000)
419	$X=0$		Assignment 'sup3' = '1000'




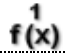


		Method	
420			Else
421			If, Else (Remove_sup3 is greater than 0)
422			Assignment X=0 'sup3' = 'Remove_sup3'
423			Else
424			Assignment X=0 'sup3' = '0'
425			End If
426			End If
427			If, Else (Remove_sup4 is greater than 1000)
428			Assignment X=0 'sup4' = '1000'
429			Else
430			If, Else (Remove_sup4 is greater than 0)
431			Assignment X=0 'sup4' = 'Remove_sup4'
432			Else
433			Assignment X=0 'sup4' = '0'
434			End If
435			End If
436			Tip Pickup on NimbusChannel Sequence: "NimbusChannel.Ham_FTR_1000_0001" Tip Type: 1000ul High Volume Tip (Ham org. name) 0 return value(s)
437			Aspirate on NimbusChannel Sequence: "NimbusChannel.UBC_RGT_CONT_50mL_0004" Individual Volumes: (sup3,sup3,sup4,sup4) 4 return value(s)
438			If, Else (loopCounter3 is less than loop34)
439			Dispense on NimbusChannel Sequence: "NimbusChannel.UBC_RoundBottom_DeepWell_Sq_24POS_0001" HxCommandDetailLevel: allDetails Individual Volumes: (sup3,sup3,sup4,sup4) 4 return value(s)
440			Else
441			Dispense on NimbusChannel Sequence: "NimbusChannel.UBC_RoundBottom_DeepWell_Sq_24POS_0001" HxCommandDetailLevel: allDetails Individual Volumes: (sup3,sup3,sup4,sup4) 4 return value(s)

		Method	
442			Aspirate on NimbusChannel Sequence: "NimbusChannel.UBC_RoundBottom_DeepWell_Sq_24POS_0001" Volume: 1000 4 return value(s) .
443			Dispense on NimbusChannel Sequence: "NimbusChannel.UBC_RoundBottom_DeepWell_Sq_24POS_0001" HxCommandDetailLevel: allDetails Volume: 0 4 return value(s) .
444			Aspirate on NimbusChannel Sequence: "NimbusChannel.UBC_RoundBottom_DeepWell_Sq_24POS_0001" Volume: 250 4 return value(s) .
445			Dispense on NimbusChannel Sequence: "NimbusChannel.UBC_RoundBottom_DeepWell_Sq_24POS_0001" HxCommandDetailLevel: allDetails Volume: 0 4 return value(s) .
446			End If
447			Tip Eject on NimbusChannel Sequence: "Waste" 0 return value(s) .
448		X=i+1	Assignment with Calculation 'Remove_sup3' = 'Remove_sup3' - '1000'
449		X=i+1	Assignment with Calculation 'Remove_sup4' = 'Remove_sup4' - '1000'
450			End Loop
451			End If
452			Comment <3rd column>
453			If, Else (Sample_num is greater than OR equal to 12)
454			Loop 'looper56' times 'loopCounter3' used as loop counter variable
455			Comment <Counting>
456			If, Else (Remove_sup5 is greater than 1000)
457		X=0	Assignment 'sup5' = '1000'
458			Else
459			If, Else (Remove_sup5 is greater than 0)
460		X=0	Assignment 'sup5' = 'Remove_sup5'
461			Else
462		X=0	Assignment 'sup5' = '0'

		Method	
463			End If
464			End If
465			If, Else (Remove_sup6 is greater than 1000)
466			Assignment X=0 'sup6' = '1000'
467			Else
468			If, Else (Remove_sup6 is greater than 0)
469			Assignment X=0 'sup6' = 'Remove_sup6'
470			Else
471			Assignment X=0 'sup6' = '0'
472			End If
473			End If
474			Tip Pickup on NimbusChannel Sequence: "NimbusChannel.Ham_FTR_1000_0001" Tip Type: 1000ul High Volume Tip (Ham org. name) 0 return value(s)
475			Aspirate on NimbusChannel Sequence: "NimbusChannel.UBC_RGT_CONT_50mL_0005" Individual Volumes: (sup5,sup5,sup6,sup6) 4 return value(s)
476			If, Else (loopCounter3 is less than loop56)
477			Dispense on NimbusChannel Sequence: "NimbusChannel.UBC_RoundBottom_DeepWell_Sq_24POS_0001" HxCommandDetailLevel: allDetails Individual Volumes: (sup5,sup5,sup6,sup6) 4 return value(s)
478			Else
479			Dispense on NimbusChannel Sequence: "NimbusChannel.UBC_RoundBottom_DeepWell_Sq_24POS_0001" HxCommandDetailLevel: allDetails Individual Volumes: (sup5,sup5,sup6,sup6) 4 return value(s)
480			Aspirate on NimbusChannel Sequence: "NimbusChannel.UBC_RoundBottom_DeepWell_Sq_24POS_0001" Volume: 1000 4 return value(s)
481			Dispense on NimbusChannel Sequence: "NimbusChannel.UBC_RoundBottom_DeepWell_Sq_24POS_0001" HxCommandDetailLevel: allDetails Volume: 0 4 return value(s)

		Method	
482			Aspirate on NimbusChannel Sequence: "NimbusChannel.UBC_RoundBottom_DeepWell_Sq_24POS_0001" Volume: 250 4 return value(s) .
483			Dispense on NimbusChannel Sequence: "NimbusChannel.UBC_RoundBottom_DeepWell_Sq_24POS_0001" HxCommandDetailLevel: allDetails Volume: 0 4 return value(s) .
484			End If
485			Tip Eject on NimbusChannel Sequence: "Waste" 0 return value(s) .
486		X=i+1	Assignment with Calculation 'Remove_sup5' = 'Remove_sup5' - '1000'
487		X=i+1	Assignment with Calculation 'Remove_sup6' = 'Remove_sup6' - '1000'
488			End Loop
489			End If
490			Comment <4th column>
491			If, Else (Sample_num is equal to 16)
492			Loop 'looper78' times 'loopCounter3' used as loop counter variable
493			Comment <Counting>
494			If, Else (Remove_sup7 is greater than 1000)
495		X=0	Assignment 'sup7' = '1000'
496			Else
497			If, Else (Remove_sup7 is greater than 0)
498		X=0	Assignment 'sup7' = 'Remove_sup7'
499			Else
500		X=0	Assignment 'sup7' = '0'
501			End If
502			End If
503			If, Else (Remove_sup8 is greater than 1000)
504		X=0	Assignment 'sup8' = '1000'

		Method	
505			Else
506			If, Else (Remove_sup8 is greater than 0)
507		X=0	Assignment 'sup8' = 'Remove_sup8'
508			Else
509		X=0	Assignment 'sup8' = '0'
510			End If
511			End If
512		1000	Tip Pickup on NimbusChannel Sequence: "NimbusChannel.Ham_FTR_1000_0001" Tip Type: 1000ul High Volume Tip (Ham org. name) 0 return value(s)
513		1000	Aspirate on NimbusChannel Sequence: "NimbusChannel.UBC_RGT_CONT_50mL_0005" Individual Volumes: (sup7,sup7,sup8,sup8) 4 return value(s)
514			If, Else (loopCounter3 is less than looper78)
515		1000	Dispense on NimbusChannel Sequence: "NimbusChannel.UBC_RoundBottom_DeepWell_Sq_24POS_0001" HxCommandDetailLevel: allDetails Individual Volumes: (sup7,sup7,sup8,sup8) 4 return value(s)
516			Else
517		1000	Dispense on NimbusChannel Sequence: "NimbusChannel.UBC_RoundBottom_DeepWell_Sq_24POS_0001" HxCommandDetailLevel: allDetails Individual Volumes: (sup7,sup7,sup8,sup8) 4 return value(s)
518		1000	Aspirate on NimbusChannel Sequence: "NimbusChannel.UBC_RoundBottom_DeepWell_Sq_24POS_0001" Volume: 1000 4 return value(s)
519		1000	Dispense on NimbusChannel Sequence: "NimbusChannel.UBC_RoundBottom_DeepWell_Sq_24POS_0001" HxCommandDetailLevel: allDetails Volume: 0 4 return value(s)
520		1000	Aspirate on NimbusChannel Sequence: "NimbusChannel.UBC_RoundBottom_DeepWell_Sq_24POS_0001" Volume: 250 4 return value(s)
521		1000	Dispense on NimbusChannel Sequence: "NimbusChannel.UBC_RoundBottom_DeepWell_Sq_24POS_0001" HxCommandDetailLevel: allDetails Volume: 0 4 return value(s)
522			End If

		Method	
523			Tip Eject on NimbusChannel Sequence: "Waste" 0 return value(s)
524		$X=i+1$	Assignment with Calculation 'Remove_sup7' = 'Remove_sup7' - '1000'
525		$X=i+1$	Assignment with Calculation 'Remove_sup8' = 'Remove_sup8' - '1000'
526			End Loop
527			End If
528		1	Write2 of HSLTipCountingNimbusLib TipCount1::Write2(NimbusChannel.Ham_FTR_1000_0001, Tip_Cnt1000FTR, NimbusChannel)
529			Comment <Done removing supernatant and replenishing and resuspending with new media.>
530			User Output Dialog Title: ", Return Value: ", Buttons: 'Only 'OK' button', Default: 'OK', Icons: 'Display information message icon', Sound: ", Timeout: 'infinite' Output: "Method complete!"
531			

Appendix B: Microfluidic Fabrication Protocols

Fabrication Protocol: Midiclone Devices with Osmotic Bath

Sylgard cell culture chips (v1.1, 2.0, 2.1, 2.2)

- 1) prepare Sylgard for bath and control 1:10 (5 g + 50 g)
- 2) make bath, **bake for 50 min**
- 3) spin control at 1500 rpm (use the rest of PDMS that's left from bath), wait for 10 min after spinning until the features on the wafer get flat, bake at the same time as the bath for 50 min
- 4) cut out the bath from the mold and cut the membrane in the place of the array out, oxidize the top part of the bath (where the membrane has been cut) and the control for 25 s
- 5) align control with bath, **bake for 20 min**
- 6) in the meantime prepare GE plug 1:10 (5 g + 50 g) and degas in the cup
- 7) oxidize the bath + control combo for 15 - 20 s, treat with **fluorosilane for 8 min**
- 8) pour GE 1:10 (5 g + 50 g) into the bath and make another thick layer, **bake for 50 min**
- 9) in the mean time prepare 1:10 (2 g + 20 g) of Sylgard per wafer for blank and flow
- 10) make the blank for membrane between flow and control - spin at 3500 rpm, **bake for 50 min**
- 11) prepare the flow: spin at 300 rpm, pour on top extra PDMS (~10 g), **degas in Dixie cup first**, oxidize glass slide for 15 s on medium, put the flow wafer on a tin foil, put the glass slide on the wafer starting from one side, pushing out bubbles, squeeze any bubbles out, tape the slide to the wafer, pack the tin foil, put a 500 g weight on it (optional) and **bake it for 50 min**
- 12) peel off the bath + control, oxidize B + C and blank for 25 s, bond together, **bake for 15 min**

13) peel off bath + control + blank from wafer, (if version v2.1 cut into individual chips), peel off flow wafer from the slide by cutting around and gently lifting it at a few sides with a small tweezers, slowly, wait until you hear it is peeling off

14) oxidize B + C + B and flow on slide for 12 s, align under the microscope, probably have 2 - 3 shots of peeling off and trying again

15) **bake for 1 - 2 h**, peel off from slide (**can leave overnight after removing from oven**)

16) cut into chips, peel off the GE plug

17) punch holes

18) oxidize chips and slides for 25 s and bond (careful to place it in the middle if v2.0, 2.1), start bonding from one side and push to the other side to avoid any bubbles under the array

(make sure to bond on black background like an alignment scope bed so you can see the bubbles when bonding)

4 Layer - hESC Bath Chip Fabrication Protocol (3 sets of wafers)

Cleaning Layer (10:1)

- Foiled 9 shallow petrie dishes
- Treated wafers with TMCS for ~10 min.
- Mixed 60.0 g RTV A (GE 09H101) with 6.0 g RTV B (GE 09H102) [cup #1]
- Mixed 60.0 g RTV A (GE 09H101) with 6.0 g RTV B (GE 09H102) [cup #2]
- Mixed 60.0 g RTV A (GE 09H101) with 6.0 g RTV B (GE 09H102) [cup #3]
- Poured PDMS onto wafers
- Cured for 45 min @ 80°C

Flow Layer (5:1)

- Foiled 3 deep petrie dishes
- Treated bath wafers with TMCS for ~10 min.
- Mixed **12.5 g** RTV A (GE 09H101) with **2.5 g** RTV B (GE 09H102) [cup #1]
- Mixed **12.5 g** RTV A (GE 09H101) with **2.5 g** RTV B (GE 09H102) [cup #2]
- Mixed **12.5 g** RTV A (GE 09H101) with **2.5 g** RTV B (GE 09H102) [cup #3]
- Poured PDMS onto wafers in deep foil dishes
- Degassed for 45 min in “BIG DEGASSER” (Foil shallow petrie dishes while degassing)
- Straightened wafers & removed bubbles with pipette tips
- Cured for **40 min** @ 80°C

Control Layer (20:1)

- Foiled 3 shallow petrie dishes
- Treated control wafers with TMCS for ~10 min.
- Mixed **60.0 g** RTV A (GE 09H102) with **3.0 g** RTV B (GE 09H102)
- Poured PDMS onto wafers in spinner & spin coated wafers
- Used Recipe #7:
 1. Ramp to 500 for 10 s
 2. Ramp to 1650 for 60 s
 3. Ramp to 0
- Cured for **25 min** @ 80°C

Alignment (precise)

- Removed chips from oven
- Cut out around flow wafer inside the edge of the wafer.
- Placed control wafer under microscope
- Peeled off flow layer from flow wafer & aligned flow to control wafer under microscope (~20 min per wafer)
- Cured aligned FLOW/CTRL for **1 h** @ 80°C

Blank Layer (20:1)

- Foiled 3 shallow petrie dishes
- Treated 3 blank wafers with TMCS for ~10 min.
- Mixed **60.0 g** RTV A (GE 09H102) with **3.0 g** RTV B (GE 09H102)

- Poured PDMS onto wafers in spinner & spin coated wafers
- Used Recipe #2:
 1. Ramp to 500 for 10 s
 2. Ramp to 1650 for 60 s
 3. Ramp to 0
- Cured for **25 min @ 80°C**
- Cut out around ctrl wafer inside the edge of the wafer.
- Peel off bonded FLOW/CTRL from ctrl wafer.
- Aligned CTRL side down for each chip and bonded FLOW/CTRL to BLANK. Made sure no bubbles were present btw CTRL and BLANK layers.
- Cured FLOW/CTRL/BLANK **~1 h @ 80°C**.

Can be left in the oven overnight after this step

BLANK Bath Layer (10:1)

- Foiled 4 deep petrie dishes
- Treated 4 BLANK wafers with TMCS for ~10 min.
- Mixed **40.0 g** RTV A (GE 09H102) with **4.0 g** RTV B (GE 09H102) [**cup #1**]
- Mixed **40.0 g** RTV A (GE 09H102) with **4.0 g** RTV B (GE 09H102) [**cup #2**]
- Mixed **40.0 g** RTV A (GE 09H102) with **4.0 g** RTV B (GE 09H102) [**cup #3**]
- Mixed **40.0 g** RTV A (GE 09H102) with **4.0 g** RTV B (GE 09H102) [**cup #4**]
- Poured PDMS onto wafers in deep foil dishes.
- Degassed for 1 h in “BIG DEGASSER” (until no visible bubbles were left)
- Straightened wafers & removed bubbles with pipette tips
- Cured for **40 min @ 80°C**.
- Remove FLOW/CONTROL/BLANK & Blank BATH layer from oven.
- Cut around outside of FLOW/CTRL/Blank layer & remove any excess PDMS.
- Dice into individual chips.
- Clean ALL chips vigorously with tape.
- Dice Blank BATH layers (into 4 pieces each) and mark/cut inside to create bath area. Make sure to leave enough space for the ports & edges. Punch out holes for BATH (**MAKE SURE NOT TO CROSS ANY CTRL/FLOW PUNCH HOLES!!!**)

Stamping 1

- Foiled 4 shallow petrie dishes
- Treated 4 blank wafers with TMCS for ~10 min (OPTIONAL)
- Mixed **60.0 g** RTV A (GE 09H102) with **6.0 g** RTV B (GE 09H102)
- Poured PDMS onto wafers in spinner & spin coated wafers
- Used Recipe #2:
 1. Ramp to 500 for 10 s
 2. Ramp to 6000 for 60 s
 3. Ramp to 0

- “STAMP” each THICK blank portion onto the liquid blank wafer and leave for 30 s.
- Remove from wafer and stick together with TOP of FLOW/CTRL/BLANK portion. Make sure to remove bubbles between layers.
- Place all “stamped” chips onto ball bearings in oven and bake for at least **1 h @ 80°C**.

Can be left in the oven overnight after this step

Final TOP Blank & stamping 2:

- Foiled 4 deep petrie dishes
- Treated 4 blank wafers with TMCS for ~10 min (OPTIONAL)
- Mixed **12.5 g** RTV A (GE 09H102) with **2.5 g** RTV B (GE 09H102) [**cup #1**]
- Mixed **12.5 g** RTV A (GE 09H102) with **2.5 g** RTV B (GE 09H102) [**cup #2**]
- Mixed **12.5 g** RTV A (GE 09H102) with **2.5 g** RTV B (GE 09H102) [**cup #3**]
- Poured PDMS onto wafers in deep foil dishes.
- Degassed for 30 – 45 min in “BIG DEGASSER” (until no visible bubbles were left)
- Straightened wafers & removed bubbles with pipette tips
- Cured for **40 min @ 80°C**.

- Foiled 4 shallow petrie dishes
- Treated 4 blank wafers with TMCS for ~10 min (OPTIONAL)
- Mixed **60.0 g** RTV A (GE 09H102) with **6.0 g** RTV B (GE 09H102)
- Poured PDMS onto wafers in spinner & spin coated wafers
- Used Recipe #2:
 4. Ramp to 500 for 10 s
 5. Ramp to 6000 for 60 s
 6. Ramp to 0

- Remove TOP Blank layer as well as BATH layers stamped to chips from oven. Dice TOP Blank layers (into 4 pieces each) & cut off any excess PDMS from chips.
- “STAMP” the TOP of each THICK blank portion (now attached to the FLOW/CTRL/thin BLANK) onto the liquid blank wafer and leave for 30 s.
- Remove from wafer and stick together with TOP Blank layer portion. Make sure to remove bubbles between layers.
- Place all “stamped” chips onto ball bearings in oven and bake for at least **1 h @ 80°C**.

Can be left in the oven overnight after this step

Punching/Bonding to Glass

- Remove BATH chips from oven & cut off any excess PDMS from chips.
- Punched holes in TOP blank/BATH/FLOW/CTRL/BLANK layer (~2-3 h)
- Clean glass slides with IPA and clean chips vigorously with tape.

- Use plasma bonder to bond chips to glass slides (20 s; follow proper plasma bonding protocol).
- Cure all chips at least overnight (or all weekend) @ 80°C.

Appendix C: Bead Segmentation Algorithm

```
cd('D:\Darek\2015_06_01 - Dilution Series Test 2');

clear
clc

f = 'D:\Darek\2015_06_01 - Dilution Series Test 2';

%%
% post_inc
% subtract bg with post_load?

days = {...
    'Day 1\Array 1 - 0 ugpmL'...
    'Day 1\Array 2 - pt01 ugpmL'...
    'Day 1\Array 3 - pt1 ugpmL'...
    'Day 1\Array 4 - 1 ugpmL'...
    'Day 2\Array 1 - 0 ugpmL'...
    'Day 2\Array 2 - 1 ugpmL'...
    'Day 2\Array 3 - 10 ugpmL'...
    'Day 2\Array 4 - 100 ugpmL'...
};

patterns = {...
    '*Postload*1s*00_Red.tif'...
    '*Postinc*1s*00_Red.tif'...
};

folder = fullfile(f,days{1});
pattern = patterns{1};
D = parseFolder(folder,pattern,false);

FLsum1 = zeros(length(patterns),length(days),length(D));
FLmean1 = zeros(length(patterns),length(days),length(D));
%FLsum2 = zeros(length(patterns),length(days),length(D));
%FLmean2 = zeros(length(patterns),length(days),length(D));

for kp = 1:length(patterns)

    pattern = patterns{kp};

    for kd = 1:length(days)

        folder = fullfile(f,days{kd});
        D = parseFolder(folder,pattern,false);
```

```

for k = 1:length(D)

    % Load image
    A = imread(fullfile(folder,D(k).name));
    figure(1); imagesc(I0); colormap gray
    %I = 1-double(I0)/65536;

    %switch kp
    % case {1,2}
    %     threshold = 1-3500/65536;
    % case {3,4}
    %     threshold = 1-17500/65536;
    % case {5,6}
    %     threshold = 1-35000/65536;
    %end

%     [mask,info] = dd_segBeads(I,threshold);

    % Background illumination is usually brighter at centre.
    % Use imopen to estimate the background illumination.
    background = imopen(A,strel('disk',20));

    % Subtract background from initial image
    I2 = A - background;

    % Filter the image with a 10x10 median filter
    I3 = medfilt2(I2,[10 10],'symmetric');

    % Increase contrast so it can be thresholded
    I4 = imadjust(I3);

    %Repeat process
    background2 = imopen(I4,strel('disk',20));
    I5 = I4 - background2;
    I6 = medfilt2(I5,[10 10],'symmetric');
    I7 = imadjust(I6);

    % Create a new binary image (mask) via thresholding.
    level = graythresh(I7);
    mask = im2bw(I7,level);

    % Remove background noise with bwareaopen.
    mask = bwareaopen(mask, 50);

```



```

% Apply mask to original image
value = mask.*im2double(A);

%figure(2); imshow(B);

[PATHSTR,NAME,EXT] = fileparts(D(k).name);
imwrite(mask,fullfile(folder,PATHSTR,[NAME,'_mask',EXT]),'TIFF');

figure(1); imagesc(mask); colormap gray

value1 = value;%(:,1:256);
%value2 = value(:,257:end);
%   value = I0;
FLsum1(kp,kd,k) = sum(value1(:));
FLmean1(kp,kd,k) = mean(value1(value1>0));
%FLsum2(kp,kd,k) = sum(value2(:));
%FLmean2(kp,kd,k) = mean(value2(value2>0));

end

end

end

return

%%

figure(1); clf;

subplot(3,1,1)
data = reshape(FLsum(2,::),4,size(FLsum,3)) - reshape(FLsum(1,::),4,size(FLsum,3));
plot(1:4,data);
title('100ms exposure');
xlabel('time');

subplot(3,1,2);
data = reshape(FLsum(4,::),4,size(FLsum,3)) - reshape(FLsum(3,::),4,size(FLsum,3));
plot(1:4,data);
title('500ms exposure');
xlabel('time');

subplot(3,1,3);
data = reshape(FLsum(6,::),4,size(FLsum,3)) - reshape(FLsum(5,::),4,size(FLsum,3));
plot(1:4,data);
title('1000ms exposure');

```

```

xlabel('time');

name = {...
    'postload00',...
    'postinc00',...
    'postload01',...
    'postinc01',...
    'postload02',...
    'postinc02',...
};

xlname = 'imageseg.xlsx';

for kp = 1:length(name)

    fname = ['imageSum',name{kp},' .txt'];
    data = reshape(FLsum(kp,,:),8,128);
    csvwrite(fname,data);
    xlswrite(xlname,data,name{kp});

end

figure(1); clf;
data = reshape(FLsum(2,,:),8,size(FLsum,3)) - reshape(FLsum(1,,:),8,size(FLsum,3));
plot(1:8,data);
title('100ms exposure');
xlabel('time');

figure(2); clf;
data = reshape(FLmean(2,[1 2 3 4 7 8],:),6,size(FLmean,3)) - reshape(FLmean(1,[1 2 3 4
7 8],:),6,size(FLsum,3));
plot(1:6,data);
title('100ms exposure');
xlabel('time');

```